Closed-form Solution of Timoshenko Frames on Elastic Winkler Foundation Using the Green's Function Stiffness Method

Solución Analítica de Marcos de Timoshenko Sobre Fundación Elástica de Winkler Usando el Método de Rigidez con Funciones de Green

CRISTIAN DANIEL POSSO SABOGAL

JUAN CAMILO MOLINA VILLEGAS

JORGE ELIECER BALLESTEROS ORTEGA

Artículo

Asesor, docente

JUAN CAMILO MOLINA VILLEGAS

UNIVERSIDAD EAFIT

ESCUELA DE CIENCIAS APLICADAS E INGENIERÍA

MAESTRÍA EN INGENIERÍA

MEDELLÍN

2024

European Journal of Mechanics / A Solids 109 (2025) 105457

Contents lists available at ScienceDirect

European Journal of Mechanics / A Solids

journal homepage: www.elsevier.com/locate/ejmsol

Full Length Article

Closed-form solution of Timoshenko frames on elastic Winkler foundation using the Green's function stiffness method

Cristian Posso [a], Juan Camilo Molina-Villegas [a,*], Jorge Eliecer Ballesteros Ortega [b]

[a] Escuela de Ciencias Aplicadas e Ingeniería, Universidad EAFIT, Medellín, Colombia
[b] Dept. of Civil, Environmental, and Construction Engineering, University of Central Florida, Orlando, FL 32816, USA

ARTICLE INFO

Keywords:
Timoshenko beam
Elastic Winkler foundation
Static analysis
Closed-form solution
Green's functions
Mesh reduction method
Green's function stiffness method
Finite element method
Transcendental Finite element method

ABSTRACT

This paper presents a method to obtain the exact closed-form solution for the static analysis of Timoshenko beams and frames on elastic Winkler foundation, subjected to arbitrary external loads and bending moments. The solution is derived using the Green's Functions Stiffness Method (GFSM), a novel mesh reduction method that combines the strengths of the Stiffness Method (SM) and Green's Functions (GFs). By incorporating the core concepts of the SM, the GFSM exhibits similarities to the Finite Element Method (FEM), including the use of shape functions, stiffness matrices, and fixed-end forces. The application of GFs facilitates the derivation of analytical expressions for displacement and internal force fields for arbitrary external loads and bending moments. Three examples are presented: a single-span beam, a two-span beam, and a one-bay, one-story plane frame on elastic Winkler foundations; which demonstrate applicability and efficacy of the method.

1. Introduction

The analysis of beams on elastic foundations is fundamental in various engineering disciplines, including geotechnical, civil, mechanical, biomechanical, and aerospace engineering. This modeling approach has been extensively utilized for analyzing foundation beams and piles (Hetényi and Hetbenyi, 1946), pavements (Beskou and Muho, 2023), railroad tracks (Lamprea-Pineda et al., 2022), orthopedic implants (Bechtold and Riley, 1991), the deformation of the Earth's lithosphere (Turcotte and Schubert, 2002), and numerous other engineering applications (Frydrýšek et al., 2023). In recent decades, the application of this structural model in nanomechanics has grown exponentially. Nanobeams on nano-foundations have been used to model advanced structural elements, such as functionally graded porous nanobeams employed in MicroElectroMechanical Systems (MEMS), sensors, and solar cells; where the unique combination of mechanical strength and electrical conductivity of carbon nanotubes is advantageous (Pham et al., 2022). Also, they are used to simulate protein microtubules within cellular structures (Alhebshi et al., 2022) and viruses (Dastjerdi et al., 2022). The versatility and effectiveness of this approach make it an indispensable tool for understanding the behavior and interaction of macro and microstructures with their foundations.

The Euler–Bernoulli Beam Model (EBBM) (Euler, 1744) is the most widely used model for analyzing beams. The EBBM assumes that shear deformation is negligible, and the transverse cross-sections of an undeformed beam remain plane and perpendicular to the neutral axis after deformation. This assumption limits its applicability primarily to slender beams. To overcome these limitations, more advanced beam theories have been developed, with the Timoshenko Beam Model (TBM) (Timoshenko, 1921; Elishakoff, 2019) and the Reddy Beam Model (RBM) (Ruocco and Reddy, 2023) being among the most prominent. The TBM incorporates a first-order shear deformation theory, which considers that plane sections remain plane but not necessarily perpendicular to the neutral axis. In contrast, the RBM is a third-order theory which proposes that sections after deformation are neither plane nor perpendicular to the neutral axis, ensuring zero shear stress at the beam's top and bottom surfaces. Unlike the TBM, the RBM does not require a shear correction factor (Timoshenko, 1922; Cowper, 1966; Faghidian and Elishakoff, 2023). Other significant beam models have been developed to address these and additional common limitations (Touratier, 1991; Silvestre and Camotim, 2002; Shi and Voyiadjis, 2010; Neves et al., 2011; Carrera et al., 2011; Mantari et al., 2011; Challamel et al., 2013; Zenkour, 2013; Benzid and Tati, 2023; Kenanda and Hammadi, 2023).

Despite the complexity of soil mechanical properties and their interaction with beams, two recognized models offer different approaches to study these aspects. The first is the Continuous Medium Model (CMM) (Boussinesq, 1885; Worku, 2012; Worku and Degu, 2012) which analyzes

* Corresponding author.
E-mail address: jmolina2@eafit.edu.co (J.C. Molina-Villegas).

https://doi.org/10.1016/j.euromechsol.2024.105457
Received 6 June 2024; Received in revised form 20 August 2024; Accepted 23 September 2024
Available online 1 October 2024

a beam resting on a half-space, considering the soil as a continuous tridimensional medium. The second approach involves Mechanical Models (MMs), where the soil is idealized using simplified models that can be readily integrated into traditional beam models. Although MMs generally offer less accuracy compared to CMMs, they have simpler mathematical formulations enabling analytical solutions. MMs are typically categorized into one-parameter, two-parameter, and three-parameter models, depending on the complexity of the represented soil behavior.

The Winkler model (Winkler, 1867) is a well-known one-parameter model that represents the foundation as a continuous series of infinite, independent, linear-elastic transverse springs. This model offers a simplified approximation of soil behavior while providing reasonable results in many practical scenarios (Shirima and Giger, 1992). To address the limitations of one-parameter models, two-parameter models have been developed, incorporating a second parameter to consider the coupling effects among the springs. Notable examples include models proposed by Filonenko-Borodich, Pasternak, Vlasov, Hetényi, and Selvadurai, among others (Filonenko-Borodich, 1940; Pasternak, 1954; Vlasov, 1966; Fletcher and Hermann, 1971; Selvadurai, 1979; Scott, 1981; Zhaohua and Cook, 1983; Nogami and O'Neill, 1985). Three-parameter models further enhance the representation of stress distribution by introducing an additional parameter (Avramidis and Morfidis, 2006). Significant contributions in this area have been made by Kerr, Reissner, and others (Hetényi, 1950; Kerr, 1965; Reissner, 1967; Vallabhan and Das, 1988).

Numerous studies have investigated the static behavior of various beam types on different foundation models using MMs. Hetényi and Hetbenyi (1946) presented analytical solutions for displacement and internal force fields were derived for Euler–Bernoulli frames with constant and variable flexural rigidity on elastic Winkler foundation. Stiffness matrices and fixed-end force vectors for Timoshenko beams on elastic Winkler foundation were determined by Cheng and Pantelides (1988), and Aydoğan (1995). Additionally, Lignola et al. (2017) derived equations applicable to only one of the three cases of the characteristic equation obtained in the analysis of Timoshenko beams on Winkler's foundation. Yin (2000a) provided solutions for the displacement and internal force fields of reinforced Timoshenko beams on elastic Winkler foundations using Fourier series.

The concept of Green's Functions (GFs), also known as fundamental solutions, is a key mathematical tool for solving complex problems governed by Differential Equations (DEs) (Challis and Sheard, 2003), and form the basis of the Direct Boundary Element Method (BEM) (Banerjee and Butterfield, 1981) and Indirect Boundary Element Method (Sánchez-Sesma et al., 1993). They have been widely used to solve structural problems, Ghannadiasl and Mofid (2014), Hozhabrossadati et al. (2015) and Han et al. (2017) used GFs that involve the dynamic response of Euler–Bernoulli and Timoshenko beams. Rezaiee-Pajand et al. (2018) obtained exact thermo-mechanical static responses of curved circular Euler–Bernoulli beams using GFs. For beams on elastic foundations, Molina-Villegas et al. (2021) computed the response of Euler–Bernoulli beams on elastic Winkler foundation. Wang and He (1998) extended the GFs developed by Lueschen et al. (1996) to calculate the response of Timoshenko beams on Winkler, Pasternak, generalized, and Vlasov foundation models. Additionally, Naghdi (1980) derived GFs for thin elastic semicircular plates and used them to obtain closed-form solutions.

For the dynamic analysis, Ruge and Birk (2007) explored frequency and time domain solutions to compare infinite Euler–Bernoulli and Timoshenko beams on elastic Winkler foundation. Arboleda-Monsalve et al. (2008) determined the dynamic stiffness matrix and fixed-end forces for Timoshenko beam–columns on elastic foundation. Deng et al. (2017) computed the exact dynamic stiffness matrix for a double-functionally graded Timoshenko beam. Esen (2019) developed a Finite Element Method (FEM) formulation to analyze the vibration of functionally graded Timoshenko beams. The aforementioned studies utilized two-parameter foundation models, whereas (Morfidis, 2010) investigated the natural vibration of Timoshenko beams on a Kerr-type three-parameter foundation. Also, the analysis of dynamic nanobeams on elastic foundation have been studied (Akgöz and Civalek, 2018; Al-Furjan et al., 2021; Avcar et al., 2021).

Despite the development of numerous methods for the static analysis of Timoshenko beams and frames on elastic Winkler foundations, a closed-form solution for these elements under arbitrary external loads and bending moments has not yet been developed. This paper addresses that gap by introducing a novel formulation of the Green's Functions Stiffness Method (GFSM) for the static analysis of Timoshenko beams and frames on elastic Winkler foundations.

The GFSM is a novel mesh reduction technique that combines the strengths of the Stiffness Method (SM) and GFs (Molina-Villegas and Ballesteros Ortega, 2023a). By integrating core concepts from the SM, the GFSM shares similarities with the FEM, such as shape functions, stiffness matrices, and fixed-end forces. The primary advantage of the GFSM over FEM and other numerical methods, such as the Finite Difference Method (FDM), the differential quadrature method, and the Rayleigh–Ritz method, is its ability, as an analytical method, to achieve closed-form solutions for linear problems without the need of the dense meshes typically required in FEM and FDM. Moreover, the GFSM is a specialized form of the Transcendental Finite Element Method (TFEM) (Kennedy et al., 2004; Ilanko, 2005; Onu, 2008; Adhikari et al., 2021; Adhikari and Bhattacharya, 2021; Adhikari, 2021) in which are included GFs to achieve closed-form solutions.

The GFSM has proven its effectiveness in the analysis of uniform Euler–Bernoulli beams on elastic Winkler foundations with and without semi-rigid connections (Molina-Villegas, 2021; Molina-Villegas et al., 2022), uniform Timoshenko frames with and without semi-rigid connections (Molina-Villegas and Ballesteros Ortega, 2023b,c), and axially non-uniform Euler–Bernoulli and Timoshenko frames (Molina-Villegas et al., 2023, 2024). This paper is unique in its focus on the analysis of uniform Timoshenko beams and frames on elastic Winkler foundations.

This paper is organized into seven sections. Section 2 describes the decomposition of the Timoshenko frame on elastic Winkler foundation into Timoshenko beam on elastic foundation and rod elements. Sections 3 and 4 present the formulation of the GFSM for the Timoshenko beam on elastic Winkler foundation and the rod element, respectively, focusing on the most practical case of the characteristic equation. Section 5 combines the results from the two previous sections to develop the GFSM formulation for the Timoshenko frame on elastic Winkler foundation element. Section 6 provides three examples demonstrating the applicability and effectiveness of the GFSM. Section 7 summarizes the key findings and conclusions. Finally, Appendices A and B offer the GFSM formulation for the Timoshenko frame on elastic Winkler foundation in the remaining cases of the characteristic equation, while Appendix C introduces a novel variational FEM formulation based on the relation between the analytical cross-section rotation and the analytical transverse displacement shape functions.

2. Decomposition of the frame element

The element to be analyzed is the Timoshenko frame on elastic Winkler foundation, as shown in Fig. 1. It is subjected to: (a) an external distributed axial load along the x-axis direction $p(x)$, (b) an external distributed transverse load along the y-axis direction $q_v(x)$, (c) a distributed load exerted by the soil along the local y-axis $f_s(x)$, and (d) external distributed bending moments about the z-axis direction $q_\theta(x)$. The material of the element is homogeneous and linear-elastic, characterized by Young's modulus E and shear modulus G. Its transverse cross-sectional properties include a shear coefficient κ, an area A, a shear area A_s ($A_s = \kappa A$), and the second moment of area about the z-axis I. The soil is modeled as a linear-elastic Winkler foundation with a stiffness per unit length denoted by k.

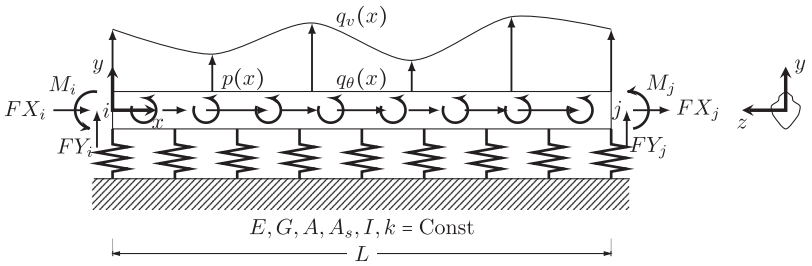

Fig. 1. Timoshenko frame on elastic Winkler foundation element and its transverse cross-section.

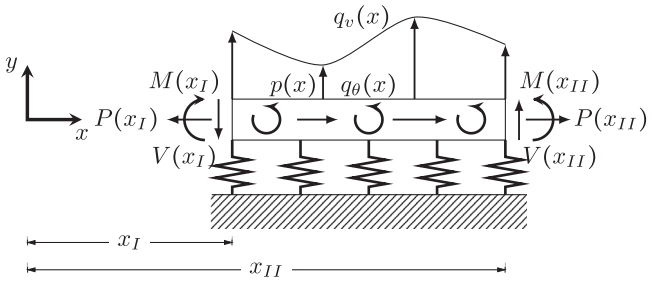

Fig. 2. Internal forces positive sign convention.

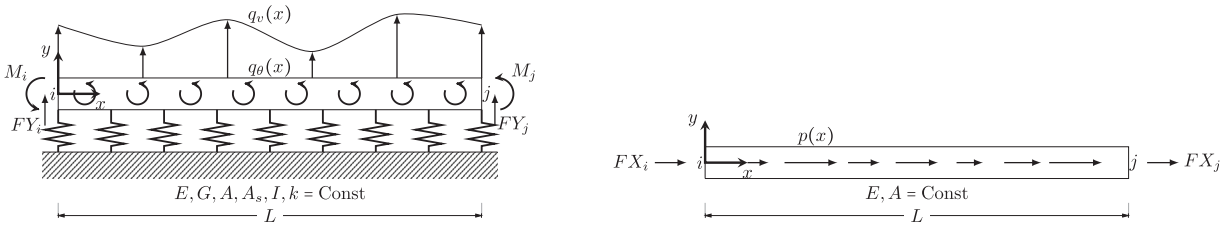

(a) Timoshenko beam on elastic Winkler foundation element. (b) Rod element.

Fig. 3. Decomposition of the Timoshenko frame on elastic Winkler foundation element as a Timoshenko beam on elastic Winkler foundation and a rod elements.

The internal forces of the element are: axial force $P(x)$, shear force $V(x)$, and bending moment $M(x)$, all of which follow to the positive sign convention depicted in Fig. 2.

Utilizing a first-order theory, where the transverse and axial behaviors of the element are decoupled, allows the independent analysis of a Timoshenko beam on elastic Winkler foundation element (Section 3) and a rod element (Section 4), as illustrated in Fig. 3.

3. Formulation of the GFSM for the Timoshenko beam on elastic Winkler foundation element

By applying Hooke's law and integrating the stresses over the transverse cross-section, the internal forces in the Timoshenko beam on elastic Winkler foundation can be determined as follows Reddy (2019):

$$V(x) = A_s G \left[\frac{\mathrm{d}v}{\mathrm{d}x}(x) - \theta(x)\right], \tag{1a}$$

$$M(x) = EI\frac{\mathrm{d}\theta}{\mathrm{d}x}(x), \tag{1b}$$

where $v(x)$ is the transverse displacement field, positive in the y-axis direction, and $\theta(x)$ is the cross-section rotation field, positive about the z-axis (counterclockwise).

The transverse and rotational equilibrium for each point of the Timoshenko beam on elastic Winkler foundation element leads to the following DEs:

$$\frac{\mathrm{d}V}{\mathrm{d}x}(x) - k \cdot v(x) = -q_v(x), \tag{2a}$$

$$\frac{\mathrm{d}M}{\mathrm{d}x}(x) + V(x) = -q_\theta(x), \tag{2b}$$

where the term $-k \cdot v(x)$ in Eq. (2a) represents the distributed load exerted by the soil in the transverse direction (Lamprea-Pineda et al., 2022):

$$f_s(x) = -k \cdot v(x). \tag{3}$$

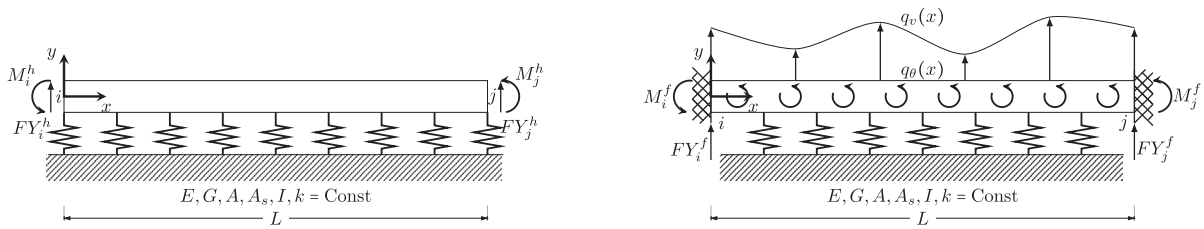

(a) Homogeneous response. (b) Fixed response.

Fig. 4. Decomposition of the response of the Timoshenko beam on elastic Winkler foundation element.

Using Eqs. (1) and (2), the governing DE for the Timoshenko beam on elastic Winkler foundation element (Li et al., 2016) is obtained:

$$\frac{\mathrm{d}^4 v}{\mathrm{d}x^4}(x) - \frac{k}{A_s G}\frac{\mathrm{d}^2 v}{\mathrm{d}x^2}(x) + \frac{k}{EI}v(x) = \frac{1}{EI}q_v(x) - \frac{1}{A_s G}\frac{\mathrm{d}^2 q_v}{\mathrm{d}x^2}(x) - \frac{1}{EI}\frac{\mathrm{d}q_\theta}{\mathrm{d}x}(x), \tag{4}$$

also, using a similar approach (Yin, 2000b; Al-Sadder and Wahshat, 2012), a relation between the cross-section rotation and the transverse displacement fields can be obtained:

$$\theta(x) = \frac{EI}{A_s G}\frac{\mathrm{d}^3 v}{\mathrm{d}x^3}(x) + \left[1 - \frac{EIk}{\left(A_s G\right)^2}\right]\frac{\mathrm{d}v}{\mathrm{d}x}(x) + \frac{EI}{\left(A_s G\right)^2}\frac{\mathrm{d}q_v}{\mathrm{d}x}(x) + \frac{1}{A_s G}q_\theta(x). \tag{5}$$

The formulation of the GFSM for the Timoshenko beam on elastic Winkler foundation is based on the solution of the DE (4), utilizing a strong formulation. This approach requires specifying four prescribed Boundary Conditions (BCs), which are the transverse displacements and cross-section rotations at the element ends. The resulting Boundary Value Problem (BVP) is defined as follows:

$$\frac{\mathrm{d}^4 v}{\mathrm{d}x^4}(x) - \frac{k}{A_s G}\frac{\mathrm{d}^2 v}{\mathrm{d}x^2}(x) + \frac{k}{EI}v(x) = \frac{1}{EI}q_v(x) - \frac{1}{A_s G}\frac{\mathrm{d}^2 q_v}{\mathrm{d}x^2}(x) - \frac{1}{EI}\frac{\mathrm{d}q_\theta}{\mathrm{d}x}(x), \tag{6a}$$

$$v(0) = v_i, \tag{6b}$$

$$\theta(0) = \theta_i, \tag{6c}$$

$$v(L) = v_j, \tag{6d}$$

$$\theta(L) = \theta_j, \tag{6e}$$

where v_i and v_j are the y-axis displacements at $x = 0$ and $x = L$, respectively, whereas θ_i and θ_j denote the rotations of the transverse cross-section at the same points.

To solve the BVP (6), the transverse displacement field is decomposed into a homogeneous solution $v_h(x)$ (see Fig. 4(a) for its physical interpretation), and a particular or "fixed" solution $v_f(x)$ (see Fig. 4(b) for its physical interpretation). This implies that the response fields are decomposed as:

$$v(x) = v_h(x) + v_f(x), \tag{7a}$$

$$\theta(x) = \theta_h(x) + \theta_f(x), \tag{7b}$$

$$V(x) = V_h(x) + V_f(x), \tag{7c}$$

$$M(x) = M_h(x) + M_f(x), \tag{7d}$$

where the terms with the subscript h correspond to the homogeneous solution, while those with the subscript f belong to the fixed solution.

The homogeneous response is determined in Section 3.1, while the fixed response is obtained in Section 3.2.

3.1. Homogeneous response

The governing BVP for the homogeneous problem of the Timoshenko beam on elastic Winkler foundation element is:

$$\frac{\mathrm{d}^4 v_h}{\mathrm{d}x^4}(x) - \frac{k}{A_s G}\frac{\mathrm{d}^2 v_h}{\mathrm{d}x^2}(x) + \frac{k}{EI}v_h(x) = 0, \tag{8a}$$

$$v_h(0) = v_i, \tag{8b}$$

$$\theta_h(0) = \theta_i, \tag{8c}$$

$$v_h(L) = v_j, \tag{8d}$$

$$\theta_h(L) = \theta_j. \tag{8e}$$

A straightforward method to compute the homogeneous transverse displacement field is to rewrite the homogeneous governing DE (8a) as follows:

$$\frac{\mathrm{d}^4 v_h}{\mathrm{d}x^4}(x) - 4\lambda_s^2\frac{\mathrm{d}^2 v_h}{\mathrm{d}x^2}(x) + 4\lambda_f^4 v_h(x) = 0, \tag{9}$$

where

$$\lambda_s = \sqrt{\frac{k}{4A_sG}}, \tag{10a}$$

$$\lambda_f = \sqrt[4]{\frac{k}{4EI}}. \tag{10b}$$

From Eq. (5), the homogeneous cross-section rotation field can be obtained in terms of λ_s and λ_f as:

$$\theta_h(x) = \frac{\mathrm{d}v_h}{\mathrm{d}x}(x) + \frac{\lambda_s^2}{\lambda_f^4}\left[\frac{\mathrm{d}^3v_h}{\mathrm{d}x^3}(x) - 4\lambda_s^2\frac{\mathrm{d}v_h}{\mathrm{d}x}(x)\right]. \tag{11}$$

The homogeneous DE (9) can be solved using the test solution $v_h(x) = \mathrm{e}^{\lambda x}$. Substituting this into Eq. (9) yields the following equation:

$$\lambda^4 - 4\lambda_s^2\lambda^2 + 4\lambda_f^4 = 0. \tag{12}$$

Using the change of variable $s = \lambda^2$ in expression (12), the characteristic equation is obtained:

$$s^2 - 4\lambda_s^2 s + 4\lambda_f^4 = 0, \tag{13}$$

from which it is clear that its solution is:

$$s = 2\lambda_s^2 \pm 2\sqrt{\left(\lambda_s - \lambda_f\right)\left(\lambda_s + \lambda_f\right)\left(\lambda_s^2 + \lambda_f^2\right)}. \tag{14}$$

In Eq. (14), three cases are identified for the solution of the characteristic equation: $\lambda_s < \lambda_f$, $\lambda_s = \lambda_f$, and $\lambda_s > \lambda_f$. Throughout the remaining sections of the paper, including the current one, the focus is primarily directed towards the scenario where $\lambda_s < \lambda_f$ because it is the most widely used in real-world problems. However, in Appendices A and B, there are provided solutions for the cases where $\lambda_s = \lambda_f$, and $\lambda_s > \lambda_f$, respectively.

In light of the aforementioned case of interest, Eq. (14) can be expressed as:

$$s = (\alpha \pm \beta\mathrm{i})^2, \tag{15}$$

where

$$\alpha = \sqrt{\lambda_f^2 + \lambda_s^2}, \tag{16a}$$

$$\beta = \sqrt{\lambda_f^2 - \lambda_s^2}, \tag{16b}$$

$$\mathrm{i} = \sqrt{-1}. \tag{16c}$$

Then, the four roots of Eq. (12) are given by:

$$\lambda_1 = +\alpha + \beta\mathrm{i}, \tag{17a}$$

$$\lambda_2 = +\alpha - \beta\mathrm{i}, \tag{17b}$$

$$\lambda_3 = -\alpha + \beta\mathrm{i}, \tag{17c}$$

$$\lambda_4 = -\alpha - \beta\mathrm{i}, \tag{17d}$$

and the solution for $v_h(x)$ can be written as:

$$v_h(x) = D_1\cosh(\alpha x)\cos(\beta x) + D_2\cosh(\alpha x)\sin(\beta x) + D_3\sinh(\alpha x)\cos(\beta x) + D_4\sinh(\alpha x)\sin(\beta x). \tag{18}$$

By substituting Eq. (18) into Eq. (11), the homogeneous cross-section rotation field is obtained:

$$\theta_h(x) = R_1\cosh(\alpha x)\cos(\beta x) + R_2\cosh(\alpha x)\sin(\beta x) + R_3\sinh(\alpha x)\cos(\beta x) + R_4\sinh(\alpha x)\sin(\beta x), \tag{19}$$

where

$$R_1 = \eta D_3 + \phi D_2, \tag{20a}$$

$$R_2 = \eta D_4 - \phi D_1, \tag{20b}$$

$$R_3 = \eta D_1 + \phi D_4, \tag{20c}$$

$$R_4 = \eta D_2 - \phi D_3; \tag{20d}$$

$$\eta = \alpha\left(\frac{3\beta^2 - \alpha^2}{\alpha^2 + \beta^2}\right), \tag{20e}$$

$$\phi = \beta\left(\frac{3\alpha^2 - \beta^2}{\alpha^2 + \beta^2}\right). \tag{20f}$$

Finally, by using Eqs. (18) and (19) to solve the BVP (8), we obtain the solutions for the transverse displacement and cross-section rotation fields:

$$v_h(x) = \psi_2^v(x)v_i + \psi_3^v(x)\theta_i + \psi_5^v(x)v_j + \psi_6^v(x)\theta_j, \tag{21a}$$

$$\theta_h(x) = \psi_2^\theta(x)v_i + \psi_3^\theta(x)\theta_i + \psi_5^\theta(x)v_j + \psi_6^\theta(x)\theta_j, \tag{21b}$$

where

$$\psi_2^v(x) = \frac{\left(\eta^2 \cdot \mathrm{s}^2 - \phi^2 \cdot \mathrm{sh}^2\right)\cosh(\alpha x)\cos(\beta x) - \eta\,(\eta \cdot \mathrm{c} \cdot \mathrm{s} + \phi \cdot \mathrm{ch} \cdot \mathrm{sh})\cosh(\alpha x)\sin(\beta x)}{\eta^2 \cdot \mathrm{s}^2 - \phi^2 \cdot \mathrm{sh}^2} + \frac{\phi\,(\eta \cdot \mathrm{c} \cdot \mathrm{s} + \phi \cdot \mathrm{ch} \cdot \mathrm{sh})\sinh(\alpha x)\cos(\beta x) - \eta\phi\left(\mathrm{c}^2 - \mathrm{ch}^2\right)\sinh(\alpha x)\sin(\beta x)}{\eta^2 \cdot \mathrm{s}^2 - \phi^2 \cdot \mathrm{sh}^2}, \tag{22a}$$

$$\psi_3^v(x) = \frac{-\phi \cdot \mathrm{sh}^2 \cdot \cosh(\alpha x)\sin(\beta x) + \eta \cdot \mathrm{s}^2 \cdot \sinh(\alpha x)\cos(\beta x) + (\phi \cdot \mathrm{ch} \cdot \mathrm{sh} - \eta \cdot \mathrm{c} \cdot \mathrm{s})\sinh(\alpha x)\sin(\beta x)}{\eta^2 \cdot \mathrm{s}^2 - \phi^2 \cdot \mathrm{sh}^2}, \tag{22b}$$

$$\psi_5^v(x) = \frac{(\eta \cdot \mathrm{ch} \cdot \mathrm{s} + \phi \cdot \mathrm{c} \cdot \mathrm{sh})\left[\eta \cdot \cosh(\alpha x)\sin(\beta x) - \phi \cdot \sinh(\alpha x)\cos(\beta x)\right] - \left(\eta^2 + \phi^2\right) \cdot \mathrm{sh} \cdot \mathrm{s} \cdot \sinh(\alpha x)\sin(\beta x)}{\eta^2 \cdot \mathrm{s}^2 - \phi^2 \cdot \mathrm{sh}^2}, \tag{22c}$$

$$\psi_6^v(x) = \frac{\mathrm{sh} \cdot \mathrm{s} \cdot \left[-\eta \cdot \cosh(\alpha x)\sin(\beta x) + \phi \cdot \sinh(\alpha x)\cos(\beta x)\right] + (\eta \cdot \mathrm{ch} \cdot \mathrm{s} - \phi \cdot \mathrm{c} \cdot \mathrm{sh})\sinh(\alpha x)\sin(\beta x)}{\eta^2 \cdot \mathrm{s}^2 - \phi^2 \cdot \mathrm{sh}^2}, \tag{22d}$$

$$\psi_2^\theta(x) = \frac{\left(\eta^2 + \phi^2\right)\left[\phi \cdot \mathrm{sh}^2 \cdot \cosh(\alpha x)\sin(\beta x) + \eta \cdot \mathrm{s}^2 \cdot \sinh(\alpha x)\cos(\beta x) - (\eta \cdot \mathrm{c} \cdot \mathrm{s} + \phi \cdot \mathrm{ch} \cdot \mathrm{sh})\sinh(\alpha x)\sin(\beta x)\right]}{\eta^2 \cdot \mathrm{s}^2 - \phi^2 \cdot \mathrm{sh}^2}, \tag{23a}$$

$$\psi_3^\theta(x) = \frac{\left(\eta^2 \cdot \mathrm{s}^2 - \phi^2 \cdot \mathrm{sh}^2\right)\cosh(\alpha x)\cos(\beta x) - \eta\,(\eta \cdot \mathrm{c} \cdot \mathrm{s} - \phi \cdot \mathrm{ch} \cdot \mathrm{sh})\cosh(\alpha x)\sin(\beta x)}{\eta^2 \cdot \mathrm{s}^2 - \phi^2 \cdot \mathrm{sh}^2} + \frac{-\phi\,(\eta \cdot \mathrm{c} \cdot \mathrm{s} - \phi \cdot \mathrm{ch} \cdot \mathrm{sh})\sinh(\alpha x)\cos(\beta x) + \eta \cdot \phi\left(\mathrm{c}^2 - \mathrm{ch}^2\right)\sinh(\alpha x)\sin(\beta x)}{\eta^2 \cdot \mathrm{s}^2 - \phi^2 \cdot \mathrm{sh}^2}, \tag{23b}$$

$$\psi_5^\theta(x) = \frac{\left(\eta^2 + \phi^2\right)\left\{-\mathrm{sh} \cdot \mathrm{s} \cdot \left[\eta \cdot \cosh(\alpha x)\sin(\beta x) + \phi \cdot \sinh(\alpha x)\cos(\beta x)\right] + (\eta \cdot \mathrm{ch} \cdot \mathrm{s} + \phi \cdot \mathrm{c} \cdot \mathrm{sh})\sinh(\alpha x)\sin(\beta x)\right\}}{\eta^2 \cdot \mathrm{s}^2 - \phi^2 \cdot \mathrm{sh}^2}, \tag{23c}$$

$$\psi_6^\theta(x) = \frac{(\eta \cdot \mathrm{ch} \cdot \mathrm{s} - \phi \cdot \mathrm{c} \cdot \mathrm{sh})\left[\eta \cdot \cosh(\alpha x)\sin(\beta x) + \phi \cdot \sinh(\alpha x)\cos(\beta x)\right] - \left(\eta^2 + \phi^2\right) \cdot \mathrm{sh} \cdot \mathrm{s} \cdot \sinh(\alpha x)\sin(\beta x)}{\eta^2 \cdot \mathrm{s}^2 - \phi^2 \cdot \mathrm{sh}^2}, \tag{23d}$$

being

$$\mathrm{ch} = \cosh(\alpha L), \tag{24a}$$

$$\mathrm{sh} = \sinh(\alpha L), \tag{24b}$$

$$\mathrm{c} = \cos(\beta L), \tag{24c}$$

$$\mathrm{s} = \sin(\beta L). \tag{24d}$$

The functions $\psi_n^v(x)$ and $\psi_n^\theta(x)$ $(n = 2, 3, 5, 6)$ are defined as the analytical transverse displacement and analytical cross-section rotation shape functions for the Timoshenko beam on elastic Winkler foundation element, respectively. These functions are equivalent to those used in the TFEM (Xia, 2022).

Additionally, using Eqs. (1), the homogeneous internal force fields can be computed from the homogeneous transverse displacement and cross-section rotation fields presented in Eqs. (21a) and (21b), respectively, obtaining:

$$V_h(x) = \psi_2^V(x)v_i + \psi_3^V(x)\theta_i + \psi_5^V(x)v_j + \psi_6^V(x)\theta_j, \tag{25a}$$

$$M_h(x) = \psi_2^M(x)v_i + \psi_3^M(x)\theta_i + \psi_5^M(x)v_j + \psi_6^M(x)\theta_j, \tag{25b}$$

where

$$\psi_2^V(x) = \frac{EI\left(\eta^2 + \phi^2\right)^2}{2\,(\alpha \cdot \eta - \beta \cdot \phi)\left(\eta^2 \cdot \mathrm{s}^2 - \phi^2 \cdot \mathrm{sh}^2\right)}\Big\{ (\eta \cdot \mathrm{c} \cdot \mathrm{s} + \phi \cdot \mathrm{ch} \cdot \mathrm{sh})\left\{(\beta \cdot \eta - \alpha \cdot \phi)\cosh(\alpha x)\cos(\beta x) + \left[\eta\,(\alpha - \eta) + \phi\,(\beta - \phi)\right]\sinh(\alpha x)\sin(\beta x)\right\} + \left[\alpha \cdot \eta \cdot \phi\left(\mathrm{c}^2 - \mathrm{ch}^2\right) + \eta^2\left(\beta \cdot \mathrm{s}^2 + \phi \cdot \mathrm{sh}^2\right) + \phi^2\,(\phi - \beta)\,\mathrm{sh}^2\right]\cosh(\alpha x)\sin(\beta x) + \left[\beta \cdot \eta \cdot \phi\left(\mathrm{c}^2 - \mathrm{ch}^2\right) + \phi^2\left(\alpha \cdot \mathrm{sh}^2 + \eta \cdot \mathrm{s}^2\right) + \eta^2\,(\,\eta - \alpha)\,\mathrm{s}^2\right]\sinh(\alpha x)\cos(\beta x)\Big\}, \tag{26a}$$

$$\psi_3^V(x) = \frac{EI\left(\eta^2 + \phi^2\right)^2}{2\,(\alpha \cdot \eta - \beta \cdot \phi)\left(\eta^2 \cdot \mathrm{s}^2 - \phi^2 \cdot \mathrm{sh}^2\right)}\Big\{ \left[\eta\,(\eta - \alpha)\,\mathrm{s}^2 + \phi\,(\beta - \phi)\,\mathrm{sh}^2\right]\cosh(\alpha x)\cos(\beta x) + (\eta \cdot \mathrm{c} \cdot \mathrm{s} - \phi \cdot \mathrm{ch} \cdot \mathrm{sh})\left[\,(\alpha - \eta)\cosh(\alpha x)\sin(\beta x) + (\beta - \phi)\sinh(\alpha x)\cos(\beta x)\,\right] + \left[\alpha \cdot \phi \cdot \mathrm{sh}^2 + \beta \cdot \eta \cdot \mathrm{s}^2 + \eta \cdot \phi\left(\mathrm{c}^2 - \mathrm{ch}^2\right)\right]\sinh(\alpha x)\sin(\beta x)\Big\}, \tag{26b}$$

$$\psi_5^V(x) = \frac{EI\left(\eta^2+\phi^2\right)^2}{2\left(\alpha\cdot\eta-\beta\cdot\phi\right)\left(\eta^2\cdot \mathrm{s}^2-\phi^2\cdot \mathrm{sh}^2\right)}\Big\{ (\eta\cdot \mathrm{ch}\cdot \mathrm{s}+\phi\cdot \mathrm{c}\cdot \mathrm{sh})\{(\alpha\cdot\phi-\beta\cdot\eta)\cosh(\alpha x)\cos(\beta x) + [\eta(\eta-\alpha)+\phi(\phi-\beta)]\sinh(\alpha x)\sin(\beta x)\} + \left(\eta^2+\phi^2\right)\mathrm{s}\cdot\mathrm{sh}[(\alpha-\eta)\cosh(\alpha x)\sin(\beta x) + (\beta-\phi)\sinh(\alpha x)\cos(\beta x)]\Big\}, \tag{26c}$$

$$\psi_6^V(x) = \psi_6^V(x) = \frac{EI\left(\eta^2+\phi^2\right)^2}{2\left(\alpha\cdot\eta-\beta\cdot\phi\right)\left(\eta^2\cdot \mathrm{s}^2-\phi^2\cdot \mathrm{sh}^2\right)}\Big\{\mathrm{s}\cdot\mathrm{sh}\{(\beta\cdot\eta-\alpha\cdot\phi)\cosh(\alpha x)\cos(\beta x) + [\eta(\alpha-\eta)+\phi(\beta-\phi)]\sinh(\alpha x)\sin(\beta x)\} + (\eta\cdot \mathrm{ch}\cdot \mathrm{s}-\phi\cdot \mathrm{c}\cdot \mathrm{sh})[(\eta-\alpha)\cosh(\alpha x)\sin(\beta x) + (\phi-\beta)\sinh(\alpha x)\cos(\beta x)]\Big\}, \tag{26d}$$

$$\psi_2^M(x) = \frac{EI\left(\eta^2+\phi^2\right)}{\eta^2\cdot \mathrm{s}^2-\phi^2\cdot \mathrm{sh}^2}\Big\{\left(\alpha\cdot\eta\cdot \mathrm{s}^2+\beta\cdot\phi\cdot \mathrm{sh}^2\right)\cosh(\alpha x)\cos(\beta x) + \left(\alpha\cdot\phi\cdot \mathrm{sh}^2-\beta\cdot\eta\cdot \mathrm{s}^2\right)\sinh(\alpha x)\sin(\beta x) - (\eta\cdot \mathrm{c}\cdot \mathrm{s}+\phi\cdot \mathrm{ch}\cdot \mathrm{sh})[\alpha\cdot\cosh(\alpha x)\sin(\beta x) + \beta\cdot\sinh(\alpha x)\cos(\beta x)]\Big\}, \tag{27a}$$

$$\psi_3^M(x) = \frac{EI}{\eta^2\cdot \mathrm{s}^2-\phi^2\cdot \mathrm{sh}^2}\Big\{(\alpha\cdot\phi+\beta\cdot\eta)(\phi\cdot \mathrm{ch}\cdot \mathrm{sh}-\eta\cdot \mathrm{c}\cdot \mathrm{s})\cosh(\alpha x)\cos(\beta x) + \left[\alpha\cdot\eta\cdot\phi\left(\mathrm{c}^2-\mathrm{ch}^2\right)+\beta\left(\phi^2\cdot \mathrm{sh}^2-\eta^2\cdot \mathrm{s}^2\right)\right]\cosh(\alpha x)\sin(\beta x) + \left[\alpha\left(\eta^2\cdot \mathrm{s}^2-\phi^2\cdot \mathrm{sh}^2\right)+\beta\cdot\eta\cdot\phi\left(\mathrm{c}^2-\mathrm{ch}^2\right)\right]\sinh(\alpha x)\cos(\beta x) + (\alpha\cdot\eta-\beta\cdot\phi)(\phi\cdot \mathrm{ch}\cdot \mathrm{sh}-\eta\cdot \mathrm{c}\cdot \mathrm{s})\sinh(\alpha x)\sin(\beta x)\Big\}, \tag{27b}$$

$$\psi_5^M(x) = \frac{EI\left(\eta^2+\phi^2\right)}{\eta^2\cdot \mathrm{s}^2-\phi^2\cdot \mathrm{sh}^2}\Big\{\mathrm{s}\cdot\mathrm{sh}[(\beta\cdot\phi-\alpha\cdot\eta)\sinh(\alpha x)\sin(\beta x) - (\alpha\cdot\phi+\beta\cdot\eta)\cosh(\alpha x)\cos(\beta x)] + (\eta\cdot \mathrm{ch}\cdot \mathrm{s}+\phi\cdot \mathrm{c}\cdot \mathrm{sh})[\alpha\cdot\cosh(\alpha x)\sin(\beta x) + \beta\cdot\sinh(\alpha x)\cos(\beta x)]\Big\}, \tag{27c}$$

$$\psi_6^M(x) = \frac{EI}{\eta^2\cdot \mathrm{s}^2-\phi^2\cdot \mathrm{sh}^2}\Big\{(\eta\cdot \mathrm{s}\cdot \mathrm{ch}-\phi\cdot \mathrm{c}\cdot \mathrm{sh})[(\alpha\cdot\phi+\beta\cdot\eta)\cosh(\alpha x)\cos(\beta x) + (\alpha\cdot\eta-\beta\cdot\phi)\sinh(\alpha x)\sin(\beta x)] - \left(\eta^2+\phi^2\right)\mathrm{s}\cdot\mathrm{sh}[\alpha\cdot\cosh(\alpha x)\sin(\beta x) + \beta\cdot\sinh(\alpha x)\cos(\beta x)]\Big\}, \tag{27d}$$

being the functions $\psi_n^V(x)$ and $\psi_n^M(x)$ defined as the analytical shear force and analytical bending moment shape functions for the Timoshenko beam on elastic Winkler foundation element, respectively.

By evaluating the homogeneous internal force fields presented in Eq. (25) at $x = 0$ and $x = L$, the relation for the beam element that relates its homogeneous generalized forces to its generalized displacements at the element ends is obtained (see these homogeneous generalized forces in Fig. 4(a)):

$$\begin{Bmatrix} FY_i^h \\ M_i^h \\ FY_j^h \\ M_j^h \end{Bmatrix} = \begin{Bmatrix} -V_h(0) \\ -M_h(0) \\ V_h(L) \\ M_h(L) \end{Bmatrix} = \begin{bmatrix} k_{22} & k_{23} & k_{25} & k_{26} \\ k_{32} & k_{33} & k_{35} & k_{36} \\ k_{52} & k_{53} & k_{55} & k_{56} \\ k_{62} & k_{63} & k_{65} & k_{66} \end{bmatrix} \begin{Bmatrix} v_i \\ \theta_i \\ v_j \\ \theta_j \end{Bmatrix}, \tag{28}$$

where

$$k_{22} = k_{55} = \frac{2EI\cdot\alpha\cdot\beta\left(\alpha^2+\beta^2\right)(\eta\cdot \mathrm{s}\cdot \mathrm{c}+\phi\cdot \mathrm{sh}\cdot \mathrm{ch})}{\phi^2\mathrm{sh}^2-\eta^2\mathrm{s}^2}, \tag{29a}$$

$$k_{23} = k_{32} = -k_{56} = -k_{65} = \frac{EI\left(\alpha^2+\beta^2\right)\left(\alpha\cdot\eta\cdot \mathrm{s}^2+\beta\cdot\phi\cdot \mathrm{sh}^2\right)}{\phi^2\mathrm{sh}^2-\eta^2\mathrm{s}^2}, \tag{29b}$$

$$k_{25} = k_{52} = -\frac{2EI\cdot\alpha\cdot\beta\left(\alpha^2+\beta^2\right)(\eta\cdot \mathrm{s}\cdot \mathrm{ch}+\phi\cdot \mathrm{c}\cdot \mathrm{sh})}{\phi^2\mathrm{sh}^2-\eta^2\mathrm{s}^2}, \tag{29c}$$

$$k_{26} = k_{62} = -k_{35} = -k_{53} = \frac{2EI\cdot\alpha\cdot\beta\left(\alpha^2+\beta^2\right)\mathrm{s}\cdot\mathrm{sh}}{\phi^2\mathrm{sh}^2-\eta^2\mathrm{s}^2}, \tag{29d}$$

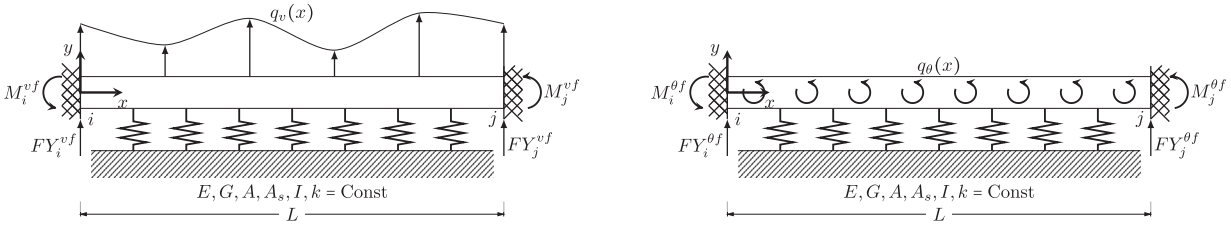

(a) Fixed response due to the external transverse load $q_v(x)$.

(b) Fixed response due to the external transverse load $q_\theta(x)$.

Fig. 5. Decomposition of the fixed response of the Timoshenko beam on elastic Winkler foundation element.

$$k_{33} = k_{66} = \frac{2EI \cdot \alpha \cdot \beta\,(\phi \cdot \text{sh} \cdot \text{ch} - \eta \cdot \text{s} \cdot \text{c})}{\phi^2 \text{sh}^2 - \eta^2 \text{s}^2}, \tag{29e}$$

$$k_{36} = k_{63} = \frac{2EI \cdot \alpha \cdot \beta\,(\eta \cdot \text{s} \cdot \text{ch} - \phi \cdot \text{c} \cdot \text{sh})}{\phi^2 \text{sh}^2 - \eta^2 \text{s}^2}. \tag{29f}$$

The stiffness matrix presented in Eq. (28) is defined as the analytical stiffness matrix for the Timoshenko beam on elastic Winkler foundation element, and it is the same as the one used in the TFEM (Aköz and Aksoydan, 2005).

3.2. Fixed response

The governing BVP for the fixed problem of the Timoshenko beam on elastic Winkler foundation element is:

$$\frac{\mathrm{d}^4 v_f}{\mathrm{d}x^4}(x) - \frac{k}{A_s G}\frac{\mathrm{d}^2 v_f}{\mathrm{d}x^2}(x) + \frac{k}{EI} v_f(x) = \frac{1}{EI} q_v(x) - \frac{1}{A_s G}\frac{\mathrm{d}^2 q_v}{\mathrm{d}x^2}(x) - \frac{1}{EI}\frac{\mathrm{d}q_\theta}{\mathrm{d}x}(x), \tag{30a}$$

$$v_f(0) = 0, \tag{30b}$$

$$\theta_f(0) = 0, \tag{30c}$$

$$v_f(L) = 0, \tag{30d}$$

$$\theta_f(L) = 0. \tag{30e}$$

To solve the BVP (30), the fixed response is decomposed into two distinct components: one generated by the external distributed transverse load $q_v(x)$ (see Fig. 5(a) for its physical interpretation), and another resulting from the external distributed bending moments $q_\theta(x)$ (see Fig. 5(b) for its physical interpretation). Consequently, the fixed transverse displacement, cross-section rotation, and internal force fields can be expressed as follows:

$$v_f(x) = v_f^v(x) + v_f^\theta(x), \tag{31a}$$

$$\theta_f(x) = \theta_f^v(x) + \theta_f^\theta(x), \tag{31b}$$

$$V_f(x) = V_f^v(x) + V_f^\theta(x), \tag{31c}$$

$$M_f(x) = M_f^v(x) + M_f^\theta(x), \tag{31d}$$

where superscript v corresponds to the response generated by the external distributed transverse load $q_v(x)$, while the superscript θ pertains to the response generated by the external distributed bending moments $q_\theta(x)$.

In Sections 3.2.1 and 3.2.2 the solutions to the fixed problems generated by $q_v(x)$ and $q_\theta(x)$ are presented, respectively.

3.2.1. Fixed response due to $q_v(x)$

Applying a method similar to that presented in Molina-Villegas and Ballesteros Ortega (2023b), the fixed transverse displacement $v_f^v(x)$ and the cross-section rotation $\theta_f^v(x)$ fields are computed as follows:

$$v_f^v(x) = \int_0^x G_{yy}^{II}(x,\xi) q_v(\xi)\mathrm{d}\xi + \int_x^L G_{yy}^{I}(x,\xi) q_v(\xi)\mathrm{d}\xi, \tag{32a}$$

$$\theta_f^v(x) = \int_0^x G_{\theta y}^{II}(x,\xi) q_v(\xi)\mathrm{d}\xi + \int_x^L G_{\theta y}^{I}(x,\xi) q_v(\xi)\mathrm{d}\xi, \tag{32b}$$

where $G_{yy}(x,\xi)$ represents the transverse displacement GF for the element studied in this Section, describing the transverse displacement field when the element is subjected to a unit point transverse external load at ξ (see Fig. 6). Its governing BVP can be obtained from Eqs. (30) replacing $v_f(x)$ by $G_{yy}(x,\xi)$, $\theta_f(x)$ by the cross-section rotation GF $G_{\theta y}(x,\xi)$, $q_v(x)$ by $\delta(x-\xi)$, and q_θ by 0, where $\delta(\cdot)$ is the Dirac delta function, being possible to express $G_{\theta y}(x,\xi)$ in terms of $G_{yy}(x,\xi)$ using an adaptation of Eq. (5).

Using the idea that each segment of $G_{yy}(x,\xi)$ has no external load, i.e., they are solutions of the homogeneous Differential Equation (DE) (8a), both segments can be expressed as linear combinations of the transverse displacement shape functions as follows:

$$G_{yy}^{I}(x,\xi) = C_1(\xi)\psi_2^v(x) + C_2(\xi)\psi_3^v(x) + C_3(\xi)\psi_5^v(x) + C_4(\xi)\psi_6^v(x), \tag{33a}$$

$$G_{yy}^{II}(x,\xi) = C_5(\xi)\psi_2^v(x) + C_6(\xi)\psi_3^v(x) + C_7(\xi)\psi_5^v(x) + C_8(\xi)\psi_6^v(x). \tag{33b}$$

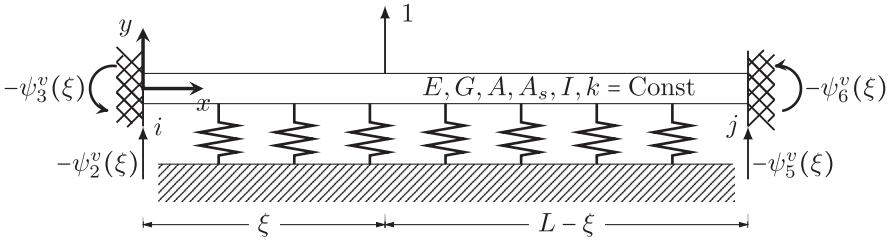

Fig. 6. Fixed Timoshenko beam on elastic Winkler foundation subjected to a unit point transverse external load whose transverse displacement, cross-section rotation, shear force and bending moment fields are $G_{yy}(x,\xi)$, $G_{\theta y}(x,\xi)$, $G_{Vy}(x,\xi)$ and $G_{My}(x,\xi)$, respectively.

To satisfy the fixed BCs at $x = 0$ and $x = L$, the functions $C_1(\xi)$, $C_2(\xi)$, $C_7(\xi)$, and $C_8(\xi)$ are equal to zero, allowing both segments of $G_{yy}(x,\xi)$ to be expressed as:

$$G_{yy}^{I}(x,\xi) = C_3(\xi)\psi_5^v(x) + C_4(\xi)\psi_6^v(x), \tag{34a}$$

$$G_{yy}^{II}(x,\xi) = C_5(\xi)\psi_2^v(x) + C_6(\xi)\psi_3^v(x). \tag{34b}$$

Assuring the compatibility and equilibrium conditions at $x = \xi$, $G_{yy}^{I}(x,\xi)$ and $G_{yy}^{II}(x,\xi)$ can be expressed as:

$$G_{yy}(x,\xi) = \begin{cases} G_{yy}^{I}(x,\xi) = W_2^v(x)\psi_2^v(\xi) + W_3^v(x)\psi_3^v(\xi),\ 0 < x \le \xi, \\ G_{yy}^{II}(x,\xi) = W_5^v(x)\psi_5^v(\xi) + W_6^v(x)\psi_6^v(\xi),\ \xi \le x < L, \end{cases} \tag{35}$$

where the symmetry properties $G_{yy}^{I}(x,\xi) = G_{yy}^{II}(\xi,x)$ and $G_{yy}^{II}(x,\xi) = G_{yy}^{I}(\xi,x)$ were employed. Additionally, for mnemonic reasons, the functions $C_3(x)$, $C_4(x)$, $C_5(x)$, and $C_6(x)$ have been redefined as $W_5^v(x)$, $W_6^v(x)$, $W_2^v(x)$, and $W_3^v(x)$, respectively. These functions are given by the following expressions:

$$W_2^v(x) = \frac{-\eta\cosh(\alpha x)\sin(\beta x) + \phi\sinh(\alpha x)\cos(\beta x)}{2EI\cdot\alpha\cdot\beta\left(\alpha^2+\beta^2\right)}, \tag{36a}$$

$$W_3^v(x) = \frac{\sinh(\alpha x)\sin(\beta x)}{2EI\cdot\alpha\cdot\beta}, \tag{36b}$$

$$W_5^v(x) = \frac{-\eta\cosh[\alpha(L-x)]\sin[\beta(L-x)] + \phi\sinh[\alpha(L-x)]\cos[\beta(L-x)]}{2EI\cdot\alpha\cdot\beta\left(\alpha^2+\beta^2\right)}, \tag{36c}$$

$$W_6^v(x) = -\frac{\sinh[\alpha(L-x)]\sin[\beta(L-x)]}{2EI\cdot\alpha\cdot\beta}. \tag{36d}$$

The cross-section rotation GF $G_{\theta y}(x,\xi)$ is expressed as follows:

$$G_{\theta y}(x,\xi) = \begin{cases} G_{\theta y}^{I}(x,\xi) = W_2^\theta(x)\psi_2^v(\xi) + W_3^\theta(x)\psi_3^v(\xi),\ 0 < x \le \xi, \\ G_{\theta y}^{II}(x,\xi) = W_5^\theta(x)\psi_5^v(\xi) + W_6^\theta(x)\psi_6^v(\xi),\ \xi \le x < L, \end{cases} \tag{37}$$

where

$$W_2^\theta(x) = -\frac{\sinh(\alpha x)\sin(\beta x)}{2EI\cdot\alpha\cdot\beta} = -W_3^v(x), \tag{38a}$$

$$W_3^\theta(x) = \frac{\eta\cosh(\alpha x)\sin(\beta x) + \phi\sinh(\alpha x)\cos(\beta x)}{2EI\cdot\alpha\cdot\beta}, \tag{38b}$$

$$W_5^\theta(x) = \frac{\sinh[\alpha(L-x)]\sin[\beta(L-x)]}{2EI\cdot\alpha\cdot\beta} = -W_6^v(x), \tag{38c}$$

$$W_6^\theta(x) = \frac{\eta\cosh[\alpha(L-x)]\sin[\beta(L-x)] + \phi\sinh[\alpha(L-x)]\cos[\beta(L-x)]}{2EI\cdot\alpha\cdot\beta}. \tag{38d}$$

Furthermore, using Eqs. (1), the fixed internal force fields generated by $q_v(x)$ can be derived from the fixed transverse displacement and cross-section rotation fields given in Eqs. (32a) and (32b), respectively, yielding:

$$V_f^v(x) = \int_0^x G_{Vy}^{II}(x,\xi)q_v(\xi)\mathrm{d}\xi + \int_x^L G_{Vy}^{I}(x,\xi)q_v(\xi)\mathrm{d}\xi, \tag{39a}$$

$$M_f^v(x) = \int_0^x G_{My}^{II}(x,\xi)q_v(\xi)\mathrm{d}\xi + \int_x^L G_{My}^{I}(x,\xi)q_v(\xi)\mathrm{d}\xi, \tag{39b}$$

being the functions $G_{Vy}(x,\xi)$ and $G_{My}(x,\xi)$ the shear force and bending moment GFs associated with the element depicted in Fig. 6. These functions represent the internal force fields of a fixed Timoshenko beam on elastic Winkler foundation when it is subjected to a unit point transverse external load at ξ, and can be obtained from the following adaptation of Eqs. (1):

$$G_{Vy}(x,\xi) = A_s G\left[\frac{\partial G_{yy}}{\partial y}(x,\xi) - G_{\theta y}(x,\xi)\right], \tag{40a}$$

$$G_{My}(x,\xi) = EI\frac{\partial G_{y\theta}}{\partial x}(x,\xi). \tag{40b}$$

These GFs are given by the following expressions:

$$G_{Vy}(x,\xi)=\begin{cases} G^{I}_{Vy}(x,\xi)=W^{V}_{2}(x)\psi^{v}_{2}(\xi)+W^{V}_{3}(x)\psi^{v}_{3}(\xi),\ 0<x<\xi,\\ G^{II}_{Vy}(x,\xi)=W^{V}_{5}(x)\psi^{v}_{5}(\xi)+W^{V}_{6}(x)\psi^{v}_{6}(\xi),\ \xi<x<L,\end{cases} \tag{41a}$$

$$G_{My}(x,\xi)=\begin{cases} G^{I}_{My}(x,\xi)=W^{M}_{2}(x)\psi^{v}_{2}(\xi)+W^{M}_{3}(x)\psi^{v}_{3}(\xi),\ 0<x\le\xi,\\ G^{II}_{My}(x,\xi)=W^{M}_{5}(x)\psi^{v}_{5}(\xi)+W^{M}_{6}(x)\psi^{v}_{6}(\xi),\ \xi\le x<L,\end{cases} \tag{41b}$$

where

$$W^{V}_{2}(x)=\frac{(\alpha\cdot\phi-\beta\cdot\eta)\cosh(\alpha x)\cos(\beta x)+[\alpha(\alpha-\eta)+\ \beta(\beta-\phi)]\sinh(\alpha x)\sin(\beta x)}{\alpha\cdot\phi-\beta\cdot\eta}, \tag{42a}$$

$$W^{V}_{3}(x)=\frac{\left(\eta^{2}+\phi^{2}\right)[(\alpha-\eta)\cosh(\alpha x)\sin(\beta x)+(\beta-\phi)\sinh(\alpha x)\cos(\beta x)]}{\alpha\cdot\phi-\beta\cdot\eta}, \tag{42b}$$

$$W^{V}_{5}(x)=-\frac{(\alpha\cdot\phi-\beta\cdot\eta)\cosh[\alpha(L-x)]\cos[\beta(L-x)]+[\alpha(\alpha-\eta)+\beta(\beta-\phi)]\sinh[\alpha(L-x)]\sin[\beta(L-x)]}{\alpha\cdot\phi-\beta\cdot\eta}, \tag{42c}$$

$$W^{V}_{6}(x)=\frac{\left(\eta^{2}+\phi^{2}\right)\{(\alpha-\eta)\cosh[\alpha(L-x)]\sin[\beta(L-x)]+(\beta-\phi)\sinh[\alpha(L-x)]\cos[\beta(L-x)]\}}{\alpha\cdot\phi-\beta\cdot\eta}, \tag{42d}$$

$$W^{M}_{2}(x)=-\frac{\alpha\cosh(\alpha x)\sin(\beta x)+\beta\sinh(\alpha x)\cos(\beta x)}{2\alpha\cdot\beta}, \tag{43a}$$

$$W^{M}_{3}(x)=\frac{(\alpha\cdot\phi+\beta\cdot\eta)\cosh(\alpha x)\cos(\beta x)+\ (\alpha\cdot\eta-\beta\cdot\phi)\sinh(\alpha x)\sin(\beta x)}{2\alpha\cdot\beta}, \tag{43b}$$

$$W^{M}_{5}(x)=-\frac{\alpha\cosh[\alpha(L-x)]\sin[\beta(L-x)]+\beta\sinh[\alpha(L-x)]\cos[\beta(L-x)]}{2\alpha\cdot\beta}, \tag{43c}$$

$$W^{M}_{6}(x)=\frac{-(\alpha\cdot\phi+\beta\cdot\eta)\cosh[\alpha(L-x)]\cos[\beta(L-x)]+(\beta\cdot\phi-\alpha\cdot\eta)\sinh[\alpha\ (L-x)]\sin[\beta(L-x)]}{2\alpha\cdot\beta}. \tag{43d}$$

By evaluating the fixed internal force fields presented in Eqs. (39) at $x=0$ and $x=L$, the fixed-end forces generated by $q_v(x)$ are obtained (see these forces in Fig. 5(a)):

$$\begin{Bmatrix} FY^{vf}_{i}\\ M^{vf}_{i}\\ FY^{vf}_{j}\\ M^{vf}_{j}\end{Bmatrix}=\begin{Bmatrix} -V^{v}_{f}(0)\\ -M^{v}_{f}(0)\\ V^{v}_{f}(L)\\ M^{v}_{f}(L)\end{Bmatrix}=-\begin{Bmatrix} \int_{0}^{L}\psi^{v}_{2}(x)q_{v}(x)\mathrm{d}x\\ \int_{0}^{L}\psi^{v}_{3}(x)q_{v}(x)\mathrm{d}x\\ \int_{0}^{L}\psi^{v}_{5}(x)q_{v}(x)\mathrm{d}x\\ \int_{0}^{L}\psi^{v}_{6}(x)q_{v}(x)\mathrm{d}x\end{Bmatrix}. \tag{44}$$

The fixed-end forces in Eq. (44) correspond to the those employed in the TFEM and conform to the general form used in the FEM (Reddy, 2019). These forces can be understood by considering that the reactions of a fixed beam subjected to a unit point load at position x (for ease of discussion, ξ has been replaced by x) are the negative of the displacement shape functions $\psi^{v}_{n}(x)$ (see Fig. 6). The expression $-\psi^{v}_{n}(x)q_{v}(x)\mathrm{d}x$ represents the reactions produced by the differential load $q_v(x)\mathrm{d}x$ located at x, while $-\int_0^L\psi^{v}_{n}(x)q_{v}(x)\mathrm{d}x$ represents the superposition of reactions generated by all external transverse loads from $x=0$ to $x=L$.

3.2.2. Fixed response due to $q_\theta(x)$

Using a strategy similar to the one used in Section 3.2.1, the fixed transverse displacement, cross-section rotation, shear force, and bending moment fields generated by the external distributed bending moments $q_\theta(x)$ are computed as follows, respectively:

$$v^{\theta}_{f}(x)=\int_{0}^{x}G^{II}_{y\theta}(x,\xi)q_{\theta}(\xi)\mathrm{d}\xi+\int_{x}^{L}G^{I}_{y\theta}(x,\xi)q_{\theta}(\xi)\mathrm{d}\xi, \tag{45a}$$

$$\theta^{\theta}_{f}(x)=\int_{0}^{x}G^{II}_{\theta\theta}(x,\xi)q_{\theta}(\xi)\mathrm{d}\xi+\int_{x}^{L}G^{I}_{\theta\theta}(x,\xi)q_{\theta}(\xi)\mathrm{d}\xi, \tag{45b}$$

$$V^{\theta}_{f}(x)=\int_{0}^{x}G^{II}_{V\theta}(x,\xi)q_{\theta}(\xi)\mathrm{d}\xi+\int_{x}^{L}G^{I}_{V\theta}(x,\xi)q_{\theta}(\xi)\mathrm{d}\xi, \tag{45c}$$

$$M^{\theta}_{f}(x)=\int_{0}^{x}G^{II}_{M\theta}(x,\xi)q_{\theta}(\xi)\mathrm{d}\xi+\int_{x}^{L}G^{I}_{M\theta}(x,\xi)q_{\theta}(\xi)\mathrm{d}\xi, \tag{45d}$$

where $G_{y\theta}(x,\xi)$, $G_{\theta\theta}(x,\xi)$, $G_{V\theta}(x,\xi)$, and $G_{M\theta}(x,\xi)$ represent the transverse displacement, cross-section rotation, shear force, and bending moment GFs, respectively, for the element studied in this Section when it is subjected to a unit point external bending moment at ξ (see Fig. 7). These GFs are given by the following expressions :

$$G_{y\theta}(x,\xi)=\begin{cases} G^{I}_{y\theta}(x,\xi)=W^{v}_{2}(x)\psi^{\theta}_{2}(\xi)+W^{v}_{3}(x)\psi^{\theta}_{3}(\xi),\ 0<x\le\xi,\\ G^{II}_{y\theta}(x,\xi)=W^{v}_{5}(x)\psi^{\theta}_{5}(\xi)+W^{v}_{6}(x)\psi^{\theta}_{6}(\xi),\ \xi\le x<L,\end{cases} \tag{46a}$$

$$G_{\theta\theta}(x,\xi)=\begin{cases} G^{I}_{\theta\theta}(x,\xi)=W^{\theta}_{2}(x)\psi^{\theta}_{2}(\xi)+W^{\theta}_{3}(x)\psi^{\theta}_{3}(\xi),\ 0<x\le\xi,\\ G^{II}_{\theta\theta}(x,\xi)=W^{\theta}_{5}(x)\psi^{\theta}_{5}(\xi)+W^{\theta}_{6}(x)\psi^{\theta}_{6}(\xi),\ \xi\le x<L,\end{cases} \tag{46b}$$

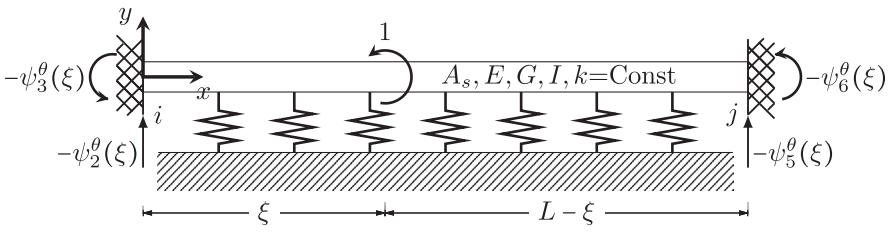

Fig. 7. Fixed Timoshenko beam on elastic Winkler foundation subjected to a unit point external bending moment whose transverse displacement, cross-section rotation, shear force and bending moment fields are $G_{y\theta}(x,\xi)$, $G_{\theta\theta}(x,\xi)$, $G_{V\theta}(x,\xi)$ and $G_{M\theta}(x,\xi)$, respectively.

$$G_{V\theta}(x,\xi)=\begin{cases} G_{V\theta}^{I}(x,\xi)=W_2^V(x)\psi_2^\theta(\xi)+W_3^V(x)\psi_3^\theta(\xi),\ 0<x\le\xi, \\ G_{V\theta}^{II}(x,\xi)=W_5^V(x)\psi_5^\theta(\xi)+W_6^V(x)\psi_6^\theta(\xi),\ \xi\le x<L, \end{cases} \tag{46c}$$

$$G_{M\theta}(x,\xi)=\begin{cases} G_{M\theta}^{I}(x,\xi)=W_2^M(x)\psi_2^\theta(\xi)+W_3^M(x)\psi_3^\theta(\xi),\ 0<x<\xi, \\ G_{M\theta}^{II}(x,\xi)=W_5^M(x)\psi_5^\theta(\xi)+W_6^M(x)\psi_6^\theta(\xi),\ \xi<x<L. \end{cases} \tag{46d}$$

By comparing the GFs of the fixed element subjected to a unit point transverse external load (Eqs. (35), (37), and (41)) with those generated by a unit point external bending moment (Eqs. (46)), it becomes evident that the latter can be derived from the former by substituting the shape functions $\psi_n^v(\xi)$ with $\psi_n^\theta(\xi)$.

Implementing the same technique described in Section 3.2.1, the fixed-end forces generated by $q_\theta(x)$ (see these forces in Fig. 5(b)) are computed:

$$\begin{Bmatrix} FY_i^{\theta f} \\ M_i^{\theta f} \\ FY_j^{\theta f} \\ M_j^{\theta f} \end{Bmatrix} = \begin{Bmatrix} -V_f^\theta(0) \\ -M_f^\theta(0) \\ V_f^\theta(L) \\ M_f^\theta(L) \end{Bmatrix} = -\begin{Bmatrix} \int_0^L \psi_2^\theta(x)q_\theta(x)\mathrm{d}x \\ \int_0^L \psi_3^\theta(x)q_\theta(x)\mathrm{d}x \\ \int_0^L \psi_5^\theta(x)q_\theta(x)\mathrm{d}x \\ \int_0^L \psi_6^\theta(x)q_\theta(x)\mathrm{d}x \end{Bmatrix}. \tag{47}$$

4. Formulation of the GFSM for the rod element

The GFSM formulation for the rod element was previously presented in Molina-Villegas and Ballesteros Ortega (2023c). However, to keep the paper self-contained, this section summarizes that part of the study.

For the rod element, the axial force field is computed using the following formula:

$$P(x)=EA\frac{\mathrm{d}u}{\mathrm{d}x}(x), \tag{48}$$

where $u(x)$ is the axial displacement field, positive in the x-axis direction.

The equilibrium DE associated with the rod element is:

$$\frac{\mathrm{d}P}{\mathrm{d}x}(x)=-p(x). \tag{49}$$

The axial displacement and axial force fields are decomposed into their homogeneous and fixed solutions, as follows:

$$u(x)=u_h(x)+u_f(x), \tag{50a}$$

$$P(x)=P_h(x)+P_f(x). \tag{50b}$$

4.1. Homogeneous response

The homogeneous axial displacement and axial force fields are computed as:

$$u_h(x)=\psi_1^u(x)u_i+\psi_4^u(x)u_j, \tag{51a}$$

$$P_h(x)=\psi_1^P(x)u_i+\psi_4^P(x)u_j, \tag{51b}$$

where

$$\psi_1^u(x)=1-\frac{x}{L}, \tag{52a}$$

$$\psi_4^u(x)=\frac{x}{L}, \tag{52b}$$

$$-\psi_1^P(x)=\psi_4^P(x)=\frac{EA}{L}, \tag{53}$$

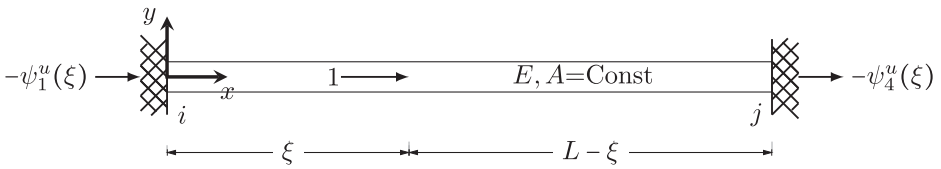

Fig. 8. Fixed rod subjected to a unit point axial external load whose axial displacement and axial force fields are $G_{xx}(x,\xi)$ and $G_{Px}(x,\xi)$, respectively.

being the functions $\psi_m^u(x)$ and $\psi_m^P(x)$ $(m=1,4)$ defined as the analytical axial displacement and analytical axial force shape functions, respectively.

By evaluating the homogeneous axial force field (51b) at $x=0$ and $x=L$, the relation for the rod element that relates its homogeneous generalized forces to its generalized displacements at the element ends is obtained:

$$\begin{Bmatrix} FX_i^h \\ FX_j^h \end{Bmatrix} = \begin{Bmatrix} -P_h(0) \\ P_h(L) \end{Bmatrix} = \begin{bmatrix} k_{11} & k_{14} \\ k_{41} & k_{44} \end{bmatrix} \begin{Bmatrix} u_i \\ u_j \end{Bmatrix}, \tag{54}$$

where

$$k_{11} = k_{44} = -k_{14} = -k_{41} = \frac{EA}{L}, \tag{55}$$

being the matrix presented in Eq. (54) defined as the analytical stiffness matrix for the rod element.

4.2. Fixed response

The fixed axial displacement and axial force fields are computed as follows:

$$u_f(x) = \int_0^x G_{xx}^{II}(x,\xi)p(\xi)\mathrm{d}\xi + \int_x^L G_{xx}^{I}(x,\xi)p(\xi)\mathrm{d}\xi, \tag{56a}$$

$$P_f(x) = \int_0^x G_{Px}^{II}(x,\xi)p(\xi)\mathrm{d}\xi + \int_x^L G_{Px}^{I}(x,\xi)p(\xi)\mathrm{d}\xi, \tag{56b}$$

where $G_{xx}(x,\xi)$ and $G_{Px}(x,\xi)$ represent the axial displacement and axial force GFs, respectively, for the element studied in this Section when it is fixed and subjected to a unit point axial external load (see Fig. 8). These GFs are given by the following expressions:

$$G_{xx}(x,\xi) = \begin{cases} G_{xx}^{I}(x,\xi) = W_1^u(x)\psi_1^u(\xi),\ 0 < x \le \xi, \\ G_{xx}^{II}(x,\xi) = W_4^u(x)\psi_4^u(\xi),\ \xi \le x < L, \end{cases} \tag{57a}$$

$$G_{Px}(x,\xi) = \begin{cases} G_{Px}^{I}(x,\xi) = W_1^P(x)\psi_1^u(\xi),\ 0 < x < \xi, \\ G_{Px}^{II}(x,\xi) = W_4^P(x)\psi_4^u(\xi),\ \xi < x < L, \end{cases} \tag{57b}$$

where

$$W_1^u(x) = \frac{x}{EA}, \tag{58a}$$

$$W_4^u(x) = \frac{L-x}{EA}, \tag{58b}$$

$$W_1^P(x) = -W_4^P(x) = 1. \tag{59}$$

By evaluating the fixed axial force field in Eq. (56b) at $x=0$ and $x=L$, the fixed-end forces generated by $p(x)$ are obtained:

$$\begin{Bmatrix} FX_i^f \\ FX_j^f \end{Bmatrix} = \begin{Bmatrix} -P_f(0) \\ P_f(L) \end{Bmatrix} = -\begin{Bmatrix} \int_0^L \psi_1^u(x)p(x)\mathrm{d}x \\ \int_0^L \psi_4^u(x)p(x)\mathrm{d}x \end{Bmatrix}. \tag{60}$$

5. Formulation of the GFSM for the timoshenko frame on elastic Winkler foundation element

The GFSM formulation for the Timoshenko frame on elastic Winkler foundation element, depicted in Fig. 1, is derived by superposing the formulations of the Timoshenko beam on elastic Winkler foundation element (Section 3) and the rod element (Section 4). As a result, the analytical relation for the frame element that relates its generalized forces to its generalized displacements at the element ends is obtained (see these generalized forces in Fig. 1):

$$\begin{Bmatrix} FX_i \\ FY_i \\ M_i \\ FX_j \\ FY_j \\ M_j \end{Bmatrix} = \begin{Bmatrix} FX_i^h + FX_i^f \\ FY_i^h + FY_i^f \\ M_i^h + M_i^f \\ FX_j^h + FX_j^f \\ FY_j^h + FY_j^f \\ M_j^h + M_j^f \end{Bmatrix} = \begin{bmatrix} k_{11} & 0 & 0 & k_{14} & 0 & 0 \\ 0 & k_{22} & k_{23} & 0 & k_{25} & k_{26} \\ 0 & k_{32} & k_{33} & 0 & k_{35} & k_{36} \\ k_{41} & 0 & 0 & k_{44} & 0 & 0 \\ 0 & k_{52} & k_{53} & 0 & k_{55} & k_{56} \\ 0 & k_{62} & k_{63} & 0 & k_{65} & k_{66} \end{bmatrix} \begin{Bmatrix} u_i \\ v_i \\ \theta_i \\ u_j \\ v_j \\ \theta_j \end{Bmatrix} + \begin{Bmatrix} FX_i^f \\ FY_i^f \\ M_i^f \\ FX_j^f \\ FY_j^f \\ M_j^f \end{Bmatrix}, \tag{61}$$

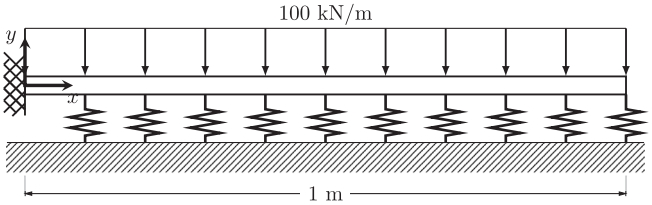

Fig. 9. Single-span Timoshenko beam on elastic Winkler foundation.

where

$$\begin{Bmatrix} FY_i^f \\ M_i^f \\ FY_j^f \\ M_j^f \end{Bmatrix} = \begin{Bmatrix} FY_i^{vf} + FY_i^{\theta f} \\ M_i^{vf} + M_i^{\theta f} \\ FY_j^{vf} + FY_j^{\theta f} \\ M_j^{vf} + M_j^{\theta f} \end{Bmatrix}. \tag{62}$$

The total response of the element is obtained by adding the homogeneous and fixed solutions, as follows:

$$v(x) = \psi_2^v(x)v_i + \psi_3^v(x)\theta_i + \psi_5^v(x)v_j + \psi_6^v(x)\theta_j + \int_0^x \left[G_{yy}^{II}(x,\xi)q_v(\xi) + G_{y\theta}^{II}(x,\xi)q_\theta(\xi)\right]\mathrm{d}\xi + \int_x^L \left[G_{yy}^{I}(x,\xi)q_v(\xi) + G_{y\theta}^{I}(x,\xi)q_\theta(\xi)\right]\mathrm{d}\xi, \tag{63a}$$

$$\theta(x) = \psi_2^\theta(x)v_i + \psi_3^\theta(x)\theta_i + \psi_5^\theta(x)v_j + \psi_6^\theta(x)\theta_j + \int_0^x \left[G_{\theta y}^{II}(x,\xi)q_v(\xi) + G_{\theta\theta}^{II}(x,\xi)q_\theta(\xi)\right]\mathrm{d}\xi + \int_x^L \left[G_{\theta y}^{I}(x,\xi)q_v(\xi) + G_{\theta\theta}^{I}(x,\xi)q_\theta(\xi)\right]\mathrm{d}\xi, \tag{63b}$$

$$u(x) = \psi_1^u(x)u_i + \psi_4^u(x)u_j + \int_0^x G_{xx}^{II}(x,\xi)p(\xi)\mathrm{d}\xi + \int_x^L G_{xx}^{I}(x,\xi)p(\xi)\mathrm{d}\xi, \tag{63c}$$

$$V(x) = \psi_2^V(x)v_i + \psi_3^V(x)\theta_i + \psi_5^V(x)v_j + \psi_6^V(x)\theta_j + \int_0^x \left[G_{Vy}^{II}(x,\xi)q_v(\xi) + G_{V\theta}^{II}(x,\xi)q_\theta(\xi)\right]\mathrm{d}\xi + \int_x^L \left[G_{Vy}^{I}(x,\xi)q_v(\xi) + G_{V\theta}^{I}(x,\xi)q_\theta(\xi)\right]\mathrm{d}\xi, \tag{63d}$$

$$M(x) = \psi_2^M(x)v_i + \psi_3^M(x)\theta_i + \psi_5^M(x)v_j + \psi_6^M(x)\theta_j + \int_0^x \left[G_{My}^{II}(x,\xi)q_v(\xi) + G_{M\theta}^{II}(x,\xi)q_\theta(\xi)\right]\mathrm{d}\xi + \int_x^L \left[G_{My}^{I}(x,\xi)q_v(\xi) + G_{M\theta}^{I}(x,\xi)q_\theta(\xi)\right]\mathrm{d}\xi, \tag{63e}$$

$$P(x) = \psi_1^P(x)u_i + \psi_4^P(x)u_j + \int_0^x G_{Px}^{II}(x,\xi)p(\xi)\mathrm{d}\xi + \int_x^L G_{Px}^{I}(x,\xi)p(\xi)\mathrm{d}\xi, \tag{63f}$$

and the distributed load exerted by the soil on the element can be computed using Eq. (63a) along with Eq. (3).

From Eqs. (61) and (63) is evident that in a FEM formulation employing analytical stiffness matrices and analytical shape functions, as in the TFEM, the GFSM can be utilized to "fix" the results with an additional post-processing step by adding the fixed fields for each element during the analysis.

It is also important to mention that Eqs. (63a) to (63f) could alternatively be computed using the BEM. The key difference between the two approaches lies in the use of GFs for infinite elements in the BEM formulation, which results in a loss of interpretability for each term and a more tenuous relationship with the FEM and the TFEM.

6. Examples

Unless otherwise specified, the units used for solving the examples are kilonewtons (kN) for force and meters (m) for length.

6.1. Example 1

Calculate the response of the single-span Timoshenko beam on elastic Winkler foundation shown in Fig. 9. The beam has a Young's modulus of $E = 15\,000$ MPa, a Poisson's ratio of $\nu = 0.3$, and a rectangular cross-section with a base of 15 cm and a height of 20 cm. The Winkler foundation has a stiffness per unit length of $k = 5000$ kPa.

Preliminary calculations

According to the theory of elasticity (Timoshenko and Goodier, 1951), the shear modulus can be calculated from the Young's modulus as follows:

$$G = \frac{E}{2(1+\nu)} = \frac{75000}{13}\ \text{MPa}, \tag{64}$$

and following Timoshenko (1922), Kaneko (1975), Rosinger and Ritchie (1977) and Kaneko (1978), the shear coefficient for rectangular cross-sections can be determined as:

$$\kappa = \frac{5(1+\nu)}{6+5\nu} = \frac{13}{15}. \tag{65}$$

Computation of unknown degrees of freedom in global coordinates

The equilibrium of the node at the right end of the beam yields the following system of equations:

$$\begin{Bmatrix} FY_j \\ M_j \end{Bmatrix} = \begin{Bmatrix} 0 \\ 0 \end{Bmatrix} = \begin{bmatrix} 17532 & -8238 \\ -8238 & 5554 \end{bmatrix} \begin{Bmatrix} v_j \\ \theta_j \end{Bmatrix} + \begin{Bmatrix} 49.706 \\ -8.272 \end{Bmatrix}, \tag{66}$$

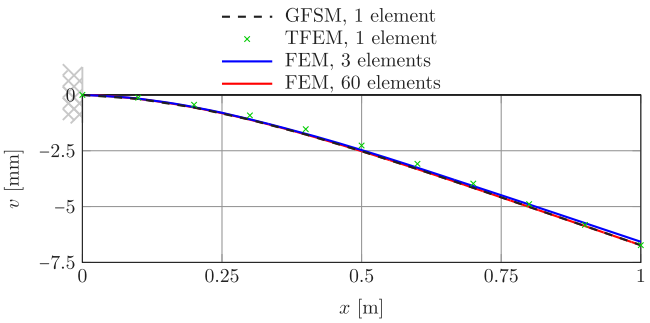

Fig. 10. Deformed shape: Computed using the GFSM with 1 element, the TFEM with 1 element and two FEM discretizations with 3 and 60 elements.

Table 1
Comparison of the computed transverse displacement and cross-section rotation fields using the GFSM with 1 element and the FEM with 60 elements, at points spaced 0.1 m apart.

x (m)	v_{GFSM} (mm)	v_{FEM} (mm)	ε_v (%)	θ_{GFSM} (rad)	θ_{FEM} (rad)	ε_θ (%)
0.1	−0.178	−0.178	2.541×10^{-3}	-2.395×10^{-3}	-2.395×10^{-3}	3.478×10^{-3}
0.2	−0.564	−0.564	3.096×10^{-3}	-4.282×10^{-3}	-4.282×10^{-3}	3.841×10^{-3}
0.3	−1.109	−1.108	3.474×10^{-3}	-5.728×10^{-3}	-5.727×10^{-3}	4.252×10^{-3}
0.4	−1.772	−1.772	3.807×10^{-3}	-6.794×10^{-3}	-6.794×10^{-3}	4.715×10^{-3}
0.5	−2.520	−2.520	4.130×10^{-3}	-7.545×10^{-3}	-7.545×10^{-3}	5.233×10^{-3}
0.6	−3.324	−3.324	4.455×10^{-3}	-8.039×10^{-3}	-8.038×10^{-3}	5.803×10^{-3}
0.7	−4.161	−4.161	4.786×10^{-3}	-8.332×10^{-3}	-8.332×10^{-3}	6.422×10^{-3}
0.8	−5.015	−5.015	5.125×10^{-3}	-8.480×10^{-3}	-8.479×10^{-3}	7.075×10^{-3}
0.9	−5.873	−5.873	5.470×10^{-3}	-8.533×10^{-3}	-8.533×10^{-3}	7.739×10^{-3}
1.0	−6.729	−6.729	5.816×10^{-3}	-8.541×10^{-3}	-8.540×10^{-3}	8.377×10^{-3}

whose solution is the degrees of freedom of the beam:

$$\begin{Bmatrix} v_j \\ \theta_j \end{Bmatrix} = \begin{Bmatrix} -7.04530 \times 10^{-3} \\ -8.96003 \times 10^{-3} \end{Bmatrix}. \tag{67}$$

Computation of joint reactions in global coordinates

The equilibrium of the node at the left end of the beam leads to the determination of the reactions:

$$\begin{Bmatrix} FY_i \\ M_i \end{Bmatrix} = \begin{bmatrix} -15544 & 7907 \\ -7907 & 2488 \end{bmatrix} \begin{Bmatrix} v_j \\ \theta_j \end{Bmatrix} + \begin{Bmatrix} 49.706 \\ 8.272 \end{Bmatrix} = \begin{Bmatrix} 88.369 \\ 41.686 \end{Bmatrix}. \tag{68}$$

Computation of displacement and cross-section rotation fields

By using the computed degrees of freedom (67), along with Eqs. (63a) and (63b), the transverse displacement and cross-section rotation fields are obtained. In Fig. 10, the deformed shape of the structure computed with the 1 element GFSM solution obtained in this example is compared with an own TFEM implementation with 1 element (computed using the TFEM formulation provided in Appendix C), and the FEM software OpenSees (Mazzoni et al., 2006) with 3 and 60 elements.

Table 1 presents the computed transverse displacement and cross-section rotation fields using the GFSM with 1 element and the FEM with 60 elements, at points spaced 0.1 m apart. The subscripts GFSM and FEM of v and θ (as well as for V and M in Table 2) indicate the method used for calculation. The absolute relative error ε_O is calculated as $\varepsilon_O = \left|\left(O_{\text{GFSM}} - O_{\text{FEM}}\right)/O_{\text{FEM}}\right| \cdot 100\%;\ O \in \{v, \theta, V, M\}$. From Fig. 10 and Table 1 it can be concluded that the three methods are in agreement.

Computation of internal force fields

By using the computed degrees of freedom (67), along with Eqs. (63d) and (63e), the shear force and bending moment fields are obtained. In Fig. 11, the internal force fields computed using the GFSM and the two previously mentioned methods are compared. In this instance, the results from the GFSM and the fine FEM mesh exhibit excellent agreement, whereas the coarse FEM mesh does not.

Table 2 shows the internal force fields computed using the GFSM with 1 element and the FEM with 60 elements at points spaced 0.1 m apart. From its results, it can be concluded that the GFSM method is in agreement with the fine FEM mesh.

Source file

From the following link can be downloaded the Python source file used to solve this example: https://figshare.com/s/98f32449e82d0705a2a9, DOI 10.6084/m9.figshare.26789926.

6.2. Example 2

Calculate the response of the two-span Timoshenko beam on elastic Winkler foundation shown in Fig. 12(a). The beam has a Young's modulus $E = 25\,000$ MPa, a Poisson's ratio of $\nu = 0.2$, and a rectangular cross-section with a base of 20 cm and a height of 30 cm. The Winkler foundation has a stiffness per unit length of $k = 6000$ kPa.

Preliminary calculations

The shear modulus can be determined from the Young's modulus as shown below (Timoshenko and Goodier, 1951):

$$G = \frac{E}{2(1+\nu)} = \frac{31\,250}{3}\ \text{MPa}, \tag{69}$$

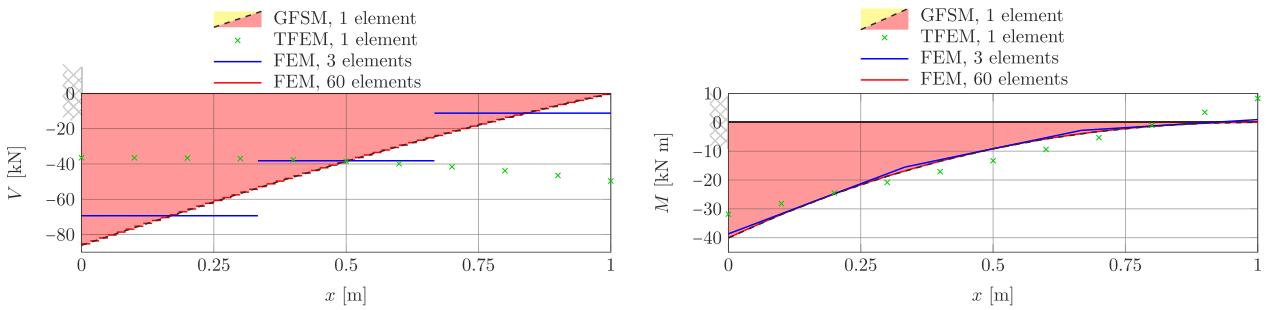

(a) Shear force field. (b) Bending moment field.

Fig. 11. Internal force fields: Computed using the GFSM with 1 elements, the TFEM with 1 elements and two FEM discretizations with 3 and 60 elements.

Table 2
Comparison of the computed internal force fields using the GFSM with 1 element and the FEM with 60 elements, at points spaced 0.1 m apart.

x (m)	V_{GFSM} (kN)	V_{FEM} (kN)	ε_V (%)	M_{GFSM} (kN m)	M_{FEM} (kN m)	ε_M (%)
0.0	−86.093	−85.259	0.978	−40.063	−40.059	0.009
0.1	−76.128	−75.302	1.097	−31.953	−31.949	0.011
0.2	−66.306	−65.496	1.236	−24.833	−24.829	0.014
0.3	−56.718	−55.931	1.407	−18.684	−18.680	0.018
0.4	−47.434	−46.675	1.626	−13.479	−13.476	0.024
0.5	−38.504	−37.776	1.927	−9.185	−9.182	0.034
0.6	−29.963	−29.269	2.372	−5.765	−5.762	0.052
0.7	−21.834	−21.174	3.115	−3.179	−3.176	0.089
0.8	−14.127	−13.503	4.622	−1.384	−1.381	0.194
0.9	−6.849	−6.261	9.399	−0.339	−0.336	0.744
1.0	0	−0.553	100	0	0.002	100

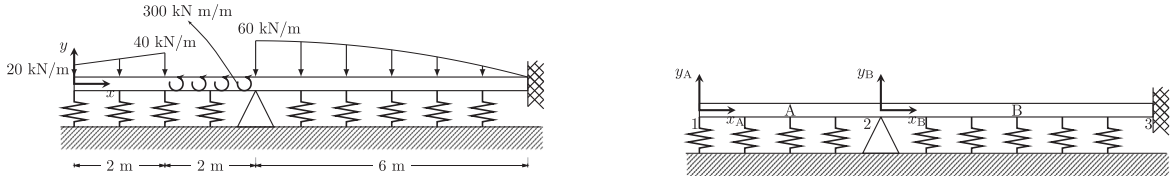

(a) Model. (b) Discretization.

Fig. 12. Model and discretization of a two-span Timoshenko beam on elastic Winkler foundation.

and according to Timoshenko (1922), Kaneko (1975), Rosinger and Ritchie (1977) and Kaneko (1978), the shear coefficient can be determined as follows:

$$\kappa_{\text{A}} = \kappa_{\text{B}} = \frac{5(1+\nu)}{6+5\nu} = \frac{6}{7}. \tag{70}$$

Computation of unknown degrees of freedom in global coordinates

The equilibrium of nodes 1 and 2 yields the following system of equations:

$$\begin{Bmatrix} FY_1 \\ M_1 \\ M_2 \end{Bmatrix} = \begin{Bmatrix} FY_1^{\text{A}} \\ M_1^{\text{A}} \\ M_2^{\text{A}} + M_2^{\text{B}} \end{Bmatrix} = \begin{Bmatrix} 0 \\ 0 \\ 0 \end{Bmatrix} = \begin{bmatrix} 9955 & 8318 & 1942 \\ 8318 & 14051 & 3415 \\ 1942 & 3415 & 27505 \end{bmatrix} \begin{Bmatrix} v_1 \\ \theta_1 \\ v_2 \end{Bmatrix} + \begin{Bmatrix} 147.048 \\ 133.410 \\ -55.599 \end{Bmatrix}, \tag{71}$$

being its solution the degrees of freedom of the beam

$$\begin{Bmatrix} v_1 \\ \theta_1 \\ v_2 \end{Bmatrix} = \begin{Bmatrix} -1.34789 \times 10^{-2} \\ -2.30760 \times 10^{-3} \\ 3.25977 \times 10^{-3} \end{Bmatrix}. \tag{72}$$

Computation of joint reactions in global coordinates

The equilibrium of nodes 2 and 3 leads to the determination of the reactions:

$$\begin{Bmatrix} FY_2 \\ FY_3 \\ M_3 \end{Bmatrix} = \begin{Bmatrix} FY_2^{\text{A}} + FY_2^{\text{B}} \\ FY_3^{\text{B}} \\ M_3^{\text{B}} \end{Bmatrix} = \begin{bmatrix} 138 & -1942 & -217 \\ 0 & 0 & 382 \\ 0 & 0 & 316 \end{bmatrix} \begin{Bmatrix} v_1 \\ \theta_1 \\ v_2 \end{Bmatrix} + \begin{Bmatrix} -80.252 \\ 33.894 \\ -42.421 \end{Bmatrix} = \begin{Bmatrix} -78.341 \\ 35.141 \\ -41.388 \end{Bmatrix}. \tag{73}$$

Computation of displacement and cross-section rotation fields

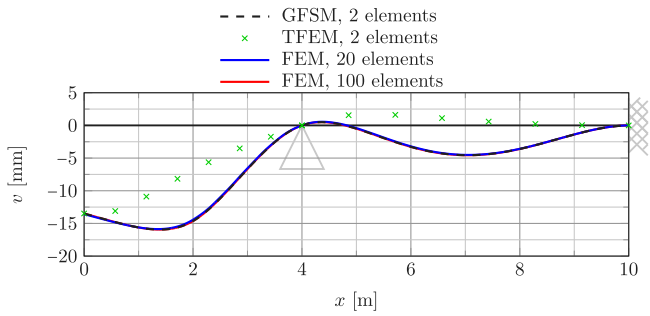

Fig. 13. Deformed shape: Computed using the GFSM with 2 elements, the TFEM with 2 elements and two FEM discretizations with 20 and 100 elements (10 and 50 elements per structural member, respectively).

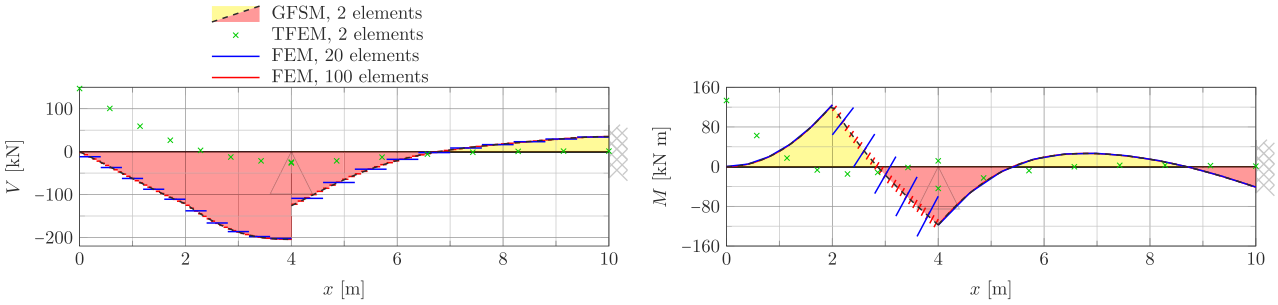

(a) Shear force field. (b) Bending moment field.

Fig. 14. Internal force fields: Computed using the GFSM with 2 elements, the TFEM with 2 elements and two FEM discretizations with 20 and 100 elements (10 and 50 elements per structural member, respectively).

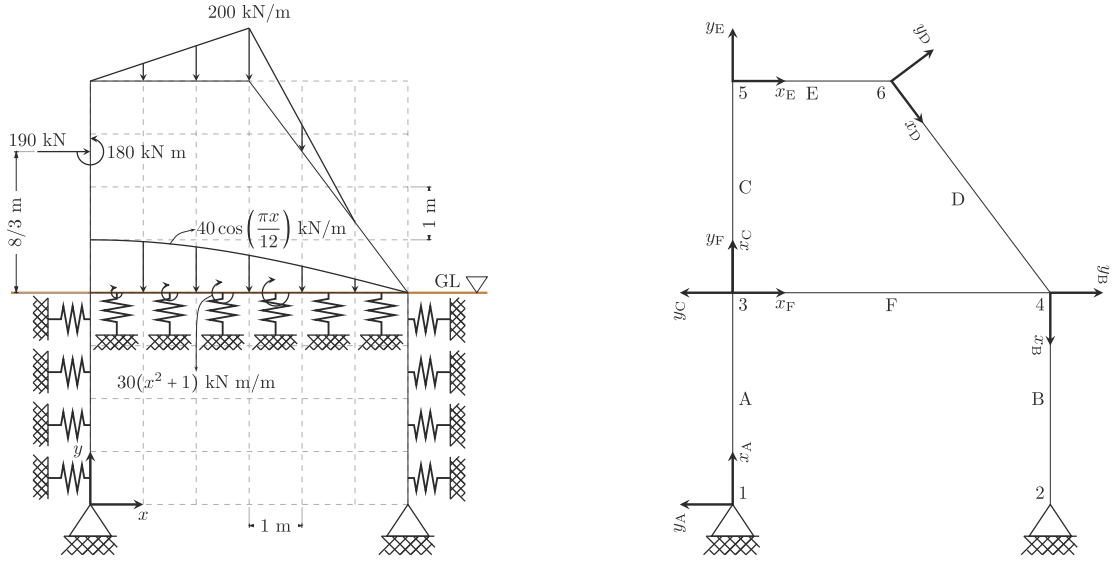

(a) Model. (b) Discretization.

Fig. 15. Model and discretization of a one-bay, one-story Timoshenko plane frame with foundation beam and piles.

The transverse displacement and cross-section rotation fields of elements A and B are obtained using the computed degrees of freedom presented in Eq. (72), along with Eqs. (63a) and (63b). The structure's deformed shape is presented in Fig. 13.

Computation of internal force fields

By using the computed degrees of freedom (72), along with Eqs. (63d) and (63e), the shear force and bending moment fields of elements A and B are obtained. The internal force fields are shown in Fig. 14, from which it can be concluded that the GFSM and the fine FEM mesh agree excellently; however, the coarse mesh does not.

Source file

From the following link can be downloaded the Python source file used to solve this example: https://figshare.com/s/c8a95dc7b5b412bfc954, DOI 10.6084/m9.figshare.26789938.

6.3. Example 3

Compute the response of the Timoshenko plane frame shown in Fig. 15(a), where the Ground Level is defined as GL. All the elements of the structure have a linear elastic material with Young's modulus $E = 20\ 000$ MPa, and Poisson's ratio of $\nu = 0.25$. The pile elements (A and B) are modeled as Timoshenko frames on elastic Winkler foundation elements, have a circular cross-section with a diameter of 60 cm, and a Winkler foundation with stiffness per unit length $k = 7000$ kPa. The element F is a ground beam with a rectangular cross-section, having a base of 40 cm and a height of 50 cm and is modeled as a Timoshenko frame on elastic Winkler foundation, with the Winkler foundation having a stiffness per unit length of $k = 7000$ kPa. Elements C, D, and E are Timoshenko frames with the same cross-section of the element F.

The element F has distributed bending moments from $x = 0$ to $x = 4$ m, defined with the function $30\left(x^2 + 1\right)$ kN m/m (see Fig. 15(a)), with the remaining applied loads presented in the same figure.

Preliminary calculations

The shear modulus can be computed from the Young modulus as follows Timoshenko and Goodier (1951):

$$G = \frac{E}{2(1+\nu)} = 8000 \text{ MPa}, \tag{74}$$

and, the shear coefficients can be determined for the circular and rectangular cross-sections (Timoshenko, 1922; Kaneko, 1975; Rosinger and Ritchie, 1977; Kaneko, 1978), respectively:

$$\kappa_{\mathrm{A}} = \kappa_{\mathrm{B}} = \frac{6 + 12\nu + 6\nu^2}{7 + 12\nu + 4\nu^2} = \frac{75}{82}, \tag{75a}$$

$$\kappa_{\mathrm{C}} = \kappa_{\mathrm{D}} = \kappa_{\mathrm{E}} = \kappa_{\mathrm{F}} = \frac{5(1+\nu)}{6 + 5\nu} = \frac{25}{29}. \tag{75b}$$

Computation of unknown degrees of freedom in global coordinates

The equilibrium of nodes yields the following system of equations:

$$\begin{Bmatrix} 0 \\ 0 \\ 0 \\ 0 \\ 0 \\ 0 \\ 0 \\ 0 \\ 0 \\ 0 \\ 0 \\ 0 \\ 0 \\ 0 \end{Bmatrix} = \begin{Bmatrix} M_1'^{\mathrm{A}} \\ M_2'^{\mathrm{A}} \\ FX_3'^{\mathrm{A}} + FX_3'^{\mathrm{C}} + FX_3'^{\mathrm{F}} \\ FY_3'^{\mathrm{A}} + FY_3'^{\mathrm{C}} + FY_3'^{\mathrm{F}} \\ M_3'^{\mathrm{A}} + M_3'^{\mathrm{C}} + M_3'^{\mathrm{F}} \\ FX_4'^{\mathrm{B}} + FX_4'^{\mathrm{D}} + FX_4'^{\mathrm{F}} \\ FY_4'^{\mathrm{B}} + FY_4'^{\mathrm{D}} + FY_4'^{\mathrm{F}} \\ M_4'^{\mathrm{B}} + M_4'^{\mathrm{D}} + M_4'^{\mathrm{F}} \\ FX_5'^{\mathrm{C}} + FX_5'^{\mathrm{E}} \\ FY_5'^{\mathrm{C}} + FY_5'^{\mathrm{E}} \\ M_5'^{\mathrm{C}} + M_5'^{\mathrm{E}} \\ FX_6'^{\mathrm{D}} + FX_6'^{\mathrm{E}} \\ FY_6'^{\mathrm{D}} + FY_6'^{\mathrm{E}} \\ M_6'^{\mathrm{D}} + M_6'^{\mathrm{E}} \end{Bmatrix}$$

$$= \begin{bmatrix} 127127 & 0 & 42211 & 0 & 56278 & 0 & 0 & 0 & 0 & 0 & 0 & 0 & 0 & 0 \\ 0 & 127127 & 0 & 0 & 0 & 42211 & 0 & 56278 & 0 & 0 & 0 & 0 & 0 & 0 \\ 42211 & 0 & 714592 & 0 & 21373 & -666666 & 0 & 0 & -14947 & 0 & -29895 & 0 & 0 & 0 \\ 0 & 0 & 0 & 2432304 & 24870 & 0 & -422 & 7487 & 0 & -1000000 & 0 & 0 & 0 & 0 \\ 56278 & 0 & 21373 & 24870 & 274444 & 0 & -7487 & 18351 & 29895 & 0 & 38957 & 0 & 0 & 0 \\ 0 & 42211 & -666666 & 0 & 0 & 992620 & -380268 & 35719 & 0 & 0 & 0 & -292975 & 380268 & -15549 \\ 0 & 0 & 0 & -422 & -7487 & -380268 & 1947103 & -36532 & 0 & 0 & 0 & 380268 & -514798 & -11661 \\ 0 & 56278 & 0 & 7487 & 18351 & 35719 & -36532 & 259077 & 0 & 0 & 0 & 15549 & 11661 & 31924 \\ 0 & 0 & -14947 & 0 & 29895 & 0 & 0 & 0 & 1348281 & 0 & 29895 & -1333333 & 0 & 0 \\ 0 & 0 & 0 & -1000000 & 0 & 0 & 0 & 0 & 0 & 1034275 & 51413 & 0 & -34275 & 51413 \\ 0 & 0 & -29895 & 0 & 38957 & 0 & 0 & 0 & 29895 & 51413 & 185522 & 0 & -51413 & 49343 \\ 0 & 0 & 0 & 0 & 0 & -292975 & 380268 & 15549 & -1333333 & 0 & 0 & 1626309 & -380268 & 15549 \\ 0 & 0 & 0 & 0 & 0 & 380268 & -514798 & 11661 & 0 & -34275 & -51413 & -380268 & 549074 & -39752 \\ 0 & 0 & 0 & 0 & 0 & -15549 & -11661 & 31924 & 0 & 51413 & 49343 & 15549 & -39752 & 170156 \end{bmatrix}$$

$$\times \begin{Bmatrix} \theta_1 \\ \theta_2 \\ u_3 \\ v_3 \\ \theta_3 \\ u_4 \\ v_4 \\ \theta_4 \\ u_5 \\ v_5 \\ \theta_5 \\ u_6 \\ v_6 \\ \theta_6 \end{Bmatrix} + \begin{Bmatrix} 0 \\ 0 \\ -107.268 \\ -73.292 \\ 88.897 \\ -5.529 \\ 241.847 \\ -219.169 \\ -82.732 \\ 90.746 \\ -55.456 \\ 5.529 \\ 368.956 \\ -27.161 \end{Bmatrix}, \tag{76}$$

being its solution the unknown degrees of freedom of the structure

$$\begin{Bmatrix} \theta_1 \\ \theta_2 \\ u_3 \\ v_3 \\ \theta_3 \\ u_4 \\ v_4 \\ \theta_4 \\ u_5 \\ v_5 \\ \theta_5 \\ u_6 \\ v_6 \\ \theta_6 \end{Bmatrix} = \begin{Bmatrix} -1.33252 \times 10^{-3} \\ -1.96862 \times 10^{-3} \\ 4.80900 \times 10^{-3} \\ -8.16833 \times 10^{-5} \\ -5.96926 \times 10^{-4} \\ 4.86328 \times 10^{-3} \\ -3.40131 \times 10^{-4} \\ 7.99248 \times 10^{-4} \\ 8.13442 \times 10^{-4} \\ -2.80688 \times 10^{-4} \\ 1.95943 \times 10^{-4} \\ 6.97609 \times 10^{-4} \\ -3.92986 \times 10^{-3} \\ -5.23087 \times 10^{-4} \end{Bmatrix}. \tag{77}$$

Computation of joint reactions in global coordinates

The equilibrium of nodes 1 and 2 leads to the determination of the reactions:

$$\begin{Bmatrix} FX'_1 \\ FY'_1 \\ FX'_2 \\ FY'_2 \end{Bmatrix} = \begin{bmatrix} -51268 & 0 & -19304 & 0 & -42211 & 0 & 0 & 0 \\ 0 & 0 & 0 & -1413716 & 0 & 0 & 0 & 0 \\ 0 & -51268 & 0 & 0 & 0 & -19304 & 0 & -42211 \\ 0 & 0 & 0 & 0 & 0 & 0 & -1413716 & 0 \end{bmatrix} \begin{Bmatrix} \theta_1 \\ \theta_2 \\ u_3 \\ v_3 \\ \theta_3 \\ u_4 \\ v_4 \\ \theta_4 \end{Bmatrix} = \begin{Bmatrix} 0.679 \\ 115.477 \\ -26.691 \\ 480.848 \end{Bmatrix}. \tag{78}$$

Computation of displacements and cross-section rotation fields

By using the computed degrees of freedom in Eq. (77) along with Eqs. (63a), (63b) and (63f), the transverse displacement, cross-section rotation, and axial displacement fields of each element are obtained. The structure's deformed shape with a scale factor of 150 is presented in Fig. 16, from which it is evident that the three methods exhibit agreement, particularly, the GFSM has excellent agreement with the fine FEM mesh.

Computation of internal force fields

By using the computed degrees of freedom presented in Eq. (77) along with Eqs. (63d), (63e) and (63f), the shear force, bending moment, and axial force fields of each element are obtained. The internal force fields are shown in Fig. 17, from which it can be concluded that the GFSM and the fine FEM mesh agree excellently; however, the coarse mesh does not.

Source file

From the following link can be downloaded the Python source file used to solve this example: https://figshare.com/s/f6107de174b5eed8ca99, DOI 10.6084/m9.figshare.25984141.

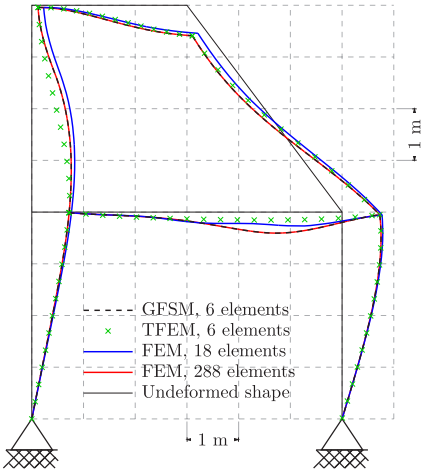

Fig. 16. Deformed shape: Computed using the GFSM with 6 elements, the TFEM with 6 elements and two FEM discretizations with 18 and 48 elements (3 and 48 elements per structural member, respectively). A scale factor of 150 has been used.

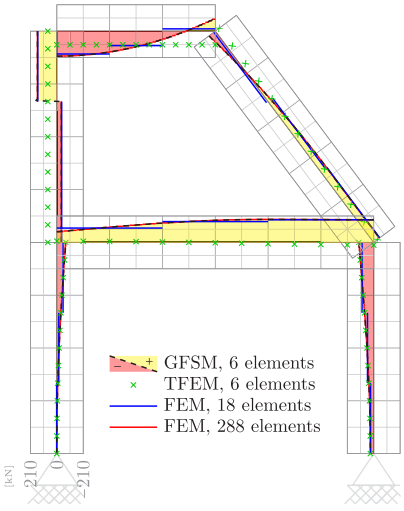

(a) Shear force field.

(b) Bending moment field.

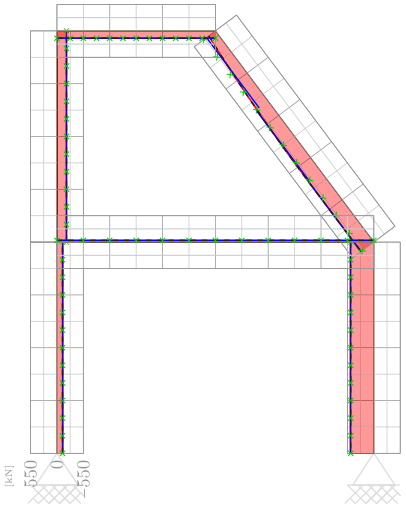

(c) Axial force field.

Fig. 17. Internal force fields: Computed using the GFSM with 6 elements, the TFEM with 6 elements and two FEM discretizations with 18 and 288 elements (3 and 48 elements per structural member, respectively).

7. Conclusions

1. The formulation of the GFSM for the static analysis of Timoshenko beams and frames on elastic Winkler foundation subjected to arbitrary external loads and bending moments, is presented for all three cases of the characteristic equation. This approach enables the calculation of closed-form solutions for any combination of soil and structural parameters.
2. The GFSM is an analytical mesh reduction method for structural analysis that uses only one element per structural member, due to its analytical nature.
3. The GFSM solves the strong formulation of the DE, in contrast to the FEM, which solves the weak formulation. This allows to obtain coherent solutions, helping to avoid common issues such as shear locking (Rakowski, 1990) and discontinuities in the internal force fields which can manifest as sawtooth behavior in FEM, as observed in Figs. 11, 14 and 17.
4. The GFSM idea of decomposing the solution of the problems into homogeneous and fixed (particular) solutions, and solving the latter with GFs, can be readily extended to other linear physical problems such as fluid mechanics, quantum field theory, aerodynamics, heat transfer, aeroacoustics, electrodynamics, seismology, and statistical field theory.
5. This study serves as a generalization of simpler models such as the Timoshenko frame, Euler–Bernoulli frame on elastic Winkler foundation, and the Euler–Bernoulli frame. By taking the limit of the Winkler foundation parameter as it tends to zero, analytical expressions for the Timoshenko frame are derived. Evaluating shear rigidity as it approaches infinity yields analytical expressions for the Euler–Bernoulli frame on elastic Winkler foundation. Simultaneously, approaching zero soil stiffness and infinite shear rigidity leads to analytical expressions for the Euler–Bernoulli frame.
6. Three examples are presented to demonstrate the benefits of the GFSM. These examples involve the analysis of a single-span beam, a two-span beam, and a one-bay, one-story plane frame on elastic Winkler foundations. The GFSM is utilized to achieve closed-form solutions, which are then compared with numerical solutions obtained using the TFEM and the FEM software OpenSees. These comparisons highlight the applicability and efficacy of the GFSM.
7. A novel unified variational formulation is presented for the finite element analysis of Timoshenko beams and frames supported on elastic Winkler foundation, utilizing the relation between the analytical cross-section rotation and analytical transverse displacement shape functions.

CRediT authorship contribution statement

Cristian Posso: Writing – original draft, Validation, Software, Formal analysis. **Juan Camilo Molina-Villegas:** Writing – review & editing, Methodology, Formal analysis, Conceptualization. **Jorge Eliecer Ballesteros Ortega:** Writing – review & editing, Formal analysis, Conceptualization.

Declaration of competing interest

The authors declare that they have no known competing financial interests or personal relationships that could have appeared to influence the work reported in this paper.

Data availability

No data was used for the research described in the article. The Python code used for the elaboration of the examples is provided at the end of each.

Appendix A. Case $\lambda_s = \lambda_f$

In this appendix, formulas for using Eqs. (61) and (63) in the case where $\lambda_s = \lambda_f$ are provided. First, the coefficients of the stiffness matrix associated with the beam element in Eq. (61) need to be replaced with the following:

$$k_{22} = k_{55} = \frac{2EI\left[3\left(\varepsilon^2 - \varepsilon^{-2}\right) - 4\imath\right]\rho^3}{9\left(\varepsilon^2 + \varepsilon^{-2}\right) - 18 - 4\imath^2}, \tag{A.1a}$$

$$k_{23} = k_{32} = -k_{56} = -k_{65} = \frac{EI\left[3\left(\varepsilon^2 + \varepsilon^{-2}\right) - 2\left(3 + 2\imath^2\right)\right]\rho^2}{9\left(\varepsilon^2 + \varepsilon^{-2}\right) - 18 - 4\imath^2}, \tag{A.1b}$$

$$k_{25} = k_{52} = \frac{4EI\left[3\left(\varepsilon^{-1} - \varepsilon\right) + \left(\varepsilon + \varepsilon^{-1}\right)\imath\right]\rho^3}{9\left(\varepsilon^2 + \varepsilon^{-2}\right) - 18 - 4\imath^2}, \tag{A.1c}$$

$$k_{26} = k_{62} = -k_{35} = -k_{53} = \frac{4EI\left(\varepsilon - \varepsilon^{-1}\right)\imath \cdot \rho^2}{9\left(\varepsilon^2 + \varepsilon^{-2}\right) - 18 - 4\imath^2}, \tag{A.1d}$$

$$k_{33} = k_{66} = \frac{2EI\left[3\left(\varepsilon^2 - \varepsilon^{-2}\right) + 4\imath\right]\rho}{9\left(\varepsilon^2 + \varepsilon^{-2}\right) - 18 - 4\imath^2}, \tag{A.1e}$$

$$k_{36} = k_{63} = -\frac{4EI\left[3\left(\varepsilon - \varepsilon^{-1}\right) + \left(\varepsilon + \varepsilon^{-1}\right)\imath\right]\rho}{9\left(\varepsilon^2 + \varepsilon^{-2}\right) - 18 - 4\imath^2}, \tag{A.1f}$$

where

$$\varepsilon = \mathrm{e}^{\rho L}, \tag{A.2a}$$

$$\iota = \rho \cdot L; \tag{A.2b}$$

$$\rho = \sqrt{2}\lambda_s, \tag{A.2c}$$

this implies that the remaining stiffness matrix coefficients, derived from the rod element, do not require any modifications.

Subsequently, the transverse displacement and cross-section rotation shape functions needed to compute the fixed-end force vector in Eq. (61), as well as the transverse displacement and cross-section rotation fields in Eqs. (63a) and (63b), should be replaced with the following expressions in those equations, respectively:

$$\psi_2^v(x) = \left[\frac{9\left(\varepsilon^{-2}-1\right)+(6-2\iota)\,\iota+\left[3\left(\varepsilon^{-2}-1\right)+2\iota\right]\rho\cdot x}{9\left(\varepsilon^2+\varepsilon^{-2}\right)-18-4\iota^2}\right]\mathrm{e}^{\lambda_5 x}+\left[\frac{9\left(\varepsilon^2-1\right)-(6+2\iota)\,\iota+\left[3\left(1-\varepsilon^2\right)+2\iota\right]\rho\cdot x}{9\left(\varepsilon^2+\varepsilon^{-2}\right)-18-4\iota^2}\right]\mathrm{e}^{\lambda_7 x}, \tag{A.3a}$$

$$\psi_3^v(x) = \left[\frac{2\tau+\left[3\left(\varepsilon^{-2}-1\right)-2\iota\right]x}{9\left(\varepsilon^2+\varepsilon^{-2}\right)-18-4\iota^2}\right]\mathrm{e}^{\lambda_5 x}+\left[\frac{-2\tau+\left[3\left(\varepsilon^2-1\right)+2\iota\right]x}{9\left(\varepsilon^2+\varepsilon^{-2}\right)-18-4\iota^2}\right]\mathrm{e}^{\lambda_7 x}, \tag{A.3b}$$

$$\begin{aligned}\psi_5^v(x) = &\left[\frac{3\left[3\left(\varepsilon-\varepsilon^{-1}\right)-\left(\varepsilon+\varepsilon^{-1}\right)\iota\right]+\left[3\left(\varepsilon-\varepsilon^{-1}\right)-2\varepsilon^{-1}\cdot\iota\right]\rho\cdot x}{9\left(\varepsilon^2+\varepsilon^{-2}\right)-18-4\iota^2}\right]\mathrm{e}^{\lambda_5 x}\\ &+\left[\frac{3\left[-3\left(\varepsilon-\varepsilon^{-1}\right)+\left(\varepsilon+\varepsilon^{-1}\right)\iota\right]+\left[3\left(\varepsilon-\varepsilon^{-1}\right)-2\varepsilon\cdot\iota\right]\rho\cdot x}{9\left(\varepsilon^2+\varepsilon^{-2}\right)-18-4\iota^2}\right]\mathrm{e}^{\lambda_7 x},\end{aligned} \tag{A.3c}$$

$$\psi_6^v(x) = \left[\frac{-3\sigma+\left[3\left(\varepsilon-\varepsilon^{-1}\right)+2\varepsilon^{-1}\cdot\iota\right]x}{9\left(\varepsilon^2+\varepsilon^{-2}\right)-18-4\iota^2}\right]\mathrm{e}^{\lambda_5 x}+\left[\frac{3\sigma+\left[3\left(\varepsilon^{-1}-\varepsilon\right)-2\varepsilon\cdot\iota\right]x}{9\left(\varepsilon^2+\varepsilon^{-2}\right)-18-4\iota^2}\right]\mathrm{e}^{\lambda_7 x}, \tag{A.3d}$$

$$\psi_2^\theta(x) = \left\{\left[\frac{2\iota^2-\left[3\left(\varepsilon^{-2}-1\right)+2\iota\right]\rho\cdot x}{9\left(\varepsilon^2+\varepsilon^{-2}\right)-18-4\iota^2}\right]\mathrm{e}^{\lambda_5 x}+\left[\frac{-2\iota^2+\left[3\left(1-\varepsilon^2\right)+2\iota\right]\rho\cdot x}{9\left(\varepsilon^2+\varepsilon^{-2}\right)-18-4\iota^2}\right]\mathrm{e}^{\lambda_7 x}\right\}\rho, \tag{A.4a}$$

$$\psi_3^\theta(x) = \left[\frac{9\left(\varepsilon^{-2}-1\right)-2\,(3+\iota)\,\iota+\left[-3\left(\varepsilon^{-2}-1\right)+2\iota\right]\rho\cdot x}{9\left(\varepsilon^2+\varepsilon^{-2}\right)-18-4\iota^2}\right]\mathrm{e}^{\lambda_5 x}+\left[\frac{9\left(\varepsilon^2-1\right)-2\,(3-\iota)\,\iota+\left[3\left(\varepsilon^2-1\right)+2\iota\right]\rho\cdot x}{9\left(\varepsilon^2+\varepsilon^{-2}\right)-18-4\iota^2}\right]\mathrm{e}^{\lambda_7 x}, \tag{A.4b}$$

$$\psi_5^\theta(x) = \left\{\left[\frac{3\left(\varepsilon-\varepsilon^{-1}\right)\iota+\left[-3\left(\varepsilon-\varepsilon^{-1}\right)+2\varepsilon^{-1}\cdot\iota\right]\rho\cdot x}{9\left(\varepsilon^2+\varepsilon^{-2}\right)-18-4\iota^2}\right]\mathrm{e}^{\lambda_5 x}+\left[\frac{3\left(-\varepsilon+\varepsilon^{-1}\right)\iota+\left[3\left(\varepsilon-\varepsilon^{-1}\right)+2\varepsilon\cdot\iota\right]\rho\cdot x}{9\left(\varepsilon^2+\varepsilon^{-2}\right)-18-4\iota^2}\right]\mathrm{e}^{\lambda_7 x}\right\}\rho, \tag{A.4c}$$

$$\begin{aligned}\psi_6^\theta(x) = &\left[\frac{3\left[3\left(\varepsilon-\varepsilon^{-1}\right)+\left(\varepsilon+\varepsilon^{-1}\right)\iota\right]+\left[-3\left(\varepsilon-\varepsilon^{-1}\right)-2\varepsilon^{-1}\cdot\iota\right]\rho\cdot x}{9\left(\varepsilon^2+\varepsilon^{-2}\right)-18-4\iota^2}\right]\mathrm{e}^{\lambda_5 x}\\ &+\left[\frac{3\left[3\left(\varepsilon^{-1}-\varepsilon\right)-\left(\varepsilon+\varepsilon^{-1}\right)\iota\right]+\left[3\left(\varepsilon^{-1}-\varepsilon\right)-2\varepsilon\cdot\iota\right]\rho\cdot x}{9\left(\varepsilon^2+\varepsilon^{-2}\right)-18-4\iota^2}\right]\mathrm{e}^{\lambda_7 x},\end{aligned} \tag{A.4d}$$

where

$$\lambda_5 = \lambda_6 = +\rho, \tag{A.5a}$$

$$\lambda_7 = \lambda_8 = -\rho, \tag{A.5b}$$

$$\sigma = \left(\varepsilon-\varepsilon^{-1}\right)L, \tag{A.5c}$$

$$\tau = \iota \cdot L. \tag{A.5d}$$

No changes are required for the axial displacement shape functions needed to compute the fixed-end force vector in Eq. (61) and the axial displacement field in Eq. (63c).

The shear force and bending moment shape functions in Eqs. (63d) and (63e) should be replaced with the following expressions, respectively:

$$\begin{aligned}\psi_2^V(x) = \frac{EI\cdot\rho^3}{9\left(\varepsilon^2+\varepsilon^{-2}\right)-18-4\iota^2}\Big\{&\left\{6\left(\varepsilon^{-2}-1\right)+2\iota\,(2-\iota)+\left[3\left(\varepsilon^{-2}-1\right)+2\iota\right]\rho\cdot x\right\}\mathrm{e}^{\lambda_5 x}\\ &-\left\{6\left(\varepsilon^2-1\right)-2\iota\,(2+\iota)-\left[3\left(\varepsilon^2-1\right)-2\iota\right]\rho\cdot x\right\}\mathrm{e}^{\lambda_7 x}\Big\},\end{aligned} \tag{A.6a}$$

$$\begin{aligned}\psi_3^V(x) = -\frac{EI\cdot\rho^2}{9\left(\varepsilon^2+\varepsilon^{-2}\right)-18-4\iota^2}\Big\{&\left\{3\left(\varepsilon^{-2}-1\right)-2\iota\,(1+\iota)-\left[3\left(\varepsilon^{-2}-1\right)-2\iota\right]\rho\cdot x\right\}\mathrm{e}^{\lambda_5 x}\\ &+\left\{3\left(\varepsilon^2-1\right)+2\iota\,(1-\iota)+\left[3\left(\varepsilon^2-1\right)+2\iota\right]\rho\cdot x\right\}\mathrm{e}^{\lambda_7 x}\Big\},\end{aligned} \tag{A.6b}$$

$$\begin{aligned}\psi_5^V(x) = \frac{EI\cdot\rho^3}{9\left(\varepsilon^2+\varepsilon^{-2}\right)-18-4\iota^2}\Big\{&\left\{3\varepsilon\,(2-\iota)-\varepsilon^{-1}\,(6+\iota)+\left[3\left(\varepsilon-\varepsilon^{-1}\right)-2\varepsilon^{-1}\cdot\iota\right]\rho\cdot x\right\}\mathrm{e}^{\lambda_5 x}\\ &+\left\{\varepsilon\,(6-\iota)-3\varepsilon^{-1}\,(2+\iota)-\left[\varepsilon\,(3-2\iota)-3\varepsilon^{-1}\right]\rho\cdot x\right\}\mathrm{e}^{\lambda_7 x}\Big\},\end{aligned} \tag{A.6c}$$

$$\begin{aligned}\psi_6^V(x) = -\frac{EI\cdot\rho^2}{9\left(\varepsilon^2+\varepsilon^{-2}\right)-18-4\iota^2}\Big\{&\left\{3\varepsilon\,(1+\iota)-\varepsilon^{-1}\,(3+\iota)+\left[\varepsilon^{-1}\,(3-2\iota)-3\varepsilon\right]\rho\cdot x\right\}\mathrm{e}^{\lambda_5 x}\\ &-\left\{\varepsilon\,(3-\iota)-3\varepsilon^{-1}\,(1-\iota)+\left[\varepsilon\,(3+2\iota)-3\varepsilon^{-1}\right]\rho\cdot x\right\}\mathrm{e}^{\lambda_7 x}\Big\},\end{aligned} \tag{A.6d}$$

$$\psi_2^M(x) = -\frac{EI\cdot\rho^2}{9\left(\varepsilon^2+\varepsilon^{-2}\right)-18-4\imath^2}\left\{\left\{3\left(\varepsilon^{-2}-1\right)+2\imath\left(1-\imath\right)+\left[3\left(\varepsilon^{-2}-1\right)+2\imath\right]\rho\cdot x\right\}\mathrm{e}^{\lambda_5 x} + \left\{3\left(\varepsilon^{2}-1\right)-2\imath\left(1+\imath\right)-\left[3\left(\varepsilon^{2}-1\right)-2\imath\right]\rho\cdot x\right\}\mathrm{e}^{\lambda_7 x}\right\}, \tag{A.7a}$$

$$\psi_3^M(x) = \frac{EI\cdot\rho}{9\left(\varepsilon^2+\varepsilon^{-2}\right)-18-4\imath^2}\left\{\left\{6\left(\varepsilon^{-2}-1\right)-2\imath\left(2+\imath\right)-\left[3\left(\varepsilon^{-2}-1\right)-2\imath\right]\rho\cdot x\right\}\mathrm{e}^{\lambda_5 x} - \left\{6\left(\varepsilon^{2}-1\right)+2\imath\left(2-\imath\right)+\left[3\left(\varepsilon^{2}-1\right)+2\imath\right]\rho\cdot x\right\}\mathrm{e}^{\lambda_7 x}\right\}, \tag{A.7b}$$

$$\psi_5^M(x) = \frac{EI\cdot\rho^2}{9\left(\varepsilon^2+\varepsilon^{-2}\right)-18-4\imath^2}\left\{\left\{3\varepsilon\left(\imath-1\right)+\varepsilon^{-1}\left(3-\imath\right)+\left[\varepsilon^{-1}\left(3+2\imath\right)-3\varepsilon\right]\rho\cdot x\right\}\mathrm{e}^{\lambda_5 x} + \left\{\varepsilon\left(3+\imath\right)-3\varepsilon^{-1}\left(1+\imath\right)-\left[\varepsilon\left(3-2\imath\right)-3\varepsilon^{-1}\right]\rho\cdot x\right\}\mathrm{e}^{\lambda_7 x}\right\}, \tag{A.7c}$$

$$\psi_6^M(x) = \frac{EI\cdot\rho}{9\left(\varepsilon^2+\varepsilon^{-2}\right)-18-4\imath^2}\left\{\left\{3\varepsilon\left(2+\imath\right)-\varepsilon^{-1}\left(6-\imath\right)+\left[\varepsilon^{-1}\left(3-2\imath\right)-3\varepsilon\right]\rho\cdot x\right\}\mathrm{e}^{\lambda_5 x} + \left\{\varepsilon\left(6+\imath\right)-3\varepsilon^{-1}\left(2-\imath\right)+\left[\varepsilon\left(3+2\imath\right)-3\varepsilon^{-1}\right]\rho\cdot x\right\}\mathrm{e}^{\lambda_7 x}\right\}, \tag{A.7d}$$

no changes are required for the axial force shape functions in Eq. (63f).

Finally, the expressions listed below should be replaced in the GFs appearing in Eqs. (63a), (63b), (63d), and (63e), respectively:

$$W_2^v(x) = \frac{\left[3\left(\mathrm{e}^{2\rho x}-1\right)+\left(\mathrm{e}^{2\rho x}+1\right)\rho\cdot x\right]\mathrm{e}^{\lambda_7 x}}{4EI\cdot\rho^3}, \tag{A.8a}$$

$$W_3^v(x) = \frac{\left(\mathrm{e}^{2\rho x}-1\right)x\cdot\mathrm{e}^{\lambda_7 x}}{4EI\cdot\rho}, \tag{A.8b}$$

$$W_5^v(x) = \frac{\left[3\left(\varepsilon^2-\mathrm{e}^{2\rho x}\right)+\left(\varepsilon^2+\mathrm{e}^{2\rho x}\right)(L-x)\rho\right]\varepsilon^{-1}\cdot\mathrm{e}^{\lambda_7 x}}{4EI\cdot\rho^3}, \tag{A.8c}$$

$$W_6^v(x) = \frac{\left(\mathrm{e}^{2\rho x}-\varepsilon^2\right)(L-x)\varepsilon^{-1}\cdot\mathrm{e}^{\lambda_7 x}}{4EI\cdot\rho}, \tag{A.8d}$$

$$W_2^\theta(x) = \frac{\left(1-\mathrm{e}^{2\rho x}\right)x\cdot\mathrm{e}^{\lambda_7 x}}{4EI\cdot\rho} = -W_3^v(x), \tag{A.9a}$$

$$W_3^\theta(x) = \frac{\left[3\left(\mathrm{e}^{2\rho x}-1\right)-\left(\mathrm{e}^{2\rho x}+1\right)\rho\cdot x\right]\mathrm{e}^{\lambda_7 x}}{4EI\cdot\rho}, \tag{A.9b}$$

$$W_5^\theta(x) = \frac{\left(\varepsilon^2-\mathrm{e}^{2\rho x}\right)(L-x)\varepsilon^{-1}\cdot\mathrm{e}^{\lambda_7 x}}{4EI\cdot\rho} = -W_6^v(x), \tag{A.9c}$$

$$W_6^\theta(x) = \frac{\left[3\left(\varepsilon^2-\mathrm{e}^{2\rho x}\right)-\left(\varepsilon^2+\mathrm{e}^{2\rho x}\right)(L-x)\rho\right]\varepsilon^{-1}\cdot\mathrm{e}^{\lambda_7 x}}{4EI\cdot\rho}, \tag{A.9d}$$

$$W_2^V(x) = \frac{\left[2\left(\mathrm{e}^{2\rho x}+1\right)+\left(\mathrm{e}^{2\rho x}-1\right)\rho\cdot x\right]\mathrm{e}^{\lambda_7 x}}{4}, \tag{A.10a}$$

$$W_3^V(x) = -\frac{\left[\mathrm{e}^{2\rho x}-1-\left(\mathrm{e}^{2\rho x}+1\right)\rho\cdot x\right]\rho\cdot\mathrm{e}^{\lambda_7 x}}{4}, \tag{A.10b}$$

$$W_5^V(x) = -\frac{\left[2-(L-x)\rho\right]\varepsilon^{-1}\cdot\mathrm{e}^{\lambda_5 x}+\left[2+(L-x)\rho\right]\varepsilon\cdot\mathrm{e}^{\lambda_7 x}}{4}, \tag{A.10c}$$

$$W_6^V(x) = \frac{\left\{\left[1+(L-x)\rho\right]\varepsilon^{-1}\cdot\mathrm{e}^{\lambda_5 x}-\left[1-(L-x)\rho\right]\varepsilon\cdot\mathrm{e}^{\lambda_7 x}\right\}\rho}{4}, \tag{A.10d}$$

$$W_2^M(x) = -\frac{\left[\mathrm{e}^{2\rho x}-1+\left(\mathrm{e}^{2\rho x}+1\right)\rho\cdot x\right]\mathrm{e}^{\lambda_7 x}}{4\rho}, \tag{A.11a}$$

$$W_3^M(x) = \frac{\left[2\left(\mathrm{e}^{2\rho x}+1\right)-\left(\mathrm{e}^{2\rho x}-1\right)\rho\cdot x\right]\mathrm{e}^{\lambda_7 x}}{4}, \tag{A.11b}$$

$$W_5^M(x) = -\frac{\left[\varepsilon\left(1+\imath\right)-\varepsilon^{-1}\left(1-\imath\right)\mathrm{e}^{2\rho x}-\left(\varepsilon^{-1}\cdot\mathrm{e}^{2\rho x}+\varepsilon\right)\rho\cdot x\right]\mathrm{e}^{\lambda_7 x}}{4\rho}, \tag{A.11c}$$

$$W_6^M(x) = -\frac{\left[2+(L-x)\rho\right]\varepsilon^{-1}\cdot\mathrm{e}^{\lambda_5 x}+\left[2-(L-x)\rho\right]\varepsilon\cdot\mathrm{e}^{\lambda_7 x}}{4}, \tag{A.11d}$$

no modifications are needed for the axial displacement and axial force GFs in Eqs. (63c) and (63f).

Appendix B. Case $\lambda_s > \lambda_f$

In this appendix, formulas for using Eqs. (61) and (63) in the case where $\lambda_s > \lambda_f$ are provided. The procedure for replacing expressions in these equations is the same as explained in Appendix A. Therefore, readers are referred to the preceding appendix for instructions on how to use the formulas introduced here.

Stiffness Matrix Modifications

$$k_{22} = k_{55} = -\frac{4EI\cdot\alpha\cdot\gamma\left(\alpha^2-\gamma^2\right)\left[e_\gamma^2\left(1-e_\alpha^4\right)\zeta+e_\alpha^2\left(e_\gamma^4-1\right)\delta\right]}{e_\gamma^2\left(1+e_\alpha^4\right)\zeta^2+8e_\gamma^2\cdot e_\alpha^2\cdot\upsilon\cdot\chi-e_\alpha^2\left(1+e_\gamma^4\right)\delta^2}, \tag{B.1a}$$

$$k_{23} = k_{32} = -k_{56} = -k_{65} = \frac{2EI\left(\alpha^2-\gamma^2\right)\left[e_\gamma^2\left(e_\alpha^2-1\right)^2\gamma\cdot\zeta-e_\alpha^2\left(e_\gamma^2-1\right)^2\alpha\cdot\delta\right]}{e_\gamma^2\left(1+e_\alpha^4\right)\zeta^2+8e_\gamma^2\cdot e_\alpha^2\cdot\upsilon\cdot\chi-e_\alpha^2\left(1+e_\gamma^4\right)\delta^2}, \tag{B.1b}$$

$$k_{25} = k_{52} = \frac{8EI\cdot\alpha\cdot\gamma\left(\alpha^2-\gamma^2\right)e_\gamma\cdot e_\alpha\left\{\left[\left(e_\gamma\cdot e_\alpha\right)^2-1\right]\upsilon+\left(e_\gamma^2-e_\alpha^2\right)\chi\right\}}{e_\gamma^2\left(1+e_\alpha^4\right)\zeta^2+8e_\gamma^2\cdot e_\alpha^2\cdot\upsilon\cdot\chi-e_\alpha^2\left(1+e_\gamma^4\right)\delta^2}, \tag{B.1c}$$

$$k_{26} = k_{62} = -k_{35} = -k_{53} = \frac{8EI\cdot\alpha\cdot\gamma\left(\alpha^2-\gamma^2\right)e_\gamma\cdot e_\gamma\left(e_\gamma^2-1\right)\left(e_\gamma^2-1\right)}{e_\gamma^2\left(1+e_\alpha^4\right)\zeta^2+8e_\gamma^2\cdot e_\alpha^2\cdot\upsilon\cdot\chi-e_\alpha^2\left(1+e_\gamma^4\right)\delta^2}, \tag{B.1d}$$

$$k_{33} = k_{66} = \frac{4EI\cdot\alpha\cdot\gamma\left[e_\gamma^2\left(e_\alpha^4-1\right)\zeta+e_\alpha^2\left(e_\gamma^4-1\right)\delta\right]}{e_\gamma^2\left(1+e_\alpha^4\right)\zeta^2+8e_\gamma^2\cdot e_\alpha^2\cdot\upsilon\cdot\chi-e_\alpha^2\left(1+e_\gamma^4\right)\delta^2}, \tag{B.1e}$$

$$k_{36} = k_{63} = -\frac{8EI\cdot\alpha\cdot\gamma\cdot e_\gamma\cdot e_\alpha\left\{\left(e_\gamma^2-e_\alpha^2\right)\upsilon+\left[\left(e_\gamma\cdot e_\alpha\right)^2-1\right]\chi\right\}}{e_\gamma^2\left(1+e_\alpha^4\right)\zeta^2+8e_\gamma^2\cdot e_\alpha^2\cdot\upsilon\cdot\chi-e_\alpha^2\left(1+e_\gamma^4\right)\delta^2}, \tag{B.1f}$$

where

$$e_\gamma = \mathrm{e}^{\gamma L}, \tag{B.2a}$$

$$e_\alpha = \mathrm{e}^{\alpha L}, \tag{B.2b}$$

$$\delta = \upsilon+\chi, \tag{B.2c}$$

$$\zeta = \chi-\upsilon; \tag{B.2d}$$

$$\upsilon = \frac{(\alpha-\gamma)^2}{\alpha+\gamma}, \tag{B.2e}$$

$$\chi = \frac{(\alpha+\gamma)^2}{\alpha-\gamma}; \tag{B.2f}$$

$$\gamma = \sqrt{\lambda_s^2-\lambda_f^2}. \tag{B.2g}$$

Shape Functions Modifications

$$\begin{aligned}\psi_2^v(x) =& \frac{e_\gamma^2\cdot\chi\left(\zeta+2e_\alpha^2\cdot\upsilon-e_\gamma^{-2}\cdot e_\alpha^2\cdot\delta\right)\mathrm{e}^{\lambda_9 x}+e_\gamma^2\cdot\upsilon\left(-\zeta+2e_\alpha^2\cdot\chi-e_\gamma^2\cdot e_\alpha^2\cdot\delta\right)\mathrm{e}^{\lambda_{10}x}}{e_\gamma^2\left(1+e_\alpha^4\right)\zeta^2+8e_\gamma^2\cdot e_\alpha^2\cdot\upsilon\cdot\chi-e_\alpha^2\left(1+e_\gamma^4\right)\delta^2}\\ &+\frac{e_\alpha^2\cdot\upsilon\left(-\delta+2e_\gamma^2\cdot\chi-e_\gamma^2\cdot e_\alpha^2\cdot\zeta\right)\mathrm{e}^{\lambda_{11}x}+e_\gamma^2\cdot e_\alpha^2\cdot\chi\left(2\upsilon+e_\alpha^2\cdot\zeta-e_\gamma^2\cdot\delta\right)\mathrm{e}^{\lambda_{12}x}}{e_\gamma^2\left(1+e_\alpha^4\right)\zeta^2+8e_\gamma^2\cdot e_\alpha^2\cdot\upsilon\cdot\chi-e_\alpha^2\left(1+e_\gamma^4\right)\delta^2},\end{aligned} \tag{B.3a}$$

$$\begin{aligned}\psi_3^v(x) =& \frac{e_\gamma^2\left(\zeta-2e_\alpha^2\cdot\chi+e_\gamma^{-2}\cdot e_\alpha^2\cdot\delta\right)\mathrm{e}^{\lambda_9 x}+e_\gamma^2\left(-\zeta-2e_\alpha^2\cdot\upsilon+e_\gamma^2\cdot e_\alpha^2\cdot\delta\right)\mathrm{e}^{\lambda_{10}x}}{e_\gamma^2\left(1+e_\alpha^4\right)\zeta^2+8e_\gamma^2\cdot e_\alpha^2\cdot\upsilon\cdot\chi-e_\alpha^2\left(1+e_\gamma^4\right)\delta^2}\\ &+\frac{e_\alpha^2\left(-\delta+2e_\gamma^2\cdot\upsilon+e_\gamma^2\cdot e_\alpha^2\cdot\zeta\right)\mathrm{e}^{\lambda_{11}x}+e_\gamma^2\cdot e_\alpha^2\left(2\chi-e_\gamma^2\cdot\delta-e_\alpha^2\cdot\zeta\right)\mathrm{e}^{\lambda_{12}x}}{e_\gamma^2\left(1+e_\alpha^4\right)\zeta^2+8e_\gamma^2\cdot e_\alpha^2\cdot\upsilon\cdot\chi-e_\alpha^2\left(1+e_\gamma^4\right)\delta^2},\end{aligned} \tag{B.3b}$$

$$\begin{aligned}\psi_5^v(x) =& \frac{e_\gamma\cdot e_\alpha\cdot\chi\left(2\upsilon+e_\alpha^2\cdot\zeta-e_\gamma^2\cdot\delta\right)\mathrm{e}^{\lambda_9 x}+e_\gamma\cdot e_\alpha\cdot\upsilon\left(-\delta+2e_\gamma^2\cdot\chi-e_\gamma^2\cdot e_\alpha^2\cdot\zeta\right)\mathrm{e}^{\lambda_{10}x}}{e_\gamma^2\left(1+e_\alpha^4\right)\zeta^2+8e_\gamma^2\cdot e_\alpha^2\cdot\upsilon\cdot\chi-e_\alpha^2\left(1+e_\gamma^4\right)\delta^2}\\ &+\frac{e_\gamma\cdot e_\alpha\cdot\upsilon\left(-\zeta+2e_\alpha^2\cdot\chi-e_\gamma^2\cdot e_\alpha^2\cdot\delta\right)\mathrm{e}^{\lambda_{11}x}+e_\gamma^3\cdot e_\alpha\cdot\chi\left(\zeta+2e_\alpha^2\cdot\upsilon-e_\gamma^{-2}\cdot e_\alpha^2\cdot\delta\right)\mathrm{e}^{\lambda_{12}x}}{e_\gamma^2\left(1+e_\alpha^4\right)\zeta^2+8e_\gamma^2\cdot e_\alpha^2\cdot\upsilon\cdot\chi-e_\alpha^2\left(1+e_\gamma^4\right)\delta^2},\end{aligned} \tag{B.3c}$$

$$\psi_6^{v}(x) = \frac{e_\gamma \cdot e_\alpha \left(-2\chi + e_\gamma^2 \cdot \delta + e_\alpha^2 \cdot \zeta\right) \mathrm{e}^{\lambda_9 x} + e_\gamma \cdot e_\alpha \left(\delta - 2e_\gamma^2 \cdot \upsilon - e_\gamma^2 \cdot e_\alpha^2 \cdot \zeta\right) \mathrm{e}^{\lambda_{10} x}}{e_\gamma^2 \left(1 + e_\alpha^4\right) \zeta^2 + 8 e_\gamma^2 \cdot e_\alpha^2 \cdot \upsilon \cdot \chi - e_\alpha^2 \left(1 + e_\gamma^4\right) \delta^2} + \frac{e_\gamma \cdot e_\alpha \left(\zeta + 2e_\alpha^2 \cdot \upsilon - e_\gamma^2 \cdot e_\alpha^2 \cdot \delta\right) \mathrm{e}^{\lambda_{11} x} + e_\gamma \cdot e_\alpha \left(-e_\gamma^2 \cdot \zeta + 2e_\gamma^2 \cdot e_\alpha^2 \cdot \chi - e_\alpha^2 \cdot \delta\right) \mathrm{e}^{\lambda_{12} x}}{e_\gamma^2 \left(1 + e_\alpha^4\right) \zeta^2 + 8 e_\gamma^2 \cdot e_\alpha^2 \cdot \upsilon \cdot \chi - e_\alpha^2 \left(1 + e_\gamma^4\right) \delta^2}, \tag{B.3d}$$

$$\psi_2^{\theta}(x) = \frac{-e_\gamma^2 \cdot \upsilon \cdot \chi \left(\zeta + 2e_\alpha^2 \cdot \upsilon - e_\gamma^{-2} \cdot e_\alpha^2 \cdot \delta\right) \mathrm{e}^{\lambda_9 x} - e_\gamma^2 \cdot \upsilon \cdot \chi \left(-\zeta + 2e_\alpha^2 \cdot \chi - e_\gamma^2 \cdot e_\alpha^2 \cdot \delta\right) \mathrm{e}^{\lambda_{10} x}}{e_\gamma^2 \left(1 + e_\alpha^4\right) \zeta^2 + 8 e_\gamma^2 \cdot e_\alpha^2 \cdot \upsilon \cdot \chi - e_\alpha^2 \left(1 + e_\gamma^4\right) \delta^2} + \frac{e_\alpha^2 \cdot \upsilon \cdot \chi \left(-\delta + 2e_\gamma^2 \cdot \chi - e_\gamma^2 \cdot e_\alpha^2 \cdot \zeta\right) \mathrm{e}^{\lambda_{11} x} + e_\gamma^2 \cdot e_\alpha^2 \cdot \upsilon \cdot \chi \left(2\upsilon + e_\alpha^2 \cdot \zeta - e_\gamma^2 \cdot \delta\right) \mathrm{e}^{\lambda_{12} x}}{e_\gamma^2 \left(1 + e_\alpha^4\right) \zeta^2 + 8 e_\gamma^2 \cdot e_\alpha^2 \cdot \upsilon \cdot \chi - e_\alpha^2 \left(1 + e_\gamma^4\right) \delta^2}, \tag{B.4a}$$

$$\psi_3^{\theta}(x) = \frac{-e_\gamma^2 \cdot \upsilon \left(\zeta - 2e_\alpha^2 \cdot \chi + e_\gamma^{-2} \cdot e_\alpha^2 \cdot \delta\right) \mathrm{e}^{\lambda_9 x} - e_\gamma^2 \cdot \chi \left(-\zeta - 2e_\alpha^2 \cdot \upsilon + e_\gamma^2 \cdot e_\alpha^2 \cdot \delta\right) \mathrm{e}^{\lambda_{10} x}}{e_\gamma^2 \left(1 + e_\alpha^4\right) \zeta^2 + 8 e_\gamma^2 \cdot e_\alpha^2 \cdot \upsilon \cdot \chi - e_\alpha^2 \left(1 + e_\gamma^4\right) \delta^2} + \frac{e_\alpha^2 \cdot \chi \left(-\delta + 2e_\gamma^2 \cdot \upsilon + e_\gamma^2 \cdot e_\alpha^2 \cdot \zeta\right) \mathrm{e}^{\lambda_{11} x} + e_\gamma^2 \cdot e_\alpha^2 \cdot \upsilon \left(2\chi - e_\gamma^2 \cdot \delta - e_\alpha^2 \cdot \zeta\right) \mathrm{e}^{\lambda_{12} x}}{e_\gamma^2 \left(1 + e_\alpha^4\right) \zeta^2 + 8 e_\gamma^2 \cdot e_\alpha^2 \cdot \upsilon \cdot \chi - e_\alpha^2 \left(1 + e_\gamma^4\right) \delta^2}, \tag{B.4b}$$

$$\psi_5^{\theta}(x) = \frac{-e_\gamma \cdot e_\alpha \cdot \upsilon \cdot \chi \left(2\upsilon + e_\alpha^2 \cdot \zeta - e_\gamma^2 \cdot \delta\right) \mathrm{e}^{\lambda_9 x} - e_\gamma \cdot e_\alpha \cdot \upsilon \cdot \chi \left(-\delta + 2e_\gamma^2 \cdot \chi - e_\gamma^2 \cdot e_\alpha^2 \cdot \zeta\right) \mathrm{e}^{\lambda_{10} x}}{e_\gamma^2 \left(1 + e_\alpha^4\right) \zeta^2 + 8 e_\gamma^2 \cdot e_\alpha^2 \cdot \upsilon \cdot \chi - e_\alpha^2 \left(1 + e_\gamma^4\right) \delta^2} + \frac{e_\gamma \cdot e_\alpha \cdot \upsilon \cdot \chi \left(-\zeta + 2e_\alpha^2 \cdot \chi - e_\gamma^2 \cdot e_\alpha^2 \cdot \delta\right) \mathrm{e}^{\lambda_{11} x} + e_\gamma^3 \cdot e_\alpha \cdot \upsilon \cdot \chi \left(\zeta + 2e_\alpha^2 \cdot \upsilon - e_\gamma^{-2} \cdot e_\alpha^2 \cdot \delta\right) \mathrm{e}^{\lambda_{12} x}}{e_\gamma^2 \left(1 + e_\alpha^4\right) \zeta^2 + 8 e_\gamma^2 \cdot e_\alpha^2 \cdot \upsilon \cdot \chi - e_\alpha^2 \left(1 + e_\gamma^4\right) \delta^2}, \tag{B.4c}$$

$$\psi_6^{\theta}(x) = \frac{-e_\gamma \cdot e_\alpha \cdot \upsilon \left(-2\chi + e_\gamma^2 \cdot \delta + e_\alpha^2 \cdot \zeta\right) \mathrm{e}^{\lambda_9 x} - e_\gamma \cdot e_\alpha \cdot \chi \left(\delta - 2e_\gamma^2 \cdot \upsilon - e_\gamma^2 \cdot e_\alpha^2 \cdot \zeta\right) \mathrm{e}^{\lambda_{10} x}}{e_\gamma^2 \left(1 + e_\alpha^4\right) \zeta^2 + 8 e_\gamma^2 \cdot e_\alpha^2 \cdot \upsilon \cdot \chi - e_\alpha^2 \left(1 + e_\gamma^4\right) \delta^2} + \frac{e_\gamma \cdot e_\alpha \cdot \chi \left(\zeta + 2e_\alpha^2 \cdot \upsilon - e_\gamma^2 \cdot e_\alpha^2 \cdot \delta\right) \mathrm{e}^{\lambda_{11} x} + e_\gamma \cdot e_\alpha \cdot \upsilon \left(-e_\gamma^2 \cdot \zeta + 2e_\gamma^2 \cdot e_\alpha^2 \cdot \chi - e_\alpha^2 \cdot \delta\right) \mathrm{e}^{\lambda_{12} x}}{e_\gamma^2 \left(1 + e_\alpha^4\right) \zeta^2 + 8 e_\gamma^2 \cdot e_\alpha^2 \cdot \upsilon \cdot \chi - e_\alpha^2 \left(1 + e_\gamma^4\right) \delta^2}, \tag{B.4d}$$

$$\begin{aligned} \psi_2^{V}(x) = \frac{EI\,(\upsilon \cdot \chi)^2}{2\left(\gamma^2 + \alpha^2\right)\left[e_\gamma^2 \left(1 + e_\alpha^4\right) \zeta^2 + 8 e_\gamma^2 \cdot e_\alpha^2 \cdot \upsilon \cdot \chi - e_\alpha^2 \left(1 + e_\gamma^4\right) \delta^2\right]} \Big\{ & \left(\lambda_9 + \upsilon\right) \chi \left[e_\gamma^2 \cdot \zeta - e_\alpha^2 \left(\delta - 2e_\gamma^2 \cdot \upsilon\right)\right] \mathrm{e}^{\lambda_9 x} \\ & - e_\gamma^2 \left(\lambda_{10} + \chi\right) \upsilon \left[\zeta + e_\alpha^2 \left(e_\gamma^2 \cdot \delta - 2\chi\right)\right] \mathrm{e}^{\lambda_{10} x} \\ & - e_\alpha^2 \left(\lambda_{11} - \chi\right) \upsilon \left[\delta + e_\gamma^2 \left(e_\alpha^2 \cdot \zeta - 2\chi\right)\right] \mathrm{e}^{\lambda_{11} x} \\ & - e_\gamma^2 \cdot e_\alpha^2 \left(\lambda_{12} - \upsilon\right) \chi \left(e_\gamma^2 \cdot \delta - e_\alpha^2 \cdot \zeta - 2\upsilon\right) \mathrm{e}^{\lambda_{12} x} \Big\}, \end{aligned} \tag{B.5a}$$

$$\begin{aligned} \psi_3^{V}(x) = \frac{EI\,(\upsilon \cdot \chi)^2}{2\left(\gamma^2 + \alpha^2\right)\left[e_\gamma^2 \left(1 + e_\alpha^4\right) \zeta^2 + 8 e_\gamma^2 \cdot e_\alpha^2 \cdot \upsilon \cdot \chi - e_\alpha^2 \left(1 + e_\gamma^4\right) \delta^2\right]} \Big\{ & \left(\lambda_9 + \upsilon\right) \left[e_\gamma^2 \cdot \zeta + e_\alpha^2 \left(\delta - 2e_\gamma^2 \cdot \chi\right)\right] \mathrm{e}^{\lambda_9 x} \\ & - e_\gamma^2 \left(\lambda_{10} + \chi\right) \left[\zeta - e_\alpha^2 \left(e_\gamma^2 \cdot \delta - 2\upsilon\right)\right] \mathrm{e}^{\lambda_{10} x} \\ & - e_\alpha^2 \left(\lambda_{11} - \chi\right) \left[\delta - e_\gamma^2 \left(e_\alpha^2 \cdot \zeta + 2\upsilon\right)\right] \mathrm{e}^{\lambda_{11} x} \\ & - e_\gamma^2 \cdot e_\alpha^2 \left(\lambda_{12} - \upsilon\right) \left(e_\gamma^2 \cdot \delta + e_\alpha^2 \cdot \zeta - 2\chi\right) \mathrm{e}^{\lambda_{12} x} \Big\}, \end{aligned} \tag{B.5b}$$

$$\begin{aligned} \psi_5^{V}(x) = \frac{-EI \cdot e_\gamma \cdot e_\alpha\,(\upsilon \cdot \chi)^2}{2\left(\gamma^2 + \alpha^2\right)\left[e_\gamma^2 \left(1 + e_\alpha^4\right) \zeta^2 + 8 e_\gamma^2 \cdot e_\alpha^2 \cdot \upsilon \cdot \chi - e_\alpha^2 \left(1 + e_\gamma^4\right) \delta^2\right]} \Big\{ & \left(\lambda_9 + \upsilon\right) \chi \left(e_\gamma^2 \cdot \delta - e_\alpha^2 \cdot \zeta - 2\upsilon\right) \mathrm{e}^{\lambda_9 x} \\ & + \left(\lambda_{10} + \chi\right) \upsilon \left[\delta + e_\gamma^2 \left(e_\alpha^2 \cdot \zeta - 2\chi\right)\right] \mathrm{e}^{\lambda_{10} x} \\ & + \left(\lambda_{11} - \chi\right) \upsilon \left[\zeta + e_\alpha^2 \left(e_\gamma^2 \cdot \delta - 2\chi\right)\right] \mathrm{e}^{\lambda_{11} x} \\ & + \left(\lambda_{12} - \upsilon\right) \chi \left[e_\alpha^2 \left(\delta - 2e_\gamma^2 \cdot \upsilon\right) - e_\gamma^2 \cdot \zeta\right] \mathrm{e}^{\lambda_{12} x} \Big\}, \end{aligned} \tag{B.5c}$$

$$\psi_6^V(x) = \frac{EI \cdot e_\gamma \cdot e_\alpha (\upsilon \cdot \chi)^2}{2\left(\gamma^2+\alpha^2\right)\left[e_\gamma^2\left(1+e_\alpha^4\right)\zeta^2 + 8e_\gamma^2 \cdot e_\alpha^2 \cdot \upsilon \cdot \chi - e_\alpha^2\left(1+e_\gamma^4\right)\delta^2\right]} \left\{ \begin{array}{l} \left(\lambda_9+\upsilon\right)\left(e_\gamma^2 \cdot \delta + e_\alpha^2 \cdot \zeta - 2\chi\right) \mathrm{e}^{\lambda_9 x} \\ + \left(\lambda_{10}+\chi\right)\left[\delta - e_\gamma^2\left(e_\alpha^2 \cdot \zeta + 2\upsilon\right)\right] \mathrm{e}^{\lambda_{10} x} \\ + \left(\lambda_{11}-\chi\right)\left[\zeta - e_\alpha^2\left(e_\gamma^2 \cdot \delta - 2\upsilon\right)\right] \mathrm{e}^{\lambda_{11} x} \\ - \left(\lambda_{12}-\upsilon\right)\left[e_\gamma^2 \cdot \zeta + e_\alpha^2\left(\delta - 2e_\gamma^2 \cdot \chi\right)\right] \mathrm{e}^{\lambda_{12} x} \end{array} \right\}, \tag{B.5d}$$

$$\psi_2^M(x) = \frac{EI \cdot \upsilon \cdot \chi}{e_\gamma^2\left(1+e_\alpha^4\right)\zeta^2 + 8e_\gamma^2 \cdot e_\alpha^2 \cdot \upsilon \cdot \chi - e_\alpha^2\left(1+e_\gamma^4\right)\delta^2} \left\{ \begin{array}{l} \lambda_9\left[e_\alpha^2\left(\delta - 2e_\gamma^2 \cdot \upsilon\right) - e_\gamma^2 \cdot \zeta\right] \mathrm{e}^{\lambda_9 x} \\ + e_\gamma^2 \cdot \lambda_{10}\left[\zeta + e_\alpha^2\left(e_\gamma^2 \cdot \delta - 2 \cdot \chi\right)\right] \mathrm{e}^{\lambda_{10} x} \\ - e_\alpha^2 \cdot \lambda_{11}\left[\delta + e_\gamma^2\left(e_\alpha^2 \cdot \zeta - 2\chi\right)\right] \mathrm{e}^{\lambda_{11} x} \\ - e_\gamma^2 \cdot e_\alpha^2 \cdot \lambda_{12}\left(e_\gamma^2 \cdot \delta - e_\alpha^2 \cdot \zeta - 2\upsilon\right) \mathrm{e}^{\lambda_{12} x} \end{array} \right\}, \tag{B.6a}$$

$$\psi_3^M(x) = \frac{EI}{e_\gamma^2\left(1+e_\alpha^4\right)\zeta^2 + 8e_\gamma^2 \cdot e_\alpha^2 \cdot \upsilon \cdot \chi - e_\alpha^2\left(1+e_\gamma^4\right)\delta^2} \left\{ \begin{array}{l} \lambda_9 \cdot \upsilon\left[e_\alpha^2\left(2e_\gamma^2 \cdot \chi - \delta\right) - e_\gamma^2 \cdot \zeta\right] \mathrm{e}^{\lambda_9 x} \\ + e_\gamma^2 \cdot \lambda_{10} \cdot \chi\left[\zeta - e_\alpha^2\left(e_\gamma^2 \cdot \delta - 2\upsilon\right)\right] \mathrm{e}^{\lambda_{10} x} \\ + e_\alpha^2 \cdot \lambda_{11} \cdot \chi\left[e_\gamma^2\left(e_\alpha^2 \cdot \zeta + 2\upsilon\right) - \delta\right] \mathrm{e}^{\lambda_{11} x} \\ - e_\gamma^2 \cdot e_\alpha^2 \cdot \lambda_{12} \cdot \upsilon\left(e_\gamma^2 \cdot \delta + e_\alpha^2 \cdot \zeta - 2\chi\right) \mathrm{e}^{\lambda_{12} x} \end{array} \right\}, \tag{B.6b}$$

$$\psi_5^M(x) = \frac{EIe_\gamma \cdot e_\alpha \cdot \upsilon \cdot \chi}{e_\gamma^2\left(1+e_\alpha^4\right)\zeta^2 + 8e_\gamma^2 \cdot e_\alpha^2 \cdot \upsilon \cdot \chi - e_\alpha^2\left(1+e_\gamma^4\right)\delta^2} \left\{ \begin{array}{l} \lambda_9\left(e_\gamma^2 \cdot \delta - e_\alpha^2 \cdot \zeta - 2\upsilon\right) \mathrm{e}^{\lambda_9 x} \\ + \lambda_{10}\left[\delta + e_\gamma^2\left(e_\alpha^2 \cdot \zeta - 2\chi\right)\right] \mathrm{e}^{\lambda_{10} x} \\ - \lambda_{11}\left[\zeta + e_\alpha^2\left(e_\gamma^2 \cdot \delta - 2\chi\right)\right] \mathrm{e}^{\lambda_{11} x} \\ + \lambda_{12}\left[e_\gamma^2 \cdot \zeta - e_\alpha^2\left(\delta - 2e_\gamma^2 \cdot \upsilon\right)\right] \mathrm{e}^{\lambda_{12} x} \end{array} \right\}, \tag{B.6c}$$

$$\psi_6^M(x) = -\frac{EI \cdot e_\gamma \cdot e_\alpha}{e_\gamma^2\left(1+e_\alpha^4\right)\zeta^2 + 8e_\gamma^2 \cdot e_\alpha^2 \cdot \upsilon \cdot \chi - e_\alpha^2\left(1+e_\gamma^4\right)\delta^2} \left\{ \begin{array}{l} \lambda_9 \cdot \upsilon\left(e_\gamma^2 \cdot \delta + e_\alpha^2 \cdot \zeta - 2\chi\right) \mathrm{e}^{\lambda_9 x} \\ + \lambda_{10} \cdot \chi\left[\delta - e_\gamma^2\left(e_\alpha^2 \cdot \zeta + 2\upsilon\right)\right] \mathrm{e}^{\lambda_{10} x} \\ - \lambda_{11} \cdot \chi\left[\zeta - e_\alpha^2\left(e_\gamma^2 \cdot \delta - 2\upsilon\right)\right] \mathrm{e}^{\lambda_{11} x} \\ + \lambda_{12} \cdot \upsilon\left[e_\gamma^2 \cdot \zeta + e_\alpha^2\left(\delta - 2e_\gamma^2 \cdot \chi\right)\right] \mathrm{e}^{\lambda_{12} x} \end{array} \right\}, \tag{B.6d}$$

where

$$\lambda_9 = \alpha + \gamma, \tag{B.7a}$$

$$\lambda_{10} = \alpha - \gamma, \tag{B.7b}$$

$$\lambda_{11} = -\alpha + \gamma, \tag{B.7c}$$

$$\lambda_{12} = -\alpha - \gamma. \tag{B.7d}$$

Green's Functions Modifications

$$W_2^\upsilon(x) = \frac{\left[\alpha\left(\alpha^2+3\gamma^2\right)\left(\mathrm{e}^{2\alpha x}+1\right)\left(\mathrm{e}^{2\gamma x}-1\right) + \gamma\left(3\alpha^2+\gamma^2\right)\left(\mathrm{e}^{2\alpha x}-1\right)\left(\mathrm{e}^{2\gamma x}+1\right)\right]\mathrm{e}^{\lambda_{12} x}}{8EI \cdot \alpha \cdot \gamma\left(\alpha^2-\gamma^2\right)^2}, \tag{B.8a}$$

$$W_3^\upsilon(x) = \frac{\left(\mathrm{e}^{2\alpha x}-1\right)\left(\mathrm{e}^{2\gamma x}-1\right)\mathrm{e}^{\lambda_{12} x}}{8EI \cdot \alpha \cdot \gamma}, \tag{B.8b}$$

$$W_5^\upsilon(x) = \frac{\left\{\left[\left(e_\gamma \cdot e_\alpha\right)^2 - \mathrm{e}^{2\lambda_9 x}\right]\lambda_9^3 - \left(e_\alpha \cdot \mathrm{e}^{\gamma x}\right)^2 \lambda_{10}^3 - \left(e_\gamma \cdot \mathrm{e}^{\alpha x}\right)^2 \lambda_{11}^3\right\}\mathrm{e}^{\lambda_{12} x}}{8EI \cdot e_\gamma \cdot e_\alpha \cdot \alpha \cdot \gamma\left(\alpha^2-\gamma^2\right)^2}, \tag{B.8c}$$

$$W_6^\upsilon(x) = -\frac{\left\{\left[e_\alpha^2\left(e_\gamma^2 - \mathrm{e}^{2\gamma x}\right) + \mathrm{e}^{2\lambda_9 x}\right]\lambda_{10}^3 + \left(e_\gamma \cdot \mathrm{e}^{\alpha x}\right)^2 \lambda_{11}^3\right\}\lambda_9^3 \cdot \mathrm{e}^{\lambda_{12} x}}{8EI \cdot e_\gamma \cdot e_\alpha \cdot \alpha \cdot \gamma\left(\alpha^2-\gamma^2\right)^3}, \tag{B.8d}$$

$$W_2^{\theta}(x) = -\frac{\left(e^{2\alpha x}-1\right)\left(e^{2\gamma x}-1\right)e^{\lambda_{12}x}}{8EI\cdot\alpha\cdot\gamma} = -W_3^{v}(x), \tag{B.9a}$$

$$W_3^{\theta}(x) = \frac{v\left(e^{\lambda_{12}x}-e^{\lambda_9 x}\right)+\chi\left(e^{\lambda_{10}x}-e^{\lambda_{11}x}\right)}{8EI\cdot\alpha\cdot\gamma}, \tag{B.9b}$$

$$W_5^{\theta}(x) = \frac{\left\{\left[e_\alpha^2\left(e_\gamma^2-e^{2\gamma x}\right)+e^{2\lambda_9 x}\right]\lambda_{10}^3+\left(e_\gamma\cdot e^{\alpha x}\right)^2\lambda_{11}^3\right\}\lambda_9^3\cdot e^{\lambda_{12}x}}{8EI\cdot e_\gamma\cdot e_\alpha\cdot\alpha\cdot\gamma\left(\alpha^2-\gamma^2\right)^3} = -W_6^{v}(x), \tag{B.9c}$$

$$W_6^{\theta}(x) = \frac{\left\{\left[e^{2\lambda_9 x}-\left(e_\gamma\cdot e_\alpha\right)^2\right]\lambda_{10}^3\cdot v+\left[\left(e_\alpha\cdot e^{\gamma x}\right)^2\lambda_{10}^3+\left(e_\gamma\cdot e^{\alpha x}\right)^2\lambda_{11}^3\right]\chi\right\}\lambda_9^3\cdot e^{\lambda_{12}x}}{8EI\cdot e_\gamma\cdot e_\alpha\cdot\alpha\cdot\gamma\left(\alpha^2-\gamma^2\right)^3}, \tag{B.9d}$$

$$W_2^{V}(x) = \frac{\left[\left(\alpha^2+\gamma^2\right)\left(e^{2\alpha x}-1\right)\left(e^{2\gamma x}-1\right)+2\alpha\cdot\gamma\left(e^{2\alpha x}+1\right)\left(e^{2\gamma x}+1\right)\right](v\cdot\chi)^2 e^{\lambda_{12}x}}{8\alpha\cdot\gamma\left(\alpha^2-\gamma^2\right)^2}, \tag{B.10a}$$

$$W_3^{V}(x) = \frac{\left[\left(e^{2\lambda_9 x}-1\right)\lambda_9^2\cdot v-\left(e^{2\alpha x}-e^{2\gamma x}\right)\lambda_{10}^2\cdot\chi\right](v\cdot\chi)^2 e^{\lambda_{12}x}}{8\alpha\cdot\gamma\left(\alpha^2-\gamma^2\right)^2}, \tag{B.10b}$$

$$W_5^{V}(x) = -\frac{\left\{\left[\left(e_\gamma e_\alpha\right)^2+e^{2\lambda_9 x}\right]\lambda_9^2-\left[\left(e_\gamma e^{\alpha x}\right)^2+\left(e_\alpha e^{\gamma x}\right)^2\right]\lambda_{10}^2\right\}(v\cdot\chi)^2 e^{\lambda_{12}x}}{8e_\gamma\cdot e_\alpha\cdot\alpha\cdot\gamma\left(\alpha^2-\gamma^2\right)^2}, \tag{B.10c}$$

$$W_6^{V}(x) = \frac{\left\{\left[\left(e_\gamma e_\alpha\right)^2-e^{2\lambda_9 x}\right]\lambda_9^2\cdot v+\left[\left(e_\gamma e^{\alpha x}\right)^2-\left(e_\alpha e^{\gamma x}\right)^2\right]\lambda_{10}^2\cdot\chi\right\}(v\cdot\chi)^2 e^{\lambda_{12}x}}{8e_\gamma\cdot e_\alpha\cdot\alpha\cdot\gamma\left(\alpha^2-\gamma^2\right)^2}, \tag{B.10d}$$

$$W_2^{M}(x) = -\frac{\left[\alpha\left(e^{2\alpha x}+1\right)\left(e^{2\gamma x}-1\right)+\gamma\left(e^{2\alpha x}-1\right)\left(e^{2\gamma x}+1\right)\right]e^{\lambda_{12}x}}{8\alpha\cdot\gamma}, \tag{B.11a}$$

$$W_3^{M}(x) = \frac{v\left(\lambda_{12}e^{\lambda_{12}x}-\lambda_9 e^{\lambda_9 x}\right)+\chi\left(\lambda_{10}e^{\lambda_{10}x}-\lambda_{11}e^{\lambda_{11}x}\right)}{8\alpha\cdot\gamma}, \tag{B.11b}$$

$$W_5^{M}(x) = -\frac{\left[\alpha\left(e_\alpha^2+e^{2\alpha x}\right)\left(e_\gamma^2-e^{2\gamma x}\right)+\gamma\left(e_\alpha^2-e^{2\alpha x}\right)\left(e_\gamma^2+e^{2\gamma x}\right)\right]e^{\lambda_{12}x}}{8e_\gamma\cdot e_\alpha\cdot\alpha\cdot\gamma}, \tag{B.11c}$$

$$W_6^{M}(x) = \frac{\left\{\left[\left(e_\gamma\cdot e_\alpha\right)^2+e^{2\lambda_9 x}\right]\lambda_9\cdot v-\left[\left(e_\gamma\cdot e^{\alpha x}\right)^2+\left(e_\alpha\cdot e^{\gamma x}\right)^2\right]\lambda_{10}\cdot\chi\right\}e^{\lambda_{12}x}}{8e_\gamma\cdot e_\alpha\cdot\alpha\cdot\gamma}. \tag{B.11d}$$

Appendix C. Variational formulation of the GFSM using analytical shape functions

This appendix presents a novel formulation of the TFEM for the Timoshenko frame on elastic Winkler foundation element.

The governing DEs of the Timoshenko beam on elastic Winkler foundation element for its variational formulation can be derived by substituting the constitutive DEs (1) into the equilibrium DEs (2) (Reddy, 1997):

$$A_s G\left[\frac{d^2 v}{dx^2}(x)-\frac{d\theta}{dx}(x)\right]-k\cdot v(x) = -q_v(x), \tag{C.1a}$$

$$EI\frac{d^2\theta}{dx^2}(x)+A_s G\left[\frac{dv}{dx}(x)-\theta(x)\right] = -q_\theta(x). \tag{C.1b}$$

Subsequently, the analytical transverse displacement and analytical cross-section rotation fields in the previous equations are approximated using analytical shape functions, as shown below:

$$v(x) \approx \psi_2^{v}(x)v_i+\psi_3^{v}(x)\theta_i+\psi_5^{v}(x)v_j+\psi_6^{v}(x)\theta_j = v_h(x), \tag{C.2a}$$

$$\theta(x) \approx \psi_2^{\theta}(x)v_i+\psi_3^{\theta}(x)\theta_i+\psi_5^{\theta}(x)v_j+\psi_6^{\theta}(x)\theta_j = \theta_h(x), \tag{C.2b}$$

following that, Eqs. (C.2) are substituted into Eqs. (C.1), and Galerkin's method is applied to these approximations of the governing DEs (weak formulation) (Demir et al., 2018; Alimoradzadeh et al., 2020). This yields two variational formulations. However, in order to achieve a unified variational formulation for the beam element, the following relation between the analytical cross-section rotation and analytical transverse displacement shape functions was employed, which is derived from Eq. (11):

$$\psi_n^{\theta}(x) = \frac{EI}{A_s G}\frac{\mathrm{d}^3\psi_n^{v}}{\mathrm{d}x^3}(x) + \left[1 - \frac{EIk}{(A_s G)^2}\right]\frac{\mathrm{d}\psi_n^{v}}{\mathrm{d}x}(x). \tag{C.3}$$

The approach of mixing these two variational formulations into a single one is known as the Mixed Finite Element Method (MFEM) (Ergüven and Gedikli, 2003; Frikha et al., 2016).

In the case of the rod element, the governing DE for its variational formulation can be obtained by substitution of the constitutive DE (48) into the equilibrium DE (49):

$$EA\frac{\mathrm{d}^2u}{\mathrm{d}x^2}(x) = -p(x). \tag{C.4}$$

Then, the analytical axial displacement field in the previous equation is approximated using analytical shape functions, as shown below:

$$u(x) \approx \psi_1^{u}(x)u_i + \psi_4^{u}(x)u_j = u_h(x), \tag{C.5}$$

following that, Eq. (C.5) is substituted into Eq. (C.4), and Galerkin's method is applied to this approximation of the governing DE, yielding the variational formulation of the rod element.

Finally, the variational formulations of the beam and rod elements yield the variational formulation of the frame element, which represents the analytical relation for the frame element that relates its generalized forces to its generalized displacements at the element ends. This relation can be expressed in matrix form as:

$$\boldsymbol{F} = \boldsymbol{K}\boldsymbol{\Delta} + \boldsymbol{F}^{f}, \tag{C.6}$$

where the bold font indicates that the variable is either a matrix or a vector. Additionally, the notation $\boldsymbol{A}_{rs}$ will be used to refer to the element at position rs of matrix A, while $\boldsymbol{B}_r$ refers to the element at position r of vector $\boldsymbol{B}$. Considering this, the elements of the vectors in Eq. (C.6) correspond to the following:

$$\boldsymbol{F} = \begin{Bmatrix} \boldsymbol{F}_1 \\ \boldsymbol{F}_2 \\ \boldsymbol{F}_3 \\ \boldsymbol{F}_4 \\ \boldsymbol{F}_5 \\ \boldsymbol{F}_6 \end{Bmatrix} \equiv \begin{Bmatrix} FX_i \\ FY_i \\ M_i \\ FX_j \\ FY_j \\ M_j \end{Bmatrix}, \quad \boldsymbol{\Delta} = \begin{Bmatrix} \boldsymbol{\Delta}_1 \\ \boldsymbol{\Delta}_2 \\ \boldsymbol{\Delta}_3 \\ \boldsymbol{\Delta}_4 \\ \boldsymbol{\Delta}_5 \\ \boldsymbol{\Delta}_6 \end{Bmatrix} \equiv \begin{Bmatrix} u_i \\ v_i \\ \theta_i \\ u_j \\ v_j \\ \theta_j \end{Bmatrix}, \quad \boldsymbol{F}^{f} = \begin{Bmatrix} \boldsymbol{F}_1^{f} \\ \boldsymbol{F}_2^{f} \\ \boldsymbol{F}_3^{f} \\ \boldsymbol{F}_4^{f} \\ \boldsymbol{F}_5^{f} \\ \boldsymbol{F}_6^{f} \end{Bmatrix} \equiv \begin{Bmatrix} FX_i^{f} \\ FY_i^{f} \\ M_i^{f} \\ FX_j^{f} \\ FY_j^{f} \\ M_j^{f} \end{Bmatrix}. \tag{C.7}$$

The elements of the stiffness matrix $\boldsymbol{K}$ and the fixed-end force vector $\boldsymbol{F}^{f}$ for $r, s = 1, 4$ are computed as follows:

$$\boldsymbol{K}_{rs} = \int_0^L EA\frac{\mathrm{d}\psi_r^{u}}{\mathrm{d}x}(x)\frac{\mathrm{d}\psi_s^{u}}{\mathrm{d}x}(x)\mathrm{d}x, \tag{C.8a}$$

$$\boldsymbol{F}_r^{f} = -\int_0^L \psi_r^{u}(x)p(x)\mathrm{d}x, \tag{C.8b}$$

and the elements for $r, s = 2, 3, 5, 6$ are obtained using the following equations:

$$\boldsymbol{K}_{rs} = \int_0^L \left[EI\frac{\mathrm{d}\psi_r^{\theta}}{\mathrm{d}x}(x)\frac{\mathrm{d}\psi_s^{\theta}}{\mathrm{d}x}(x) + A_s G\left(\frac{\mathrm{d}\psi_r^{v}}{\mathrm{d}x}(x) - \psi_r^{\theta}(x)\right)\left(\frac{\mathrm{d}\psi_s^{v}}{\mathrm{d}x}(x) - \psi_s^{\theta}(x)\right) + k\psi_r^{v}(x)\psi_s^{v}(x)\right]\mathrm{d}x, \tag{C.9a}$$

$$\boldsymbol{F}_r^{f} = -\int_0^L \left[\psi_r^{v}(x)q_v(x) + \psi_r^{\theta}(x)q_{\theta}(x)\right]\mathrm{d}x. \tag{C.9b}$$

Two noteworthy remarks are made at this point: (*a*) Eqs. (C.2), (C.5), (C.8) and (C.9) can be utilized with the analytical shape functions of all three cases of the characteristic equation, and (*b*) the stiffness matrix $\boldsymbol{K}$ and the fixed-end force vector $\boldsymbol{F}^{f}$ correspond to the same analytical stiffness matrix and analytical fixed-end force vector presented in this paper for all three cases of the characteristic equation.

Nomenclature

External Loads

$f_s(x)$	Distributed load exerted by the soil in the y-axis direction
$p(x)$	External distributed load in the x-axis direction
$q_v(x)$	External distributed load in the y-axis direction
$q_\theta(x)$	External distributed bending moments about the z-axis direction

Mechanical Parameters

ν	Poisson's ratio
E	Young's modulus
G	Shear modulus
k	Soil stiffness per unit length

Geometrical Parameters

κ	Shear coefficient
A	Cross-sectional area
A_s	Cross-sectional shear area
I	Cross-sectional second moment of area about the z-axis.
L	Element length
x, y, z	Element local axes

Indices

n	Index n, where $n \in \{2, 3, 5, 6\}$
m	Index m, where $m \in \{1, 4\}$
w	Index w, where $w \in \{i, j\}$. Here, i denotes the joint at the beginning of the element ($x = 0$), and j denotes the joint at the end of the element ($x = L$)
Q	Index Q, where $Q \in \{y, \theta, V, M\}$. Here, $Q = y$, $Q = \theta$, $Q = V$ and $Q = M$ are used to obtain the transverse displacement, cross-section rotation, shear force and bending moment Green's functions, respectively
R	Index R, where $R \in \{x, P\}$. Here, $R = x$ and $R = P$ are used to obtain the axial displacement and force Green's functions, respectively
r	Index r, where $r \in \{1, 2, 3, 5, 6\}$
s	Index s, where $s \in \{1, 2, 3, 5, 6\}$

Displacements and Cross-section Rotation Fields Parameters

$\psi_n^v(x)$	Transverse displacement shape functions
$\psi_n^\theta(x)$	Cross-section rotation shape functions
$\psi_m^u(x)$	Axial displacement shape functions
$v(x)$	Transverse displacement field
$v_h(x)$	Homogeneous transverse displacement field
$v_f(x)$	Fixed transverse displacement field
$v_f^v(x)$	Fixed transverse displacement field generated by $q_v(x)$
$v_f^\theta(x)$	Fixed transverse displacement field generated by $q_\theta(x)$
$\theta(x)$	Cross-section rotation field
$\theta_h(x)$	Homogeneous cross-section rotation field
$\theta_f(x)$	Fixed cross-section rotation field
$\theta_f^v(x)$	Fixed cross-section rotation field generated by $q_v(x)$
$\theta_f^\theta(x)$	Fixed cross-section rotation field generated by $q_\theta(x)$
$u(x)$	Axial displacement field
$u_h(x)$	Homogeneous axial displacement field
$u_f(x)$	Fixed axial displacement field
v_w	Transverse displacement at the joint w
θ_w	Cross-section rotation at the joint w
u_w	Axial displacement at the joint w

Internal Force Fields Parameters

$\psi_n^V(x)$	Shear force shape functions
$\psi_n^M(x)$	Bending moment shape functions
$\psi_m^P(x)$	Axial force shape functions
$V_h(x)$	Homogeneous shear force field
$V_f(x)$	Fixed shear force field
$V_f^v(x)$	Fixed shear force field generated by $q_v(x)$
$V_f^\theta(x)$	Fixed shear force field generated by $q_\theta(x)$
$M(x)$	Bending moment field
$M_h(x)$	Homogeneous bending moment field
$M_f(x)$	Fixed bending moment field
$M_f^v(x)$	Fixed bending moment field generated by $q_v(x)$
$M_f^\theta(x)$	Fixed bending moment field generated by $q_\theta(x)$
$P(x)$	Axial force field
$P_h(x)$	Homogeneous axial force field

$P_f(x)$	Fixed axial force field
FY_w	Element end force in the y-axis direction at joint w
FY_w^h	Homogeneous element end force in the y-axis direction at joint w
FY_w^f	Fixed element end force in the y-axis direction at joint w
FY_w^{vf}	Fixed element end force in the y-axis direction at joint w generated by $q_v(x)$
$FY_w^{\theta f}$	Fixed element end force in the y-axis direction at joint w generated by $q_\theta(x)$
M_w	Element end bending moment at joint w
M_w^h	Homogeneous element end bending moment at joint w
M_w^f	Fixed element end bending moment at joint w
M_w^{vf}	Fixed element end bending moment at joint w generated by $q_v(x)$
$M_w^{\theta f}$	Fixed element end bending moment at joint w generated by $q_\theta(x)$
FX_w	Element end force in the x-axis direction at joint w
FX_w^h	Homogeneous element end force in the x-axis direction at joint w
FX_w^f	Fixed element end force in the x-axis direction at joint w
Green's Functions	
$G_{Qy}(x,\xi)$	Transverse displacement, cross-section rotation, shear force and bending moment Green's functions associated with a fixed Timoshenko beam on elastic Winkler foundation subjected to a unit point transverse external load
$G_{Q\theta}(x,\xi)$	Transverse displacement, cross-section rotation, shear force and bending moment Green's functions associated with a fixed Timoshenko beam on elastic Winkler foundation subjected to a unit point external bending moment
$G_{Rx}(x,\xi)$	Axial displacement and axial force Green's functions associated with a fixed rod subjected to an unit point axial external load
$W_n^v(x)$	Functions used to compute the Green's function $G_{yy}(x,\xi)$ and $G_{y\theta}(x,\xi)$
$W_n^\theta(x)$	Functions used to compute the Green's function $G_{\theta y}(x,\xi)$ and $G_{\theta\theta}(x,\xi)$
$W_m^u(x)$	Functions used to compute the Green's function $G_{xx}(x,\xi)$
$W_n^V(x)$	Functions used to compute the Green's function $G_{Vy}(x,\xi)$ and $G_{V\theta}(x,\xi)$
$W_n^M(x)$	Functions used to compute the Green's function $G_{My}(x,\xi)$ and $G_{M\theta}(x,\xi)$
$W_m^P(x)$	Functions used to compute the Green's function $G_{Px}(x,\xi)$

References

Adhikari, S., 2021. Exact transcendental stiffness matrices of general beam-columns embedded in elastic mediums. Comput. Struct. 255, 106617. http://dx.doi.org/10.1016/j.compstruc.2021.106617, URL https://www.sciencedirect.com/science/article/pii/S0045794921001395.

Adhikari, S., Bhattacharya, S., 2021. A general frequency adaptive framework for damped response analysis of wind turbines. Soil Dyn. Earthq. Eng. 143, 106605. http://dx.doi.org/10.1016/j.soildyn.2021.106605, URL https://www.sciencedirect.com/science/article/pii/S0267726121000270.

Adhikari, S., Karličić, D., Liu, X., 2021. Dynamic stiffness of nonlocal damped nano-beams on elastic foundation. Eur. J. Mech. A Solids 86, 104144. http://dx.doi.org/10.1016/j.euromechsol.2020.104144, URL https://www.sciencedirect.com/science/article/pii/S0997753820305313.

Akgöz, B., Civalek, Ömer, 2018. Vibrational characteristics of embedded microbeams lying on a two-parameter elastic foundation in thermal environment. Composites B 150, 68–77. http://dx.doi.org/10.1016/j.compositesb.2018.05.049, URL https://www.sciencedirect.com/science/article/pii/S1359836818309454.

Aköz, A., Aksoydan, M., 2005. Transfer and stiffnes matrix for Timoshenko beams on elastic foundations. pp. 1–16, 54.

Al-Furjan, M., Farrokhian, A., Keshtegar, B., Kolahchi, R., Trung, N.-T., 2021. Dynamic stability control of viscoelastic nanocomposite piezoelectric sandwich beams resting on kerr foundation based on exponential piezoelasticity theory. Eur. J. Mech. A Solids 86, 104169. http://dx.doi.org/10.1016/j.euromechsol.2020.104169, URL https://www.sciencedirect.com/science/article/pii/S0997753820305507.

Al-Sadder, S.Z., Wahshat, T.M., 2012. Exact secant stiffness matrix of Timoshenko beam resting on variable one-parameter Winkler foundation. pp. 263–276. http://dx.doi.org/10.1061/40735(143)22, arXiv:https://ascelibrary.org/doi/pdf/10.1061/40735%28143%2922. URL https://ascelibrary.org/doi/abs/10.1061/40735%28143%2922.

Alhebshi, A.M.S., Metwally, A.M., Al-Basyouni, K.S., Mahmoud, S.R., Al-Solami, H.M., Alwabli, A.S., 2022. Mechanical behavior and physical properties of protein microtubules in living cells using the nonlocal beam theory. Phys. Mesomech. 25 (2), 181–186. http://dx.doi.org/10.1134/S1029959922020096.

Alimoradzadeh, M., Salehi, M., Mohammadi Esfarjani, S., 2020. Nonlinear vibration analysis of axially functionally graded microbeams based on nonlinear elastic foundation using modified couple stress theory. Period. Polytech. Mech. Eng. 64 (2), 97–108. http://dx.doi.org/10.3311/PPme.11684, URL https://pp.bme.hu/me/article/view/11684.

Arboleda-Monsalve, L.G., Zapata-Medina, D.G., Aristizabal-Ochoa, J.D., 2008. Timoshenko beam-column with generalized end conditions on elastic foundation: Dynamic-stiffness matrix and load vector. J. Sound Vib. 310 (4), 1057–1079. http://dx.doi.org/10.1016/j.jsv.2007.08.014, URL https://www.sciencedirect.com/science/article/pii/S0022460X07006761.

Avcar, M., Hadji, L., Civalek, Ömer, 2021. Natural frequency analysis of sigmoid functionally graded sandwich beams in the framework of high order shear deformation theory. Compos. Struct. 276, 114564. http://dx.doi.org/10.1016/j.compstruct.2021.114564, URL https://www.sciencedirect.com/science/article/pii/S0263822321010266.

Avramidis, I., Morfidis, K., 2006. Bending of beams on three-parameter elastic foundation. Int. J. Solids Struct. 43 (2), 357–375. http://dx.doi.org/10.1016/j.ijsolstr.2005.03.033, URL https://www.sciencedirect.com/science/article/pii/S0020768305001459.

Aydoğan, M., 1995. Stiffness-matrix formulation of beams with shear effect on elastic foundation. J. Struct. Eng. 121 (9), 1265–1270. http://dx.doi.org/10.1061/(ASCE)0733-9445(1995)121:9(1265), arXiv:https://ascelibrary.org/doi/pdf/10.1061/%28ASCE%290733-9445%281995%29121%3A9%281265%29. URL https://ascelibrary.org/doi/abs/10.1061/%28ASCE%290733-9445%281995%29121%3A9%281265%29.

Banerjee, P., Butterfield, R., 1981. Boundary Element Methods in Engineering Science. McGraw-Hill, New York.

Bechtold, J.E., Riley, D.R., 1991. Application of beams on elastic foundation and b-spline solution methodologies to parametric analysis of intramedullary implant systems. J. Biomech. 24 (6), 441–448. http://dx.doi.org/10.1016/0021-9290(91)90032-I, URL https://www.sciencedirect.com/science/article/pii/002192909190032I.

Benzid, A., Tati, A., 2023. Static and buckling behaviors analysis of fg beams using a three unknowns finite element based on enhanced Timoshenko theory. Mech. Adv. Mater. Struct. 1–12. http://dx.doi.org/10.1080/15376494.2023.2270969, arXiv:https://doi.org/10.1080/15376494.2023.2270969.

Beskou, N.D., Muho, E.V., 2023. Review on dynamic response of road pavements to moving vehicle loads; part 1: Rigid pavements. Soil Dyn. Earthq. Eng. 175, 108249. http://dx.doi.org/10.1016/j.soildyn.2023.108249, URL https://www.sciencedirect.com/science/article/pii/S0267726123004943.

Boussinesq, J., 1885. Application dès Potentiels a l'Étude de l'Équilibre et du Mouvement des Solides Élastiques. Gauthier-Villars.

Carrera, E., Giunta, G., Petrolo, M., 2011. Beam Structures: Classical and Advanced Theories. John Wiley & Sons.

Challamel, N., Mechab, I., Elmeiche, N., Houari, M.S.A., Ameur, M., Atmane, H.A., 2013. Buckling of generic higher-order shear beam/columns with elastic connections: Local and nonlocal formulation. J. Eng. Mech. 139 (8), 1091–1109. http://dx.doi.org/10.1061/(ASCE)EM.1943-7889.0000542, arXiv:https://ascelibrary.org/doi/pdf/10.1061/(ASCE)EM.1943-7889.0000542. URL https://ascelibrary.org/doi/abs/10.1061/(ASCE)EM.1943-7889.0000542.

Challis, L., Sheard, F., 2003. The green of Green functions. Phys. Today 56 (12), 41–46.

Cheng, F.Y., Pantelides, C.P., 1988. Static Timoshenko beam–columns on elastic media. J. Struct. Eng. 114 (5), 1152–1172. http://dx.doi.org/10.1061/(ASCE)0733-9445(1988)114:5(1152), arXiv:https://ascelibrary.org/doi/pdf/10.1061/%28ASCE%290733-9445%281988%29114%3A5%281152%29. URL https://ascelibrary.org/doi/abs/10.1061/%28ASCE%290733-9445%281988%29114%3A5%281152%29.

Cowper, G.R., 1966. The shear coefficient in Timoshenko's beam theory. J. Appl. Mech. 33 (2), 335–340. http://dx.doi.org/10.1115/1.3625046, arXiv:https://asmedigitalcollection.asme.org/appliedmechanics/article-pdf/33/2/335/5447638/335_1.pdf.

Dastjerdi, S., Malikan, M., Akgöz, B., Civalek, Ömer, Wiczenbach, T., Eremeyev, V.A., 2022. On the deformation and frequency analyses of sars-cov-2 at nanoscale. Internat. J. Engrg. Sci. 170, 103604. http://dx.doi.org/10.1016/j.ijengsci.2021.103604, URL https://www.sciencedirect.com/science/article/pii/S0020722521001440.

Demir, C., Mercan, K., Numanoglu, H.M., Civalek, O., 2018. Bending response of nanobeams resting on elastic foundation. J. Appl. Comput. Mech. 4 (2), 105–114. http://dx.doi.org/10.22055/jacm.2017.22594.1137, arXiv:https://jacm.scu.ac.ir/article_13100_ed38f1850b2c640739f9b91952cfc134.pdf. URL https://jacm.scu.ac.ir/article_13100.html.

Deng, H., Chen, kaidong, Cheng, W., Zhao, S., 2017. Vibration and buckling analysis of double-functionally graded Timoshenko beam system on winkler-pasternak elastic foundation. Compos. Struct. 160, 152–168. http://dx.doi.org/10.1016/j.compstruct.2016.10.027, URL https://www.sciencedirect.com/science/article/pii/S0263822316314878.

Elishakoff, I., 2019. Handbook on Timoshenko-Ehrenfest Beam and Uflyand-Mindlin Plate Theories. World Scientific.

Ergüven, M., Gedikli, A., 2003. A mixed finite element formulation for Timoshenko beam on Winkler foundation. Comput. Mech. 31, 229–237. http://dx.doi.org/10.1007/s00466-003-0420-9.

Esen, I., 2019. Dynamic response of a functionally graded Timoshenko beam on two-parameter elastic foundations due to a variable velocity moving mass. Int. J. Mech. Sci. 153–154, 21–35. http://dx.doi.org/10.1016/j.ijmecsci.2019.01.033, URL https://www.sciencedirect.com/science/article/pii/S0020740318334544.

Euler, L., 1744. Methodus Inveniendi Lineas Curvas Maximi Minive Proprietate Gaudentes. Bousquet, Lausanne & Geneva, 1744 (1744).

Faghidian, S.A., Elishakoff, I., 2023. The tale of shear coefficients in Timoshenko–Ehrenfest beam theory: 130 years of progress. Meccanica 58 (1), 97–108.

Filonenko-Borodich, M., 1940. Some approximate theories of elastic foundation. Uchenyie Zap. Mosk. Gos. Univ. Mekhanika 46, 3.

Fletcher, D.Q., Hermann, L.R., 1971. Elastic foundation representation of continuum. J. Eng. Mech. Div. 97 (1), 95–107. http://dx.doi.org/10.1061/JMCEA3.0001356, arXiv:https://ascelibrary.org/doi/pdf/10.1061/JMCEA3.0001356. URL https://ascelibrary.org/doi/abs/10.1061/JMCEA3.0001356.

Frikha, A., Hajlaoui, A., Wali, M., Dammak, F., 2016. A new higher order c0 mixed beam element for fgm beams analysis. Composites B 106, 181–189. http://dx.doi.org/10.1016/j.compositesb.2016.09.024, URL https://www.sciencedirect.com/science/article/pii/S135983681631109X.

Frydrýšek, K., Čepica, D., Hrabovský, L., Nikodým, M., 2023. Experimental and stochastic application of an elastic foundation in loose material transport via sandwich belt conveyors. Machines 11 (3), http://dx.doi.org/10.3390/machines11030327, URL https://www.mdpi.com/2075-1702/11/3/327.

Ghannadiasl, A., Mofid, M., 2014. Dynamic green function for response of timoshenko beam with arbitrary boundary conditions. Mech. Based Des. Struct. Mach. 42 (1), 97–110. http://dx.doi.org/10.1080/15397734.2013.836063, arXiv:https://doi.org/10.1080/15397734.2013.836063.

Han, H., Cao, D., Liu, L., 2017. Green's functions for forced vibration analysis of bending-torsion coupled timoshenko beam. Appl. Math. Model. 45, 621–635. http://dx.doi.org/10.1016/j.apm.2017.01.014, URL https://www.sciencedirect.com/science/article/pii/S0307904X17300197.

Hetényi, M., 1950. A general solution for the bending of beams on an elastic foundation of arbitrary continuity. J. Appl. Phys. 21, 55–58, URL https://api.semanticscholar.org/CorpusID:120374892.

Hetényi, M., Hetbenyi, M.I., 1946. Beams on Elastic Foundation: Theory with Applications in the Fields of Civil and Mechanical Engineering. Vol. 16, University of Michigan Press, Ann Arbor, MI.

Hozhabrossadati, S.M., Aftabi Sani, A., Mehri, B., Mofid, M., 2015. Green's function for uniform Euler–Bernoulli beams at resonant condition: Introduction of Fredholm alternative theorem. Appl. Math. Model. 39 (12), 3366–3379. http://dx.doi.org/10.1016/j.apm.2014.11.038, URL https://www.sciencedirect.com/science/article/pii/S0307904X14006222.

Ilanko, S., 2005. Transcendental dynamic stability functions for beams carrying rigid bodies. J. Sound Vib. 279 (3), 1195–1202. http://dx.doi.org/10.1016/j.jsv.2004.01.024, URL https://www.sciencedirect.com/science/article/pii/S0022460X04001361.

Kaneko, T., 1975. On Timoshenko's correction for shear in vibrating beams. J. Phys. D: Appl. Phys. 8 (16), 1927. http://dx.doi.org/10.1088/0022-3727/8/16/003.

Kaneko, T., 1978. An experimental study of the Timoshenko's shear coefficient for flexurally vibrating beams. J. Phys. D: Appl. Phys. 11 (14), 1979. http://dx.doi.org/10.1088/0022-3727/11/14/010.

Kenanda, M.A., Hammadi, F., 2023. A novel trigonometric high-order shear deformation theory for free vibration and buckling analysis of carbon nanotube reinforced beams resting on a kerr foundation. Eng. Proc. 56 (1), http://dx.doi.org/10.3390/ASEC2023-15282, URL https://www.mdpi.com/2673-4591/56/1/209.

Kennedy, D., Djoudi, M., Williams, F., 2004. Exact determinant for infinite order fem representation of a Timoshenko beam-column via improved transcendental member stiffness matrices. Internat. J. Numer. Methods Engrg. 59, http://dx.doi.org/10.1002/nme.919.

Kerr, A.D., 1965. A study of a new foundation model. Acta Mech. 1, 135–147, URL https://api.semanticscholar.org/CorpusID:115062840.

Lamprea-Pineda, A.C., Connolly, D.P., Hussein, M.F., 2022. Beams on elastic foundations – a review of railway applications and solutions. Transp. Geotech. 33, 100696. http://dx.doi.org/10.1016/j.trgeo.2021.100696, URL https://www.sciencedirect.com/science/article/pii/S2214391221001860.

Li, P., Du, S.-J., Wang, Y.-H., Zhao, H.-H., 2016. Timoshenko beam solution for the response of existing tunnels because of tunneling underneath. Int. J. Numer. Anal. Methods Geomech. 40 (5), 766–784. http://dx.doi.org/10.1002/nag.2426, arXiv:https://onlinelibrary.wiley.com/doi/pdf/10.1002/nag.2426. URL https://onlinelibrary.wiley.com/doi/abs/10.1002/nag.2426.

Lignola, G.P., Russo Spena, F., Prota, A., Manfredi, G., 2017. Exact stiffness–matrix of two nodes Timoshenko beam on elastic medium. an analogy with eringen model of nonlocal Euler–Bernoulli nanobeams. Comput. Struct. 182, 556–572. http://dx.doi.org/10.1016/j.compstruc.2016.12.003, URL https://www.sciencedirect.com/science/article/pii/S0045794916306502.

Lueschen, G., Bergman, L., McFarland, D., 1996. Green's functions for uniform Timoshenko beams. J. Sound Vib. 194 (1), 93–102. http://dx.doi.org/10.1006/jsvi.1996.0346, URL https://www.sciencedirect.com/science/article/pii/S0022460X96903466.

Mantari, J., Oktem, A., Guedes Soares, C., 2011. Static and dynamic analysis of laminated composite and sandwich plates and shells by using a new higher-order shear deformation theory. Compos. Struct. 94 (1), 37–49. http://dx.doi.org/10.1016/j.compstruct.2011.07.020, URL https://www.sciencedirect.com/science/article/pii/S0263822311002753.

Mazzoni, S., McKenna, F., Scott, M.H., Fenves, G.L., et al., 2006. Opensees command language manual. Pac. Earthq. Eng. Res. (PEER) Cent. 264 (1), 137–158.

Molina-Villegas, J.C., 2021. Análisis Estructural - Métodos Clásicos y Matriciales. ECOE Ediciones.

Molina-Villegas, J.C., Ballesteros Ortega, J.E., 2023a. Closed-form solution of euler–bernoulli frames in the frequency domain. Eng. Anal. Bound. Elem. 155, 682–695. http://dx.doi.org/10.1016/j.enganabound.2023.06.027, URL https://www.sciencedirect.com/science/article/pii/S0955799723003430.

Molina-Villegas, J.C., Ballesteros Ortega, J.E., 2023b. Closed-form solution of Timoshenko frames using the Green's function stiffness method. Int. J. Solids Struct. 269, 112180. http://dx.doi.org/10.1016/j.ijsolstr.2023.112180, URL https://www.sciencedirect.com/science/article/pii/S002076832300077X.

Molina-Villegas, J.C., Ballesteros Ortega, J.E., 2023c. Closed-form solution of Timoshenko frames with semi-rigid connections. Structures 48, 212–225. http://dx.doi.org/10.1016/j.istruc.2022.12.082, URL https://www.sciencedirect.com/science/article/pii/S235201242201270X.

Molina-Villegas, J.C., Ballesteros Ortega, J.E., Martínez Martínez, G., 2023. Closed-form solution for non-uniform Euler–bernoulli beams and frames. Eng. Struct. 292, 116381. http://dx.doi.org/10.1016/j.engstruct.2023.116381, URL https://www.sciencedirect.com/science/article/pii/S0141029623007964.

Molina-Villegas, J.C., Ballesteros Ortega, J.E., Quintero Toro, A.C., 2021. Analysis of beams on elastic foundations using Green's functions. Rev. Int. Métodos Numér. para Cálc. Diseño Ing. 37 (2), http://dx.doi.org/10.23967/j.rimni.2021.06.002.

Molina-Villegas, J.C., Ballesteros Ortega, J.E., Ruiz Cardona, D., 2022. Formulation of the Green's functions stiffness method for Euler–Bernoulli beams on elastic winkler foundation with semi-rigid connections. Eng. Struct. 266, 114616. http://dx.doi.org/10.1016/j.engstruct.2022.114616, URL https://www.sciencedirect.com/science/article/pii/S0141029622007155.

Molina-Villegas, J.C., Ballesteros Ortega, J.E., Soto, S.B., 2024. Closed-form solutions for axially non-uniform Timoshenko beams and frames under static loading. Compos. Struct. 337, 118078. http://dx.doi.org/10.1016/j.compstruct.2024.118078, URL https://www.sciencedirect.com/science/article/pii/S026382232400206X.

Morfidis, K., 2010. Vibration of Timoshenko beams on three-parameter elastic foundation. Comput. Struct. 88 (5), 294–308. http://dx.doi.org/10.1016/j.compstruc.2009.11.001, URL https://www.sciencedirect.com/science/article/pii/S0045794909002740.

Naghdi, A., 1980. Green's function for a semicircular plate. Int. J. Solids Struct. 16 (4), 329–335. http://dx.doi.org/10.1016/0020-7683(80)90085-2, URL https://www.sciencedirect.com/science/article/pii/0020768380900852.

Neves, A., Ferreira, A., Carrera, E., Roque, C., Cinefra, M., Jorge, R., Soares, C., 2011. Bending of fgm plates by a sinusoidal plate formulation and collocation with radial basis functions. Mech. Res. Commun. 38 (5), 368–371. http://dx.doi.org/10.1016/j.mechrescom.2011.04.011, URL https://www.sciencedirect.com/science/article/pii/S0093641311000899.

Nogami, T., O'Neill, M.W., 1985. Beam on generalized two-parameter foundation. J. Eng. Mech. 111 (5), 664–679. http://dx.doi.org/10.1061/(ASCE)0733-9399(1985)111:5(664), arXiv:https://ascelibrary.org/doi/pdf/10.1061/(ASCE)0733-9399(1985)111:5(664). URL https://ascelibrary.org/doi/abs/10.1061/%28ASCE%290733-9399%281985%29111%3A5%28664%29.

Onu, G., 2008. Finite elements on generalized elastic foundation in Timoshenko beam theory. J. Eng. Mech. 134 (9), 763–776. http://dx.doi.org/10.1061/(ASCE)0733-9399(2008)134:9(763), arXiv:https://ascelibrary.org/doi/pdf/10.1061/%28ASCE%290733-9399%282008%29134%3A9%28763%29. URL https://ascelibrary.org/doi/abs/10.1061/%28ASCE%290733-9399%282008.

Pasternak, P.L., 1954. On a new method of analysis of an elastic foundation by means of two foundation constants. URL https://api.semanticscholar.org/CorpusID:124773833.

Pham, Q.-H., Tran, V.K., Tran, T.T., Nguyen, P.-C., Malekzadeh, P., 2022. Dynamic instability of magnetically embedded functionally graded porous nanobeams using the strain gradient theory. Alex. Eng. J. 61 (12), 10025–10044. http://dx.doi.org/10.1016/j.aej.2022.03.007, URL https://www.sciencedirect.com/science/article/pii/S1110016822001740.

Rakowski, J., 1990. The interpretation of the shear locking in beam elements. Comput. Struct. 37 (5), 769–776. http://dx.doi.org/10.1016/0045-7949(90)90106-C, URL https://www.sciencedirect.com/science/article/pii/004579499090106C.

Reddy, J., 1997. On locking-free shear deformable beam finite elements. Comput. Methods Appl. Mech. Engrg. 149, 113–132, URL https://api.semanticscholar.org/CorpusID:121478595.

Reddy, J.N., 2019. Introduction to the Finite Element Method. McGraw-Hill Education.

Reissner, E., 1967. Note on the formulation of the problem of the plate on an elastic foundation. Acta Mech. 4 (1), 88–91.

Rezaiee-Pajand, M., Rajabzadeh-Safaei, N., Hozhabrossadati, S.M., 2018. Three-dimensional deformations of a curved circular beam subjected to thermo-mechanical loading using Green's function method. Int. J. Mech. Sci. 142–143, 163–175. http://dx.doi.org/10.1016/j.ijmecsci.2018.04.045, URL https://www.sciencedirect.com/science/article/pii/S0020740318307100.

Rosinger, H.E., Ritchie, I.G., 1977. On Timoshenko's correction for shear in vibrating isotropic beams. J. Phys. D: Appl. Phys. 10 (11), 1461. http://dx.doi.org/10.1088/0022-3727/10/11/009.

Ruge, P., Birk, C., 2007. A comparison of infinite Timoshenko and Euler–Bernoulli beam models on winkler foundation in the frequency- and time-domain. J. Sound Vib. 304 (3), 932–947. http://dx.doi.org/10.1016/j.jsv.2007.04.001, URL https://www.sciencedirect.com/science/article/pii/S0022460X07002349.

Ruocco, E., Reddy, J., 2023. Analytical solutions of Reddy, Timoshenko and Bernoulli beam models: A comparative analysis. Eur. J. Mech. A Solids 99, 104953. http://dx.doi.org/10.1016/j.euromechsol.2023.104953, URL https://www.sciencedirect.com/science/article/pii/S0997753823000451.

Sánchez-Sesma, F.J., Ramos-Martínez, J., Campillo, M., 1993. An indirect boundary element method applied to simulate the seismic response of alluvial valleys for incident P, S and Rayleigh waves. Earthq. Eng. Struct. Dyn. 22 (4), 279–295. http://dx.doi.org/10.1002/eqe.4290220402, arXiv:https://onlinelibrary.wiley.com/doi/pdf/10.1002/eqe.4290220402. URL https://onlinelibrary.wiley.com/doi/abs/10.1002/eqe.4290220402.

Scott, R.F., 1981. Foundation Analysis. Tech. rep., Prentice-Hall, New Jersey.

Selvadurai, A.P., 1979. Elastic Analysis of Soil-Foundation Interaction. Elsevier.

Shi, G., Voyiadjis, G.Z., 2010. A sixth-order theory of shear deformable beams with variational consistent boundary conditions. J. Appl. Mech. 78 (2), 021019. http://dx.doi.org/10.1115/1.4002594, arXiv:https://asmedigitalcollection.asme.org/appliedmechanics/article-pdf/78/2/021019/5481147/021019_1.pdf.

Shirima, L.M., Giger, M.W., 1992. Timoshenko beam element resting on two-parameter elastic foundation. J. Eng. Mech. 118 (2), 280–295. http://dx.doi.org/10.1061/(ASCE)0733-9399(1992)118:2(280), arXiv:https://ascelibrary.org/doi/pdf/10.1061/(ASCE)0733-9399(1992)118:2(280). URL https://ascelibrary.org/doi/abs/10.1061/%28ASCE%290733-9399%281992%29118%3A2%28280%29.

Silvestre, N., Camotim, D., 2002. First-order generalised beam theory for arbitrary orthotropic materials. Thin-Walled Struct. 40 (9), 755–789. http://dx.doi.org/10.1016/S0263-8231(02)00025-3, URL https://www.sciencedirect.com/science/article/pii/S0263823102000253.

Timoshenko, S.P., 1921. Lxvi. on the correction for shear of the differential equation for transverse vibrations of prismatic bars. Lond. Edinb. Dublin Philos. Mag. J. Sci. 41 (245), 744–746. http://dx.doi.org/10.1080/14786442108636264.

Timoshenko, S., 1922. X. on the transverse vibrations of bars of uniform cross-section. Lond. Edinb. Dublin Philos. Mag. J. Sci. 43 (253), 125–131. http://dx.doi.org/10.1080/14786442208633855, arXiv:https://doi.org/10.1080/14786442208633855.

Timoshenko, S., Goodier, J., 1951. Theory of Elasticity, second ed. McGraw-Hill Book Company.

Touratier, M., 1991. An efficient standard plate theory. Internat. J. Engrg. Sci. 29 (8), 901–916. http://dx.doi.org/10.1016/0020-7225(91)90165-Y, URL https://www.sciencedirect.com/science/article/pii/002072259190165Y.

Turcotte, D.L., Schubert, G., 2002. Geodynamics. Cambridge University Press.

Vallabhan, C.V.G., Das, Y.C., 1988. Parametric study of beams on elastic foundations. J. Eng. Mech. 114 (12), 2072–2082. http://dx.doi.org/10.1061/(ASCE)0733-9399(1988)114:12(2072), arXiv:https://ascelibrary.org/doi/pdf/10.1061/(ASCE)0733-9399(1988)114:12(2072). URL https://ascelibrary.org/doi/abs/10.1061/%28ASCE%290733-9399%281988%29114%3A12%282072%29.

Vlasov, V.Z., 1966. Beams, Plates and Shells on Elastic Foundation. Israel Program for Scientific Translation.

Wang, K.Y.L.C.M., He, X.Q., 1998. Exact solutions for Timoshenko beams on elastic foundations using Green's functions. Mech. Struct. Mach. 26 (1), 101–113. http://dx.doi.org/10.1080/08905459808945422, arXiv:https://doi.org/10.1080/08905459808945422.

Winkler, E., 1867. Die Leher Von der Elastizitat und Festigkeit. Dominicus Prague. Dominicus, Prague.

Worku, A., 2012. Part I: A generalized formulation of continuum models for elastic foundations. pp. 1641–1650. http://dx.doi.org/10.1061/41095(365)166, arXiv:https://ascelibrary.org/doi/pdf/10.1061/41095%28365%29166. URL https://ascelibrary.org/doi/abs/10.1061/41095%28365%29166.

Worku, A., Degu, Y., 2012. Part II: Application of newly derived and calibrated continuum subgrade models in the analysis of beams on elastic foundations. pp. 1651–1660. http://dx.doi.org/10.1061/41095(365)167, arXiv:https://ascelibrary.org/doi/pdf/10.1061/41095%28365%29167. URL https://ascelibrary.org/doi/abs/10.1061/41095%28365%29167.

Xia, G., 2022. Generalized foundation Timoshenko beam and its calculating methods. Arch. Appl. Mech. 92 (3), 1015–1036. http://dx.doi.org/10.1007/s00419-021-02090-1.

Yin, J.-H., 2000a. Closed-form solution for reinforced Timoshenko beam on elastic foundation. J. Eng. Mech. 126 (8), 868–874. http://dx.doi.org/10.1061/(ASCE)0733-9399(2000)126:8(868), arXiv:https://ascelibrary.org/doi/pdf/10.1061/%28ASCE%290733-9399%282000%29126%3A8%28868%29. URL https://ascelibrary.org/doi/abs/10.1061/%28ASCE%290733-9399%282000%29126%3A8%28868%29.

Yin, J.-H., 2000b. Comparative modeling study of reinforced beam on elastic foundation. J. Geotech. Geoenviron. Eng. 126 (3), 265–271. http://dx.doi.org/10.1061/(ASCE)1090-0241(2000)126:3(265), arXiv:https://ascelibrary.org/doi/pdf/10.1061/%28ASCE%291090-0241%282000%29126%3A3%28265%29. URL https://ascelibrary.org/doi/abs/10.1061/%28ASCE%291090-0241%282000%29126%3A3%28265%29.

Zenkour, A.M., 2013. A simple four-unknown refined theory for bending analysis of functionally graded plates. Appl. Math. Model. 37 (20), 9041–9051. http://dx.doi.org/10.1016/j.apm.2013.04.022, URL https://www.sciencedirect.com/science/article/pii/S0307904X13002746.

Zhaohua, F., Cook, R.D., 1983. Beam elements on two-parameter elastic foundations. J. Eng. Mech. 109 (6), 1390–1402. http://dx.doi.org/10.1061/(ASCE)0733-9399(1983)109:6(1390), arXiv:https://ascelibrary.org/doi/pdf/10.1061/(ASCE)0733-9399(1983)109:6(1390). URL https://ascelibrary.org/doi/abs/10.1061/%28ASCE%290733-9399%281983%29109%3A6%281390%29.